AUTOMATIC GRADING OF VESSEL TORTUOSITY IN RETINAL FUNDUS IMAGES

Thesis submitted by

Debasis Maji

Doctor of Philosophy (Engineering)

Department of Electrical Engineering

Faculty Council of Engineering and Technology

Jadavpur University, Kolkata– 700032, India

2023

Index No.: 130/17/E

1. **Title of the Thesis: AUTOMATIC GRADING OF VESSEL TORTUOSITY IN RETINAL FUNDUS IMAGES**
2. **Name, Designation and Institution of the Supervisors:**

(a) Dr. Gautam Sarkar
Professor
Department of Electrical Engineering
Jadavpur University, Kolkata– 700032, India

(b) Dr. Ashis Kumar Dhara
Assistant Professor
Department of Electrical Engineering
National Institute of Technology, Durgapur, India

3. **List of Publications in Journal:**

- **Debasis Maji**, Souvik Maiti, Ashis Kumar Dhara, Gautam Sarkar, "Automatic grading of retinal blood vessel tortuosity using Modified CNN in deep retinal image diagnosis", in Biomedical Signal Processing and Control (Elsevier), Volume 74, Pp-103514, year-2022.

4. **List of Patents: NIL**

5. **List of Presentations in National/ International Conferences**

- **Debasis Maji**, Souvik Maiti, Mainak Biswas, Goutam Kumar Ghorai, Sandip Sadhukhan, Debprasad Sinha, Ashis Kumar Dhara, Gautam Sarkar, "Automatic Patch Based Tortuosity Retinal Vessel Classification using VGG16 Network", IEI Impact in Changing Energy Mix in the Power Sector, ISBN:978-81-942561-2-0,2019, Kolkata, India.
- **Debasis Maji,** Souvik Maiti, Ashis Kumar Dhara, Gautam Sarkar, "Automated Retinal Blood Vessel Segmentation Using Modified UNet Architecture", Springer Lecture Notes in Electrical Engineering (LNEE), Proceedings of the 4th International Conference on Communication, Devices and Computing, DOI : 10.1007/978-981-99-2710-4, ISBN: 978-981-99-2709-8, ICCDC 2023, Haldia, West Bengal, INDIA.
- **Debasis Maji,** Souvik Maiti, Ashis Kumar Dhara, Gautam Sarkar,,"EfficientNet Enriched Model for Implementing the Grading of Diabetic Retinopathy Based on Retinal Blood Vessel Tortuosity," in in 2023 IEEE 3rd Applied Signal Processing Conference (ASPCON), 23January-2024,PP.131-136, DOI:10.1109/ASPCON59071.2023.10396362, ISBN-979-8-3503-25881, ASPCON 2023,Haldia, West Bengal, India.

Statement of Originality

I, Debasis Maji registered on 20th March, 2017 do hereby declare that this thesis entitled "Automatic Grading of Vessel Tortuosity in Retinal Fundus Images", contains literature survey and original research work done by the undersigned candidate as part of Doctoral studies. All information in this thesis have been obtained and presented in accordance with existing academic rules and ethical conduct. I declare that, as required by these rules and conduct, I have fully cited and referred all materials and results that are not original to this work. I also declare that I have checked this thesis as per the "Policy on Anti Plagiarism, Jadavpur University, 2019", and the level of similarity as checked by iThenticate software is 6%.

Signature of Candidate: Debasis Maji

Date: 20/11/2023

Certified by Supervisors:

(Signature with date & Seal)

1. 20/11/2023 Professor Electrical Engineering Department JADAVPUR UNIVERSITY Kolkata - 700 032

(Dr. Gautam Sarkar)

Professor

Electrical Engineering Department

Jadavpur University

Kolkata – 700032, India

2. 20/11/23. Dr. Ashis Kumar Dhara Assistant Professor Electrical Engineering Department National Institute of Technology DURGAPUR - 713209

(Dr. Ashis Kumar Dhara)

Assistant Professor

Electrical Engineering Department

National Institute of Technology

Durgapur – 713209, India

CERTIFICATE

This is to certify that the thesis entitled "Automatic Grading of Vessel Tortuosity in Retinal Fundus Images" submitted by Sri. Debasis Maji, who got his name registered on 20th March, 2017, for the award of Ph.D. (Engg.) degree of Jadavpur University is absolutely based upon his own work under the supervision of Dr. Gautam Sarkar and Dr. Ashis Kumar Dhara and that neither his thesis nor any part of the thesis has been submitted for any degree/diploma or any other academic award anywhere before.

20/11/2023

Dr. Gautam Sarkar
Professor
Electrical Engineering Department
Jadavpur University
Kolkata – 700032, India

Professor
Electrical Engineering Department
JADAVPUR UNIVERSITY
Kolkata - 700 032

ashis 20/11/23

Dr. Ashis Kumar Dhara
Assistant Professor
Electrical Engineering Department
National Institute of Technology
Durgapur – 713209, India

Dr. Ashis Kumar Dhara
Assistant Professor
Electrical Engineering Department
National Institute of Technology
DURGAPUR - 713209

Dedicated to

My Parents

My Grandfather

ACKNOWLEDGEMENT

During the journey in obtaining my PhD, several domains were explored which might not be possible without the support and encouragement of numerous persons. This thesis is the end of my journey in obtaining my PhD which has been kept on track and been seen through to completion with the kind support of my family, friends, teachers, colleagues and well wishers. It would not have been possible to write this doctoral thesis without the help and support of these kind people around me. It is a pleasant task to express my thanks to all those who contributed in many ways to the success of this study and made it a memorable experience for me. At the end of this thesis, I would like to thank all those people who made this thesis possible.

First, I would like to thank my supervisors Dr. Gautam Sarkar and Dr. Ashis Kumar Dhara for their advice, guidance and support. Under their guidance, I successfully overcame many difficulties and learned a lot. I am extremely indebted to them for providing the necessary infrastructure and resources to accomplish my research work. Their advice, reviews and suggestions around my work were extremely valuable during the period of research.

I must also acknowledge the technical and administrative support provided by Jadavpur University during the research. I am obliged to Dr. Biswanath Roy, HoD, Department of Electrical Engineering, Jadavpur University for his valuable guidance during the work. I am also thankful to Prof. Sugata Munshi, Prof. Palash Kumar Kundu and Prof. Amitava Chatterjee, Prof. Arabinda Das, Dr. Debangshu Dey, Associate Professor Department of Electrical Engineering, Jadavpur University, Prof. Dilip Dey, HoD, Department of Electrical Engineering, Haldia Institute of Technology for his valuable guidance during the work.

For any errors or inadequacies that may remain in this work, of course, the responsibility is entirely my own.

Debasis Maji

Debasis Maji

PhD Fellow

Department of Electrical Engineering

Jadavpur University

Abstract

Automated grading of vessel tortuosity in retinal fundus images plays a vital role in diagnosing and monitoring various ocular diseases, such as diabetic retinopathy and hypertensive retinopathy. In this thesis, we propose a novel approach for the automatic grading of vessel tortuosity, aiming to provide an accurate and efficient tool for ophthalmologists and healthcare professionals.

The proposed method utilizes state-of-the-art computer vision techniques to extract and analyze retinal vessel structures. Initially, vessel segmentation is performed to isolate the blood vessels from the retinal fundus images. Subsequently, a tortuosity measurement algorithm is employed to quantify the level of vessel tortuosity. The algorithm utilizes advanced image processing techniques, including curve analysis and feature extraction, to capture the complex spatial characteristics of vessel curvature.

To train and validate the proposed method, a large dataset of retinal fundus images, annotated by expert ophthalmologists, is utilized. Deep learning techniques, such as convolutional neural networks (CNNs), are employed to learn the complex patterns of vessel tortuosity. The trained model achieves high accuracy and robustness in predicting the tortuosity grades of retinal vessels.

To evaluate the performance of the proposed method, a comprehensive set of experiments is conducted using various metrics, including sensitivity, specificity, and area under the receiver operating characteristic curve (AUC-ROC). The results demonstrate that the automated grading system achieves comparable or even superior performance compared to manual grading by expert ophthalmologists.

The significance of this work lies in its potential to enhance the efficiency and accuracy of vessel tortuosity grading, ultimately leading to early detection and timely treatment of ocular diseases. By providing an automated and objective assessment, this system can assist healthcare professionals in making informed decisions and improve patient care.

In conclusion, this thesis presents a novel approach for the automatic grading of vessel tortuosity in retinal fundus images. The proposed method utilizes advanced computer vision techniques, including vessel segmentation and tortuosity measurement algorithms, trained

with deep learning models. The results demonstrate the system's effectiveness in accurately and efficiently grading vessel tortuosity. The developed automated grading system has the potential to be integrated into clinical practice, aiding ophthalmologists in the diagnosis and management of ocular diseases.

Retinal imaging is a useful diagnostic tool in healthcare monitoring, particularly for conditions affecting the blood vessels in the eye. The retina is a thin layer of tissue at the back of the eye that is responsible for converting light into electrical signals that the brain can interpret. Because the retina is connected to the circulatory system, it can provide valuable information about the health of blood vessels throughout the body.

One application of retinal imaging is in the diagnosis and monitoring of diabetic retinopathy, a complication of diabetes that affects the blood vessels in the retina. By examining images of the retina, healthcare providers can detect changes in the blood vessels that may indicate the onset or progression of diabetic retinopathy. This information can then be used to adjust treatment plans and improve outcomes for patients.

Retinal imaging can also be used to detect and monitor other conditions that affect the blood vessels in the eye, such as hypertensive retinopathy (caused by high blood pressure) and macular degeneration (a leading cause of vision loss in older adults).

Overall, retinal imaging is a non-invasive, convenient, and reliable way to monitor the health of blood vessels in the eye and detect early signs of certain medical conditions. It has the potential to improve patient outcomes and reduce healthcare costs by enabling earlier diagnosis and intervention.

Retinal imaging is typically done using specialized cameras that capture high-resolution images of the retina. These images can then be analyzed by healthcare providers to look for abnormalities or changes in the blood vessels, such as narrowing, bleeding, or leakage.

One advantage of retinal imaging is that it is non-invasive, meaning it does not require any injections or other invasive procedures. This makes it a safer and more comfortable option for patients, particularly those who may be sensitive to other types of diagnostic tests.

In addition to its diagnostic applications, retinal imaging is also being used in research to better understand the relationship between the health of the blood vessels in the eye and other medical conditions, such as cardiovascular disease and stroke. By examining changes in the

retina over time, researchers may be able to develop new strategies for preventing or treating these conditions.

Retinal imaging is a diagnostic tool that enables healthcare professionals to observe and assess the health of the blood vessels in the eye. This technique is used to diagnose and monitor various medical conditions, such as diabetic retinopathy, hypertensive retinopathy, and macular degeneration. Retinal imaging provides high-resolution images of the retina, which is a thin layer of tissue at the back of the eye that is connected to the circulatory system. By examining these images, healthcare professionals can detect early signs of medical conditions affecting the blood vessels and take appropriate measures to manage or treat the condition. This paper provides an in-depth analysis of the role of retinal imaging in healthcare monitoring.

Overview of Retinal Imaging:

Retinopathy of Prematurity (ROP) is a potentially blinding disease that primarily affects premature infants, particularly those born before 31 weeks of gestation or weighing less than 1500 grams. Vessel tortuosity measurement in ROP is crucial for assessing disease progression and guiding treatment decisions. Here are some key points regarding vessel tortuosity measurement in ROP. Vessel tortuosity refers to the abnormal twisting, bending, or winding of retinal blood vessels. In ROP, this is often observed due to the physiological changes .Ophthalmologists visually inspect the retinal images to grade the severity of vessel tortuosity, often using standardized scales such as the International Classification of Retinopathy of Prematurity (ICROP).

Quantitative measurement of vessel tortuosity in ROP aids in early detection and monitoring of disease progression. Higher levels of tortuosity are often associated with more severe stages of ROP, prompting timely intervention to prevent vision-threatening complications such as retinal detachment or macular dragging.

Retinal imaging is a non-invasive diagnostic technique that uses specialized cameras to capture high-resolution images of the retina. The images are captured through the pupil of the eye, and the patient is asked to look at a fixed point during the test. There are several types of retinal imaging techniques, including fundus photography, optical coherence tomography (OCT), and fluorescein angiography.

Fundus photography is a type of retinal imaging that uses a specialized camera to capture images of the retina. The camera is placed close to the eye and focuses on the back of the eye, where the retina is located. Fundus photography is a quick and painless procedure, and the images produced provide a clear view of the retina and blood vessels.

Optical coherence tomography is a more advanced type of retinal imaging that uses light waves to produce cross-sectional images of the retina. OCT provides a highly detailed view of the retina, which enables healthcare professionals to detect even small changes in the blood vessels. OCT is a non-invasive test that is performed in a clinical setting, and the images produced are analyzed by healthcare professionals to diagnose and monitor various medical conditions affecting the eye.

Fluorescein angiography is a specialized type of retinal imaging that uses a dye injected into a vein in the arm. The dye travels through the circulatory system to the eye, where it is photographed as it flows through the blood vessels in the retina. This technique enables healthcare professionals to detect abnormalities in the blood vessels, such as blockages or leakage.Overall, retinal imaging is a valuable tool in healthcare monitoring, particularly for conditions that affect the blood vessels in the eye. Its non-invasive nature, convenience, and reliability make it a promising area for continued research and development in the years to come.

Retinal imaging has emerged as a powerful diagnostic tool in healthcare monitoring, particularly for conditions affecting the blood vessels in the eye. The retina, a thin layer of tissue at the back of the eye, is connected to the circulatory system, and can provide valuable information about the health of blood vessels throughout the body. Retinal imaging can be used to diagnose and monitor conditions such as diabetic retinopathy, hypertensive retinopathy, and macular degeneration. It is a non-invasive, convenient, and reliable way to monitor the health of blood vessels in the eye and detect early signs of certain medical conditions.

This thesis provides an in-depth analysis of the role of retinal imaging in healthcare monitoring. It covers the following topics:

Overview of retinal imaging: This section provides an overview of the retinal imaging technique, including the equipment and technology used to capture high-resolution images of the retina. It also discusses the different types of retinal imaging, such as fundus photography, optical coherence tomography, and fluorescein angiography.

Applications of retinal imaging in healthcare monitoring: This section examines the various medical conditions that can be diagnosed and monitored using retinal imaging. It discusses the role of retinal imaging in the diagnosis and monitoring of diabetic retinopathy, hypertensive retinopathy, and macular degeneration. It also covers the use of retinal imaging in research to better understand the relationship between the health of the blood vessels in the eye and other medical conditions.

Advantages of retinal imaging: This section outlines the advantages of retinal imaging compared to other diagnostic tests. It highlights the non-invasive nature of retinal imaging, which makes it a safer and more comfortable option for patients, particularly those who may be sensitive to other types of diagnostic tests.

Limitations of retinal imaging: This section discusses the limitations of retinal imaging, including the cost of the equipment and the need for trained professionals to perform the test and analyze the images. It also covers the limitations of retinal imaging in terms of its ability to detect certain medical conditions.

Future directions in retinal imaging: This section examines the future directions of retinal imaging, including the development of new imaging technologies and the integration of artificial intelligence and machine learning to improve the accuracy and efficiency of retinal imaging analysis.

Overall, this thesis provides a comprehensive overview of the role of retinal imaging in healthcare monitoring. It highlights the advantages and limitations of this diagnostic technique, and identifies future directions for research and development in this area. Retinal imaging has the potential to improve patient outcomes and reduce healthcare costs by enabling earlier diagnosis and intervention. Continued research and development in retinal imaging will be crucial in the years to come.

CONTENTS

ABSTRACT i
LIST OF FIGURES viii
LIST OF TABLES x
LIST OF SYMBOLS AND ABBREVIATIONS xi
LIST OF ALGORITHEMS xii
CHAPTER 1. INTRODUCTION 1
1.1. Retinal blood Image diagnosis in healthcare monitoring 1
1.2. Motivation 5
1.3. Problem Statement 5
1.4. Aim and Objective of the thesis 5
1.5. Structure of the thesis 6
CHAPTER 2. LITERATURE REVIEWS 8
2.1. Introduction 8
2.2. Background Study 8
2.3. Deep Learning algorithms 12
2.4. Existing related research work 15
2.5. Feature extraction methodology 25
2.6. Optimization for DR classification 27
2.7. Feature extraction 31
2.8. Receiver operating characteristic 32
CHAPTER 3. AUTOMATIC GRADING OF RETINAL BLOOD VESSEL TORTUOSITY USING MODIFIED CNN NET 36
3.1. Introduction 36
3.2. Material and method 44
3.3. Training 47
3.4. Proposed CNN 48
3.5. Implementation 48
3.6. Experimental result and discussion 50
3.7. Summary 55
CHAPTER 4. AUTOMATIC PATCH BASED TORTUOUS RETINAL VESSEL CLASSIFICATION USING VGG-16 NETWORK 56
4.1. Introduction 56
4.2. Proposed Method 58
4.3. Results and Discussions 59
4.4. Summary 64

CHAPTER 5. DIABETIC RETINOPATHY DETECTION AND GRADING OF RETINAL BLOOD VESSEL TORTUOSITY USING MODIFIED EFFICIENT NET 65
5.1. Introduction 65
5.2. Methodology 66
5.3. Experiment and result 69
5.4. Summary 73
CHAPTER 6.GRADING OF RETINAL BLOOD VESSEL TORTUOSITY USING INCEPTION V3 AND SEGMENTATION OF VESSEL USING MODIFIED U-NET ARCHITECTURE 74
6.1. Introduction 74
6.2. Related Work 77
6.3. Methodology 78
6.4. Experiment and result 79
6.5. Summary 86
CHAPTER 7. CONCLUSION AND FUTURE SCOPE OF THE WORK 87
7.1. Conclusion 87
7.2. Future work 91

REFERENCES 92

LIST OF FIGURES

Figure 2.1 Eyes structure 10

Figure 2.2 SVM architecture 13

Figure 2.3 MLP technique 14

Figure 2.4 Confusion matrix for characteristic analysis 35

Figure 3.1 Different touristy level of fundus image (a) low touristy image (b) high touristy image 42

Figure 3.2 Block diagram of proposed classification framework 43

Figure 3.3 Proposed architecture model 49

Figure 3.4 Augmented training image 50

Figure 3.5 The confusion matrix in the test case 51

Figure 3.6 ROC curve 52

Figure 3.7 Loss curve in proposed method 52

Figure 3.8 Test image of tortured eyes 53

Figure 3.9 Relationship between VTI and DI 53

Figure 4.1 Sample image of tortuosity vessel patch 57

Figure 4.2 Classification model based on VGG-16 network 58

Figure 4.3 Focus on diabetic affected vessels 59

Figure 4.4 Visualization of learned retinal pathologies with the projected pre-GAP 60

Figure 4.5 Prediction helps of confusion matrix 61

Figure 4.6 Model loss while training and testing at various epoch value 62

Figure 4.7Model Accuracy while training and testing at various epoch value 62

Figure 5.1 Framework of DR model 66

Figure 5.2 Diabetic retinopathy accuracy comparison 70

Figure 5.3 Diabetic retinopathy Loss comparison 71

Figure 5.4 Efficient Net confusion matrix 72

Figure 6.1 Different touristy level of fundus image (a) low touristy image (b) high touristy image 74

Figure 6.2 Overview of the proposed fundus images Tortuosity Measurement framework for Diagnosing Glaucoma 78

Figure 6.3 Proposed U-Net model 80

Figure 6.4 Segmentation results of two retinal image 81

Figure 6.5 Training and validation loss,f1,Accuracy during training using U-NET 82

Figure 6.6 Tortuosity Measurement result 83

Figure 6.7 Some random example of failure cases a–b and successfully obtained grade c–d using proposed method 85

LIST OF TABLES

Table 3.1 Correlation between automatic tortuosity grading results in comparison 54

Table 3.2 Automatic tortuosity grading results in comparison with different networks. 55

Table 4.1 Observation Table 60

Table 4.2 Comparative study of correlation score with existing works 63

Table 4.3 Comparative study of F1 score with different works 63

Table 5.1 Parameter comparisons for several networks 70

Table 5.2 Shows comparisons of the different networks 71

Table 5.3 On the APTOS 2019 dataset, comparison with existing research for DR severity ratings 72

Table 6.1 Performance analysis of the suggested technique and the other existing approaches on DRIVE database 82

Table 6.2 The proposed method's outcomes for the CHASE_DB1 (02_test_img.png) dataset 84

Table 6.3 Overall comparison the accuracy measure is retinopathy score (SRCC) 85

LIST OF ABBREVIATIONS

Acronyms	Meaning
ANN	Artificial Neural Network
CNN	Convolution Neural Network
DNN	Deep Neural Network
DME	Diabetic Macular Edema
GMM	Gaussian Mixture Model
NPDR	Non proliferative diabetic retinopathy
PDR	Proliferative diabetic retinopathy
VTI	Vascular Tortuosity Index
DI	Density Index
ROP	Retinopathy of Prematurity
DME	Diabetic macular edoema
SVM	Support Vector Machine
CLAHE	Contrast limited adaptive histogram equalisation
FSVM	Fuzzy Support Vector Machine
MLPNN	Multi-Layer Perceptron Neural Network
DCT	Discrete Cosine Transform
ETDRS	Early Treatment for Diabetic Retinopathy Study
EVA	Electronic visual acuity test
DWT	Discrete Wavelet Transform
OCT	Optical Coherence Tomography
ROC	Receiver Operating Characteristics Curve

LIST OF ALGORITHMS

Algorithm 1: Fundus image classification 48

CHAPTER 1

INTRODUCTION

1.1. Retinal blood Image diagnosis in healthcare monitoring

Diabetes is a condition that has a negative impact on a number of vital human organs, including the heart, eyes, and kidneys. In about 80% of patients, blood glucose levels may vary, which could cause a few ocular issues. Patients with diabetes who have had it for more than ten years may develop eye-related diseases such retinopathy and maculopathy. To stop eye damage at its earliest stage, eye-related illnesses require proper detection, diagnosis, and treatment. If eye disorders are not treated, visual loss may eventually result. Diabetes causes a condition called diabetic retinopathy, which affects the retina (DR). Visual impairment and inadequacy among adults of working age are well-known issues. When the dilated eye exam results in severe deviations in any one of the following in the retina—changes in blood vessels, newly formed blood vessels, leaking blood vessels, changes in the lens, damages to the nerve tissue, and swelling of the macula—the ophthalmologist knows they are dealing with DR. Early diagnosis of DR enables ophthalmologists to administer the proper treatment and spare patients' eyesight loss.

Retinal vessel tortuosity is a significant clinical marker used in the assessment of various ocular diseases, including diabetic retinopathy, hypertensive retinopathy, and age-related macular degeneration. The measurement of vessel tortuosity provides valuable information about the condition of retinal blood vessels and helps clinicians make informed decisions regarding patient diagnosis, monitoring, and treatment. However, the manual grading of vessel tortuosity in retinal fundus images is a time-consuming and subjective process that can be prone to inter-observer variability.

In recent years, there has been a growing interest in developing automated systems to grade vessel tortuosity in retinal fundus images. These systems aim to improve efficiency, accuracy, and consistency in clinical practice by leveraging advancements in computer vision and machine learning techniques. An automated grading system would not only alleviate the burden on clinicians but also provide a standardized and objective assessment of vessel tortuosity.

The objective of this thesis is to propose a novel framework for the automatic grading of vessel tortuosity in retinal fundus images. This framework will utilize state-of-the-art image processing techniques, feature extraction methods, and machine learning algorithms to accurately classify vessel tortuosity levels. By automating the grading process, this research aims to provide a reliable and efficient tool for clinicians, enabling them to make more accurate diagnoses and treatment decisions.

The proposed framework consists of several key components. Firstly, the retinal fundus images undergo preprocessing to enhance vessel visibility and reduce noise, ensuring optimal conditions for subsequent analysis. Next, a vessel segmentation algorithm is applied to extract the vessel network from the preprocessed images. This step plays a crucial role in isolating the vessels and preparing them for feature extraction.

Following vessel segmentation, a comprehensive set of geometric and textural features is extracted from the segmented vessels. These features capture both local and global characteristics of vessel tortuosity, providing discriminative information for classification. Various feature extraction techniques, such as shape descriptors, fractal analysis, and texture analysis, can be employed to obtain a rich representation of vessel tortuosity.

The extracted features are then used to train a machine learning model, such as a convolutional neural network (CNN) or a support vector machine (SVM), which can effectively learn the complex patterns associated with different levels of vessel tortuosity. The model is trained using a dataset of retinal fundus images with expert-annotated tortuosity grades. The performance of the system is evaluated using standard evaluation metrics, including accuracy, sensitivity, specificity, and the area under the receiver operating characteristic curve (AUC-ROC).

The expected outcomes of this research include a robust and accurate automated system for grading vessel tortuosity in retinal fundus images. The proposed framework aims to significantly reduce the time and effort required for grading, allowing clinicians to efficiently analyze large volumes of images. Moreover, the automated system seeks to enhance consistency and reduce inter-observer variability by providing an objective and standardized assessment of vessel tortuosity.

In conclusion, this thesis addresses the need for an automated system for grading vessel tortuosity in retinal fundus images. By leveraging advancements in computer vision and machine learning, the proposed framework offers a promising solution for clinicians in their

assessment of ocular diseases. The development of an automated grading system will have significant implications for improving the efficiency, accuracy, and consistency of vessel tortuosity assessment, ultimately leading to better patient care in the field of ophthalmology.

Retinal vessel tortuosity, defined as the deviation from the normal straight course of retinal blood vessels, serves as a crucial indicator for various ocular diseases, including diabetic retinopathy, hypertensive retinopathy, and age-related macular degeneration. Quantitative assessment of vessel tortuosity plays a vital role in early diagnosis, disease monitoring, and treatment planning. However, the current practice of manually grading vessel tortuosity in retinal fundus images is time-consuming, subjective, and prone to inter-observer variability.

To overcome these challenges, there is a growing need for an automated system capable of accurately grading vessel tortuosity in retinal fundus images. Such a system would offer significant advantages, including improved efficiency, enhanced accuracy, and enhanced consistency in clinical practice. Furthermore, an automated grading system would enable timely diagnosis and treatment decisions, leading to better patient outcomes.

This thesis aims to address these challenges by proposing a novel framework for the automatic grading of vessel tortuosity in retinal fundus images. Leveraging recent advancements in computer vision and machine learning, the proposed framework seeks to extract relevant features from retinal images and classify vessel tortuosity levels. By automating the grading process, this research intends to streamline the assessment of ocular diseases and provide a reliable tool for clinicians.

The framework encompasses several key components, starting with the preprocessing stage, where retinal fundus images are enhanced to improve vessel visibility and reduce noise. Subsequently, a vessel segmentation algorithm is applied to isolate the vessel network from the preprocessed images. Following this, a set of geometric and textural features is extracted from the segmented vessels, capturing their local and global characteristics.

To enable the classification of vessel tortuosity, the extracted features are then fed into a machine learning model, such as a convolutional neural network (CNN) or a support vector machine (SVM). The model is trained using a comprehensive dataset of retinal fundus images with expert-annotated tortuosity grades, covering a wide range of tortuosity levels. Various performance metrics, including accuracy, sensitivity, specificity, and the area under the receiver operating characteristic curve (AUC-ROC), are employed to evaluate the effectiveness of the system.

The expected outcomes of this research include a robust and accurate automated system for grading vessel tortuosity in retinal fundus images. The proposed framework aims to significantly reduce grading time compared to manual evaluation, facilitating timely diagnosis and treatment decisions. Moreover, the system seeks to enhance consistency in tortuosity grading across different healthcare providers, minimizing inter-observer variability.

In conclusion, this thesis presents an automated approach for the grading of vessel tortuosity in retinal fundus images. By leveraging computer vision and machine learning techniques, this research contributes to the advancement of computer-aided diagnosis in ophthalmology. The proposed framework offers a reliable and efficient solution, enabling clinicians to assess ocular diseases and monitor disease progression with improved accuracy and consistency.

The clinical examination of the ocular fundus is a crucial tool for spotting and keeping track of several pathological symptoms associated with the main disorders of the cardiovascular, neurological, and endocrine-metabolic systems [1]. If symptoms at the time of their initial manifestation could be accurately and objectively analysed, the majority of retinopathies, such as those caused by diabetes or hypertension, might be identified early and properly treated. The analysis needs to be thorough enough to compare results with those from the same patient at different times and with recognised clinical criteria, as well as sensitive enough to pick up on even the smallest abnormal indications. This last criterion is especially crucial when analysing the impact of therapeutic interventions and even more so when quantifying the effectiveness of novel medications as they are being developed.

When there are no significant retinal lesions (such as cotton wool spots, haemorrhages, or exudates), the clinical diagnostic procedure for evaluating hypertensive retinopathy entails a careful evaluation of the key characteristics of the retinal vessel network obtained from fundus camera images or ophthalmoscopic examination. When certain retinopathies first manifest, their morphological characteristics of the retinal vascular tree frequently serve as early warning signs [2] or prognostic indicators, as in the case of retinopathy of prematurity [3]. No objective and quantitative grading system has ever been used to evaluate vessel tortuosity, despite the fact that the severity of the disease has been shown to be correlated with an increase in vessel tortuosity in retinopathy of prematurity [5], hypertensive retinopathy [6], and some rarer and hereditary retinopathies (e.g. [7]). Grading is based on a subjective and qualitative metric in [6], where a five step grading scale was developed for the measurement of tortuosity. A tortuosity metric that reflects the clinical view of

ophthalmologists is urgently needed in order to assess the clinical significance of tortuosity changes over time or to compare different degrees of the same retinopathy.

First, it's important to comprehend the key elements that determine whether a vessel is considered tortuous or not. This is crucial when assessing retinal images since long, smooth veins with semicircular or parabolic shapes, as well as straight vessels, are all seen as non-tortuous due to the retina's hemispherical shape. These all are the first stage to move toward the actual diagnosis approach.

This chapter provides a brief description of the problem statement, the objectives, the suggested system, and the driving forces behind the research. In this chapter, the thesis's organisation is thoroughly addressed.

1.2. Motivation

According to the WHO's statistics estimate, 108 million individuals had diabetes in 1980, and that number rose quickly to 422 million in 2014. Diabetes and excessive blood sugar were the cause of 1.6 million fatalities in 2015. According to the WHO, diabetes will contribute significantly to deaths in the year 2030. Before the age of 70, high blood sugar causes about half of all fatalities. WHO advises people to keep a balanced diet, engage in regular physical activity, take the recommended medications, and regularly screen and test for problems in order to avoid the cause of death.

1.3. Problem Statement

The eye condition known as diabetic retinopathy affects patients who have had diabetes for more than 10 years. A well-prepared practitioner may find it difficult to diagnose DR early, which could result in postponed treatment, misunderstandings, and other problems.

In India, 10,000 ophthalmologists are available to treat the whole population (1 ophthalmologist for every 100,000 people), despite 70% of the population living in rural areas. Neural network systems were introduced in the majority of eye clinical laboratories in order to diagnose diabetic retinopathy at an earlier stage and to streamline the ophthalmologist's work.

1.4. Aim and Objective of the thesis

The suggested methodology seeks to use multiple segmentation and Deep Learning techniques to assess the severity of the early stage of diabetic retinopathy. Convolutional

Neural Network, Efficient Net, and VGG-16 Network are only a few of the learning methods used in the proposed work to detect diabetic retinopathy and grade retinopathy of prematurity(ROP) based on vessel tortuosity. An earlier diagnosis of DR may enable the administration of the proper care and the protection of the patients.

The major goals of the proposed work are to:

- Increase sensitivity, specificity, and accuracy in the diagnosis of diabetic retinopathy by detecting blood vessels and vessel tortuosity.
- To create an automatic grading system for different DR phases that is highly accurate and computationally simple.
- Development of algorithms for detection of tortuosity grade. These algorithms will be useful in the development of a DR screening tool.

1.5. Structure of the thesis

Chapter 1: The context and motivation of the current are explained in chapter 1, along with the architecture of the eye, retinal-related eye conditions, diabetic retinopathy, risk factors and complications of DR, DR screening, and a brief introduction to the classifiers utilised in the research effort.

Chapter 2: In chapter 2, the diagnostic of the retinal image, issues deduced from prior works, and suggested research goals are reviewed in the literature.

Chapter 3: In this chapter, we intend to offer a resilient Convolution Neural Networks (CNN) architecture, that can grade the disease regardless of noise and variance. We trained the model to use an open to the public dataset from Kaggle, and we verified it using EIARG2, another publicly accessible dataset. We also compare our model to standard architectures such as ResNet50, VGG16, and several others in the domain, and conclude as our architecture is better for grading retinopathy than current standard structures based on promising results.

Chapter 4: This chapter presents an automatic grading system based on a patch- based VGG16 model. The innovation of this technique resides in the forced amendments of neural organizations to 16 convolution layers, which really is more profound than prior research on gradation of vascular tortuosity. In order to reduce the boundaries in profound organizations, channels of size 3x3 are thought of in each convolution.

Chapter 5: In this chapter, Efficient Net used in order to extract more features and overcome the issue of tiny differences between lesions. Efficient Net was originally trained just on Image Net dataset using transfer-learning methods to avoid the DR's limited sample size issue. Multiple classifiers are then evolved in view of the traits gathered: one is a 5-grade classifier. Both the grade classifier as well as the factors, which incorporates classifier, have five possible approaches to establish a diagnosis: The numerals 0, 1, 2, 3, and 4 stands for absence of DR, moderate DR, medium DR, serious DR, and proliferative DR, respectively.

Chapter 6: One useful feature of automatic ophthalmological diagnostic tools is indeed the monitoring of blood vessel tortuosity. Retinopathy of Prematurity (ROP), an eye condition that affects premature infants, is one condition for which automatic tortuosity assessment is critical, in particular, is critically dependent on the automatic evaluation of tortuosity. This chapter provides a technique for segmenting blood arteries using an improved U-net architecture. These findings suggest that a deep learning framework could increase the cost effectiveness of screening and decision-making.

Chapter 7: The thesis summary, importance, and alternative extensions for future work are covered in chapter 7.

CHAPTER 2

LITERATURE REVIEWS

2.1. Introduction

Computer-aided technology development in medical picture diagnosis systems is accelerating daily. Advanced computational methods and image processing are specifically used for ophthalmic screening. The existing research on the detection of lesions and abnormal retinal characteristics such blood vessels, microaneurysms, haemorrhages, and exudates is explained in this literature review. It also reviews automated computer-aided grading for various stages of DR utilising classifier. Additionally, it describes the goals and significance of the suggested strategy.

2.2. Background Study

2.2.1. The Human eyes

Five senses, including sight, hearing, taste, smell, and touch, make up human anatomy. Every sense is crucial to daily life, but vision in particular serves a crucial role in bridging the gap between people and their surroundings. Vision is the common name for sight.

The retina receives the focused light, which stimulates the rods and cones. These nerve impulses are then sent to the optic nerve by the retina [8]. These signals are sent from the optic nerve to the brain, where the visual images are decoded.

Visual information is taken in by the brain through the eyes. The retina is a crucial component of the eye because it sends images to the brain via the optic nerve. Most eye illnesses have few symptoms in their early stages [9]. Early illness detection makes diseases like retinopathy and glaucoma easier to manage. Otherwise, the risk to the patients increases, necessitating routine examinations and diagnoses by skilled ophthalmologists and medical professionals. It is crucial to draw this conclusion early on in order to prevent diabetic retinal disorders. The majority of diabetic individuals experience eye disorders, which can have serious consequences. One of the most serious complications among the other retinal diseases is diabetic retinopathy.

2.2.2. Anatomy of the eyes

It's necessary to learn about the anatomy of the eye in order to understand the nature of eye disease. The receptor organ, which resembles a camera, is the human eye's spheroid structure. There are three protective layers inside the eyeball. The fibrous tunic, or outermost layer, is made up of the cornea and sclera [10].

The conjunctiva, a transparent membrane, covers the cornea, which is more curved and transparent. The "White of the eye" is called the sclera. It serves as the eyeball's protective membrane. The membrane that surrounds the eye's inner chambers has an exterior that is white and an interior that is brown in colour [11-14]. A region known as the limbus connects the cornea and sclera.

The vascular tunic or uvea, which is composed of the choroid, iris, ciliary body, and pigmented epithelium, is the following layer. Blood vessels and pigments make up the choroid. This layer gives rise to the ciliary body, which alters the curvature of the lens. It provides the tissues of the eyes with oxygen and a nutrition. A layer that nourishes the retina with blood vessels is called the pigmented epithelium [15]. The colourful ring around the pupil is called the iris. The retina, which is the innermost layer, is crucial in the diagnosis of diabetic retinopathy. It is a very thin layer of photosensitive tissue that receives oxygen from both the retinal blood vessels and the posterior blood vessels of the choroid (interior). There are two different kinds of photoreceptors: rods and cones.

Cones are found in the tiny macula, a region of the retina that is responsible for centre and colour vision and performs well in bright and medium light. At the macula's centre lies a little depression known as the fovea [16]. Iris, lens, and cornea make up the anterior portion.

The vitreous, retina, choroid, and sclera make up the posterior section of the eye. The human eye's anatomy is depicted in Figure 2.1 using the website https:// www.carlsonstockart.com as a source of information.

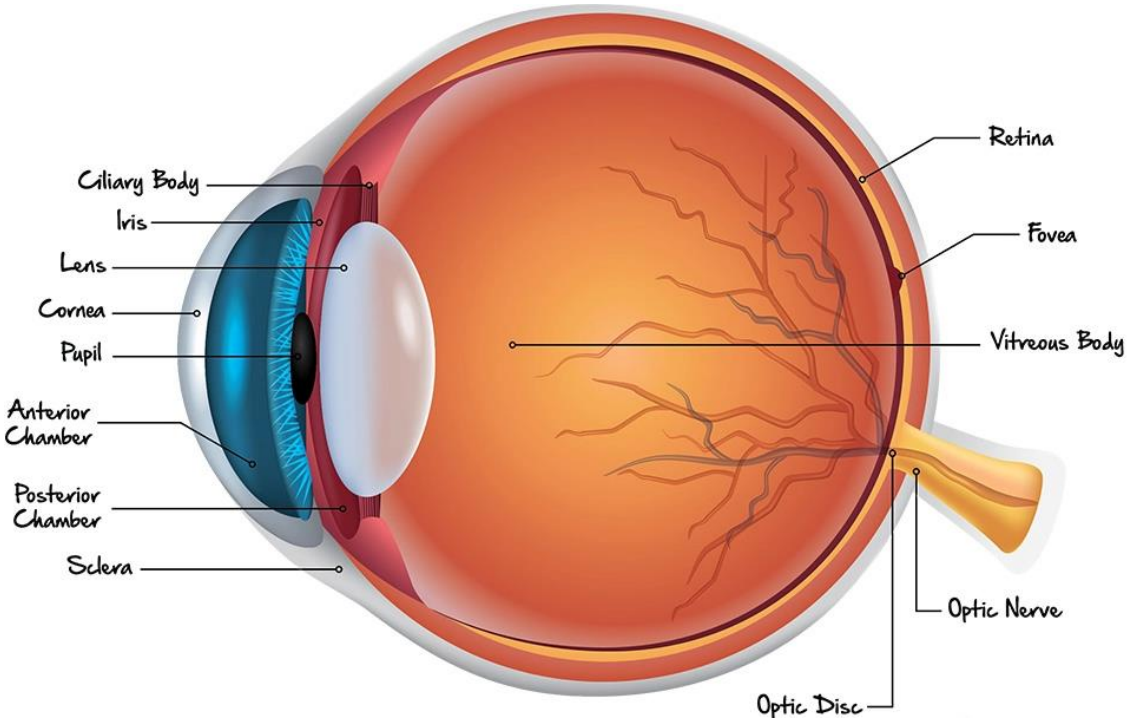

Fig .2.1. Eyes structure [14]

2.2.3. Diseases related to eyes

A condition known as diabetic retinopathy affects the blood vessels in the retina, a light-sensitive tissue located in the back of the eye. Diabetes is a common cause of vision loss in diabetics and is one of the main risk factors for vision loss and blindness in people under the age of 70 [17]. The paradoxical rise in blood glucose level, which damages the endothelium of the vessels and raises retinal vascular permeability, is the primary cause of the DR. The retinal detachment is caused by the proliferation of DR. Patients with DR do not experience any symptoms until visual impairment sets in, making treatment less effective. The initial stages of DR can be treated with laser photocoagulation, which may avoid vision loss.

Patients with diabetes are advised to have routine eye exams to screen for DR. Diabetic macular edoema, age-related macular degeneration, cataract, conjunctivitis, and glaucoma are abnormalities linked to diabetic retinal illness.

For people with diabetes, diabetic macular edoema (DME) is the predominant consequence and the main reason for visual loss [18]. It happens as a result of fluid and protein deposits on or under the macula, which cause the macula to enlarge or swell and cause vision loss. Macular edoema can be brought on by any abnormal blood vessel leaking in the adjacent retina around the macula or by any condition that harms blood vessels [19]. Florescence

angiography, which determines whether any blood vessels are leaking and, if so, how much, or Optical Coherence Tomography (OCT), which assesses retinal thickness and has a high sensitivity for detecting swelling, can be used to diagnose the condition.

Conjunctivitis is an inflammation of the conjunctiva, which is visible as lines inside the eyelid and as a thin, clear tissue at the white area of the eye [20]. Pinkeye is another name for it. It may be brought on by bacteria, viruses, irritants, or allergies. The most typical signs and symptoms are redness of the eye white or inner eyelid, more tears than usual, itchy or burning eyes, and so on. Antibiotics provided by a doctor can cure it [21].

The primary function of blood vessels in the retina is to carry oxygen and other nutrients to the eye. Since the primary blood vessels are obstructed and thickened by the presence of DR, inadequate blood flow in the retinal blood vessels may promote the growth of new, fragile blood vessels [22]. The new blood vessels are making an effort to provide the eye with nutrients and oxygen even while the primary blood arteries are obstructed. Due to the abnormality and fragility of these new blood vessels, they run the risk of rupturing and leaking blood as well as other substances including proteins and lipids [23]. If the blood leakage happened on the fovea or macula, it won't have an impact on the patient's vision.

2.2.4. Technology used for detection

Diabetes patients should have routine screening exams to identify and treat eye-related issues sooner. It is extremely challenging to treat diabetic eye disease at the point when symptoms first appear. Screening is a successful strategy for diagnosing and treating DR patients in a timely manner to prevent visual loss [24]. The screening process, which involves photographing the retina, takes 30 minutes to complete. Depending on the stage of the disease, several approaches are taken to treat DR. In order for the surgeons to confirm the proper course of treatment for the condition, the ophthalmologists or retinal surgeons execute a number of tests to observe the disease's progression [25-28].

Fluorescein angiography is a method for capturing the distinct blood vessel structure. An professional may inject a dye into the bloodstream prior to doing this test to check for blood vessel leakage, edoema, or circulation issues. Blood vessel harm can result from diabetic retinopathy [29]. The majority of medical professionals favour this test for diabetes patients. OCT, or optical coherence tomography, is a non-invasive imaging test that enables light beams to take cross-sectional pictures of the retina. The retinal specialist can analyse each of the retina's layers using OCT [30]. Additionally, it is utilised to map such layers and gauge

their thickness. This assessment will aid in further diagnosis and offer direction for therapies connected to the retina [31].

One of the techniques for screening the retina is scanning laser ophthalmoscopy. Confocal laser scanning microscopy, a method employed in SLO, produces excellent diagnostic images of the cornea and retina. To provide crisper images of the retina, it also uses adaptive optics.

2.3. Deep Learning algorithms

A computational technique called Deep Learning enables an algorithm to self-program by learning from a huge body of instances that demonstrate the desired behaviour, negating the need to explicitly express the rules [32]. It would be easier for patients and clinicians to evaluate more patients if there was a way to determine whether diabetic retinopathy was present or not using multiple classifying algorithms and proven datasets. Although training the neural network takes a long time, using Deep Learning techniques has the advantage of solving a medical image processing problem relatively effectively [33].

2.3.1. SVM

A Support Vector Machine (SVM) is a potent method that does regression, outlier detection, and linear or nonlinear classification [34]. It works well for difficult categorization with small to medium-sized datasets. It is a supervised learning technique that uses training data analysis to determine the best way to categorise photos as normal, mild, moderate, and severe. A training example consists of a label set and feature set that were each assigned to a separate class and represented by points in space. The two types of SVM classifiers are I linear SVM classifiers and (ii) nonlinear SVM classifiers.

A hyperplane is built and mapped to the space for separating the various classes in a linear SVM classifier [35]. It asserts that a good separation in view will result in less generalisation error for the SVM classifier on the hyperplane with the highest margin. The points closest to the decision surface are called support vectors.

The datasets for the various classes in the non-linear SVM classifier are somewhat spread and close together. A straight hyperplane is not favoured for dividing these various types of classes in order to tackle this problem [36]. Vapnik suggested a non-linear SVM classifier in 1998, implicitly charting the inputs in a higher-dimensional space using a kernel method to map the maximum margin space hyperplane [37]. Although there are various kernel types,

each kernel contains a non-linear kernel function. Figure 2.2, shows the SVM technique with multi input and single output.

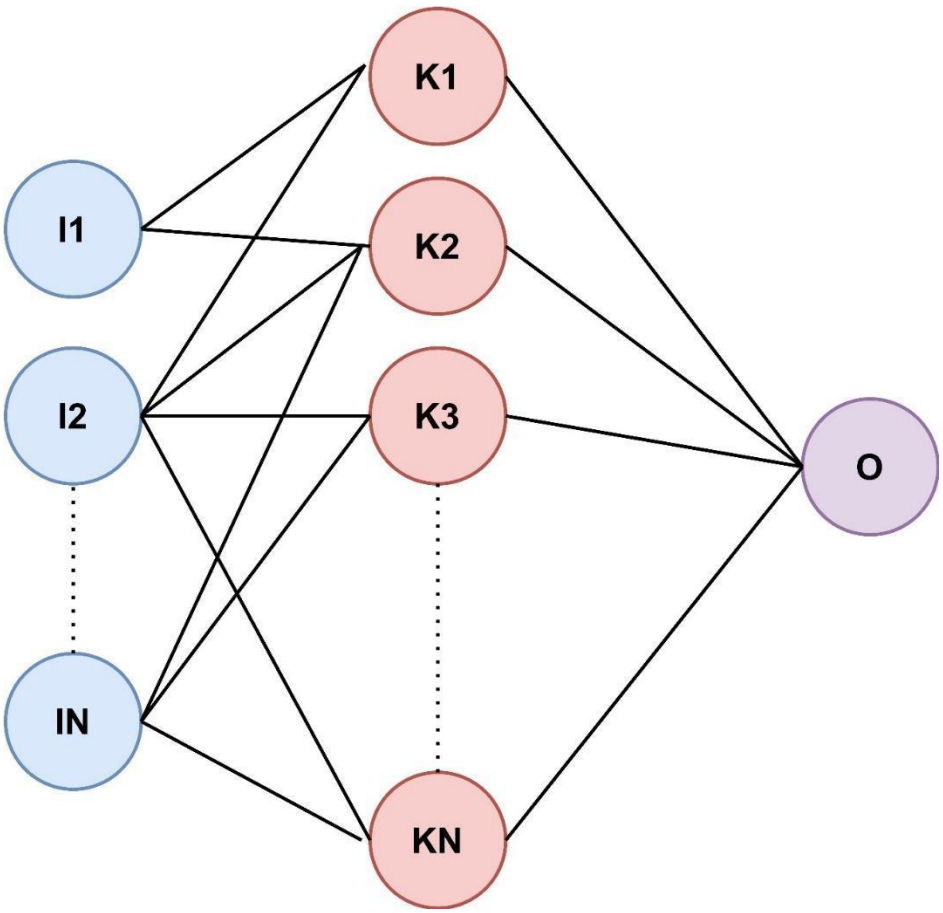

Fig. 2.2. SVM architecture

2.3.2. MLP technique

Usually referred to as multilayer perceptrons, feed forward artificial neural networks belong to this class (MLP) [38]. At least three layers of nodes make up an MLP. Except for the input nodes, each node is referred to as a neuron that employs a nonlinear activation function. Backpropagation is a supervised learning method that is used in its training. By having many layers and non-linear activation, it differs from a linear perceptron [39]. The multilayer perceptron's architecture is depicted in Figure 2.3.

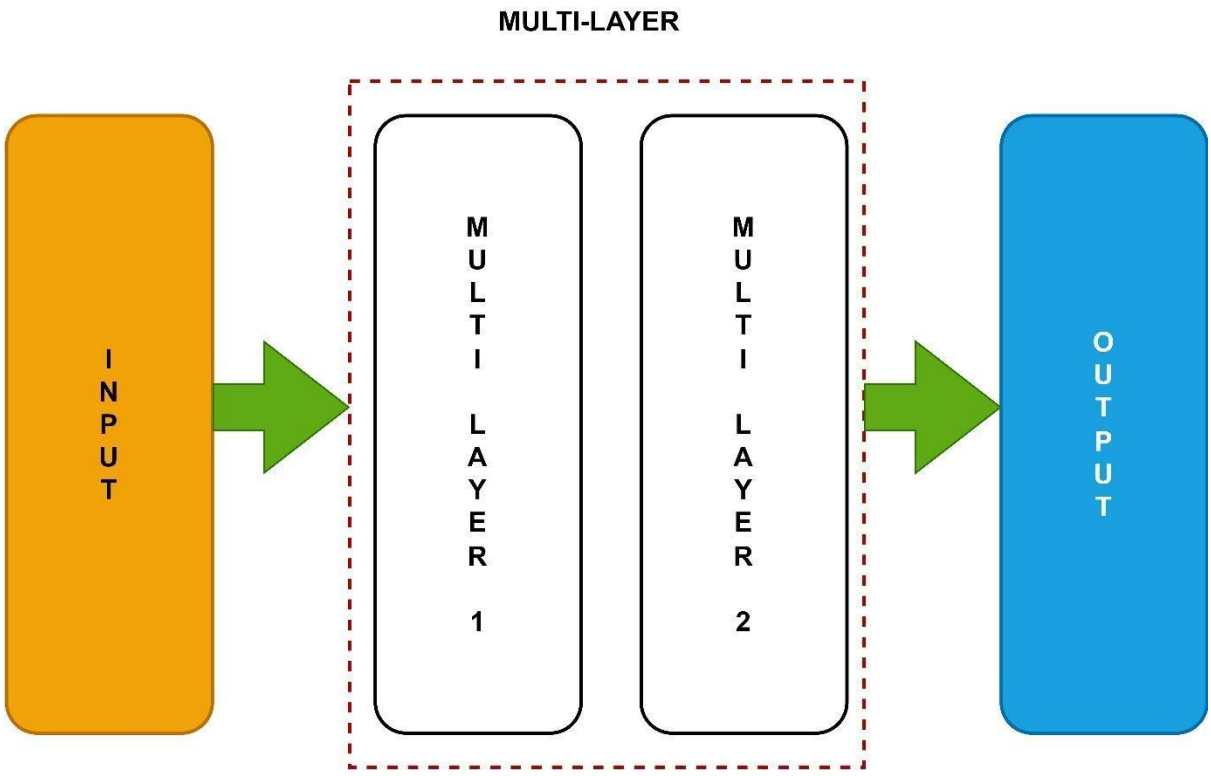

Fig. 2.3. MLP technique

Stochastic gradient descent is a popular training technique for neural networks. The row of data exposed to the network at a given time is used as the input for this method. As it repeats until an output value is produced, the network processes the exposed input by activating the neurons in the upward direction [40]. Known as a forward pass, this action. After the network has been trained to generate predictions on new data, forward pass is employed.

By contrasting the output of the network with the predicted output, an error is determined. One layer at a time, this error is transmitted back through the network, and the weights are changed while keeping the contribution they made to the error. The back propagation algorithm is what is used in this. All of the photos in the training data are subjected to this method once again. Epoch refers to the network's single update for the duration of the training. Tens, hundreds, or even thousands of training epochs can be used to train the network.

2.3.3. Convolution Neural Network

A subtype of Deep Learning called deep learning (DL) uses a cascade of different layers to extract and manipulate features. Each layer's input makes use of the previous layer's output. It will automatically pick up the features in each layer [41]. DL now has the highest level of

accuracy ever. Contrarily, DL needs a lot of categorised data and high-performance GPUs, which can cut training time to a few hours or even less. Large amounts of data are used to train DL models, and without any prior knowledge of the data through feature extraction, the neural network directly learns the features from the data. Convolutional Neural Networks, one of the most well-liked neural networks, are what we use in this situation.

The input, hidden, and output layers make up CNN. The next few layers (near the outputs) will be completely linked one-dimensional layers and normalising layers. The hidden layer comprises of alternating convolution and pooling operations to speed up processing and increase spatial and configuration invariance. The various features of an image are found using each concealed layer.

2.4. Existing related research work

Numerous academics have examined the algorithms used for the goal of extracting information from digital fundus photos. Also addressed are the methods that employ these attributes to categorise individual fundus images. It is also examined how effectively different DR systems classify data. A single result generalisation is difficult because a lot of the reported systems have been highly optimised with relation to the images of the investigated fundus. However, our analysis demonstrates that the outcomes from these classifications have lately improved and are also moving closer to the capabilities of ophthalmologists' classification.

Rema & Pradeepa [42] provided evidence that 7 percent of newly diagnosed participants have DR, demonstrating that even in situations of type 2 diabetes, frequent retinal screening for DR can aid in the optimization of laser therapy. The risk of vision loss can be decreased by a yearly retinal exam that allows for early identification, particularly in patients of type 2 diabetes. Additionally, a multidisciplinary approach to health treatment can significantly reduce visual impairment caused by DR by controlling the systematic factors that can affect the development of DR as well as how quickly it spreads.

In order to further assess DR or diabetic retinopathy for this group, Mahar et al. [43] found a frequency for type-II Diabetes mellitus or DM in the population that is indigenous in the town of Gaddap [44]. Three eye care centres with PHC facilities were established as part of this study, which was based on community data for both sexes and targeted persons over the

age of 30. Patients who need intervention were treated as such. Initially, the data was entered, then Microsoft Access and Microsoft Visual Basic 6 were used for analysis [45].

By looking for lesions in the retina, which the disease causes, ophthalmologists can predict DR. In some regions where diabetes is common and DR detection and treatment are frequently required, the proposed strategy is effective due to a lack of knowledge and resources [46]. The number of diabetics is rising, ophthalmologists are working quickly to prevent blindness, but DR infrastructure and expertise are getting worse.

Automated retinal blood vessel segmentation has garnered considerable attention during the last ten years. Unsupervised and supervised segmentation methods have been developed by Fraz et al. [47]. While unsupervised algorithms are taught while segmenting the images, supervised segmentation algorithms make advantage of the ground truth of a training set of images. Related research employ algorithms including matched filtering, vessel tracking, morphological transformations, contour models, Laplacian operators, and perceptual transformation approach in the unsupervised method [48]. The suggested study is based on supervised learning methods, and it trains the network using datasets gathered from hospitals and public databases while assigning labels like "normal," "mild," "moderate," and "severe."

The approach proposed by Marn et al. [49] does not include a network learning the features from a single expert individual. It also achieves a respectable AUC. He provided the independent training dataset and used a seven-feature set that was extracted using neighbourhood parameters and the moment invariants-based method to create neural network classifiers.

According to Soares et al. [50], the six-feature set might be extracted using Gabor wavelets and then put into practise using a GMM classifier. In this case, training data vary as well, and training GMM models with a mixture of 20 Gaussians takes longer. Fraz et al [51] 's vessel classification method employs 200 decision trees, boosting and bagging methods, and Gabor filters to extract a nine-feature set. This approach has the disadvantage of having a high computational complexity.

According to Roychowdhury et al. [52], the morphology-based method detects blood vessels and background areas while classifying a greater number of pixels than the Gaussian mixture model (GMM). The method described by Roychowdhury et al. [53], in which the blood vessels and background areas are detected by the morphology-based method, whereas more number of pixels are classified by the CNN, served as the inspiration for the proposed work

for the vessel segmentation method using CNN in tensorflow. It is suggested that the classifier's accuracy, the amount of features utilised for classification, and the number of training and test images all be increased.

Ramlugun et al. [54] used segmenting the retinal blood vessels from the digital fundus pictures as part of a systematic approach for identifying proliferative DR (PDR). The blood vessels are enhanced using 2D-Match (Gabor) filters and contrast limited adaptive histogram equalisation (CLAHE), and the vessels are segmented using a double-sided thresholding approach. High accuracy (93.1%) is achieved with this vessel extraction approach.

Franklin and Rajan [55] suggested using a feedforward network and a back propagation algorithm to adjust the effective weights in the aforementioned neural network as part of a computer-based diagnosis technique. Using a multilayer perceptron neural network with inputs derived from Gabor and moment invariants-based features, retinal blood vessels are recognised. Additionally, he saw exudates in the retinal pictures.

By utilising textural cues, Acharya et al. [56] presented automated diabetic retinopathy detection to distinguish between the various phases of DR, including normal, NPDR, PDR, and macular edoema. For the features selection, homogeneity, short- and long-run emphasis, correlation, and run percentage are computed. These features are provided as the input for the linear SVM classifier together with the radial basis function kernel and polynomial kernel of degrees 1, 2, and 3 [57]. It generates results with an accuracy of 85.2%, a sensitivity of 98.9%, and a specificity of 89.5%, respectively.

In order to categorise the DR phases, Yun et al. [58] used neural networks to determine the blood vessel area and perimeter area. The retinal pictures are preprocessed using morphological operation and histogram equalisation. The sensitivity and specificity are 90% and 100%, respectively, while the accuracy is 84% for identifying normal, moderate, severe, and proliferative [59].

A method for locating the ideal optic disc using an SVM-based optic disc localization method was proposed by Salam et al. [60]. The suggested approach offers a novel optic disc localization and segmentation technique for recognising optic disc regions from the fundus pictures. Retina exhibits many defects. It extracts the feature set for each candidate region, and the SVM classifier used these sets as input. The optic disc region is located using the Manhattan distance. Both local datasets and publically available datasets are used [61]. It demonstrates that the outcomes of the verified test are extremely ideal.

A Fuzzy Support Vector Machine (FSVM) classifier was presented by Jaya et al. [62] for the detection of hard exudates in fundus pictures. In order to avoid confusion while recognising the optic disc and exudates, false alarms were found during morphological operations. Exudates and non exudates pixels are distinguished based on colour and textural features. The FSVM classifier received these extracted features as input. 200 retinal pictures are used by this classifier in DR screening programmes. When compared to the conventional SVM classifier, it yields the best results.

Multi-Layer Perceptron Neural Network (MLPNN) classifier for the identification of DR was proposed by Bhatkar & Kharat [63]. The retinal fundus images were categorised into normal and pathological using this classifier. Based on the 64-point Discrete Cosine Transform, statistical parameters were determined (DCT). The Train N Times approach was used to train the proposed NN. The rates for normal and pathological retinal image detection during training and validation were both 100% correct [64].

By utilising basic data mining and image processing techniques, Acharya et al. suggested and demonstrated an automated method for the identification of the stages of DR [65]. Here, methods that utilised the support vector machine (SVM) or the processing of morphologically-processed pictures were applied to autonomously diagnose eye health. This has a specificity of over 86 percent, an accuracy of over 85 percent, and a sensitivity of above 82 percent. With the aid of greater features and a variety of data, performance improvement is further increased.

On the basis of the Niemeijer et al. study, Varun Saravanan and De Abhishek conducted a study for the implementation of an automated red lesion approach [66]. This technique morphologically filtered the image of the fundus to obtain the candidate's items, which were then classified using feature vector clustering's k Nearest Neighbor algorithm. A subset of the feature vectors used by Niemeijer are these ones. The representative of the data set was evaluated for the whole range of photos that were discovered in the screening set. Despite having a lower specificity or accuracy, this approach can still detect red lesions.

Rema et al. [67] conducted research on the relationship between blood lipid levels and diabetic retinopathy (DR) in Type 2 diabetes patients. Because Chennai's demographics are comparable to those of the rest of urban India, and because this allows for generalisation to the entire country of India and its urban population, the population of this study was based on a sizable population of South Indians residing in urban regions. However, the findings of this

study could not be applied generally to rural areas. This study's fundamental flaw is that it was cross-sectional; as a result, any theories about causality, as well as the association between lipid and its sub-fractions and retinopathy, require a proper investigation of follow-up. Both DR and DME have a substantial correlation with blood triglycerides and LDL cholesterol, respectively.

In addition, CSME, or clinically significant macula edoema, was found in 15 patients, or 4.1 percent of the total, and PDR, or proliferative diabetic retinopathy, was found in 18 patients, or roughly 4.6 percent of the total. NPDR, or nonproliferative diabetic retinopathy, was found in a total of 7 patients, or 1.8 percent [68]. The DR is linked to high fasting blood sugar, chronic diabetes, and high blood pressure levels. However, there was no relationship between DR and the patient's sex. The likelihood of DR in these diabetic patients is 29.2 percent, and as was already mentioned, 60.6% of them had never had a fundus exam. Due to the huge number, a stronger referral mechanism is needed to ensure early DR detection and management for this population [69].

According to Ioannidis, George, et al. [70], patients with type 2 diabetes are more likely to suffer from cardiovascular disorders, which increase their risk of morbidity and mortality [71]. Cardiovascular disorders account for more than 75% of fatalities. The relationship between RF, or risk factors, for clinical cardiovascular diseases and MA, or microalbuminuria, as well as DR, was examined. Reliable evidence for CAD, or asymptomatic coronary artery disease, was assessed using the SPECT method of RI scan with patients with DM2. The results concluded that the risk factors for MA, DR, or CAD—whether present or absent—form a part of the screening of DM2 outpatients and may also require a greater level of safety as reliable indicators of a diagnosis of asymptomatic CAD [72]. Additionally, a practitioner may be able to identify individuals who require additional diagnosis and evaluation through the use of such straightforward procedures, saving both time and money.

Niemeijer et al. reported the findings of the international microaneurysm identification and detection competition that was arranged by the ROC or the Retinopathy online challenge as a competition for the different aspects of DR detection [73]. In this study, researchers from five teams each used a different strategy to analyse the same collection of data, and the findings were compared. Utilizing a similar approach, this was done consistently. 50 separate training images with a reference standard were included in the data set used in this study, as well as

50 test images for which the organisers MN, BVG, and MDA withheld the standards. After employing standardised evaluation software to gauge performance, the test data's results were duly submitted via a website [74]. A human expert detected microaneurysms as part of the test to assure comparison with automatic techniques. The findings demonstrated that detecting microaneurysms was a very difficult task, regardless of whether the approach was automatic or human, and that there is always room for progress because even the method that performed the best could not compare to that of the human expert. The public can access all information related to the Roc microaneurysm and its detection, and the website is always accepting new submissions [75].

In order to create a computerised method for testing visual acuity for clinical research, such as the Early Treatment for Diabetic Retinopathy Study (ETDRS), Kempen John et al. [76] developed a protocol that can be tested along with the evaluation of retesting its reliability in comparison to the ETDRS standard testing. Three trial sites were organised to assess a group of 265 patients in a multicenter setting. Each patient had their visual acuity assessed twice using the SETDRS conventional ETDRS methodology and the E-ETDRS electronic visual acuity assessment algorithm. The E-ETDRS testing was properly carried out using an electronic visual acuity test (EVA) using a programmed Palm from Palm, Inc. [77], Santa Clara, California, the United States. This hand-held device was able to communicate with a personal computer that has a 17-inch monitor and a 3 metre test distance. This methodology has excellent test and retest reliability and good concordance with S-ETDRS testing. To potentially reduce testing time and technician bias, the computerised method was thought to be superior in terms of electronically gathering data for all tested letters that require only a single distance test from 20/12 to 20/800.

An automated method for segmenting the retinal vasculature in pictures was presented by Soares Joo et al. in 2006 [78]. This technique generates segmentations by classifying each image pixel as a vessel or non-vessel based on the pixel's feature vector. These vectors are made up of the pixel's intensity and the responses from the two-dimensional Morlet wavelet transform, which are taken from various frequencies and scales and allow for both noise filtering and vessel enhancement in one step [79]. Comparing them to classifiers known as linear least squared error type of classifiers, a Bayesian classifier that contains class conditional functions of probability density that are shown as Gaussian mixtures can produce a speedy classification and can model decision surfaces that are complex. On the basis of a collection of training pixels that have been manually segmented, labelled, and acquired,

probability distributions have been computed. In the DRIVE and STARE databases, which have been manually tagged with photos that aren't mydriatic, the effectiveness of various methods is assessed.

Jelinek Herbert et al. [80] developed a method that combines automated segmentation with automatic recognition of all proliferative retinopathy-related features, including median CD, wavelet moment, and other outcomes that are wavelet-derived. Additionally, a sample that is clinically significant that is still present in images that are not of the highest quality as well as those that show the scars from pan retinal laser surgery, the diverse progression of retinopathy, and finally the proliferation of all areas of ischemia as well as blood vessels that are situated close to the optic disc or in the periphery. The outcomes were attained by configuring all of the photos with similar parameters. Due to the nature of the wavelet transform, the removal of the optic disc and preprocessing is not required to enhance the segmentation of the vessel. Additionally, classifiers other than naive Bayes or the LDA can enhance the classification results. This is currently being looked into for a bigger image set [81].

Using images of the digital retina, a new approach for detecting blood vessels was presented by Marn Diego et al. in 2011 [82]. In addition to computing a 7D vector with a grey level and moment invariant features for the representation of pixels, this uses a NN technique to classify the pixels. Due to the fact that the retinal images in DRIVE and STARE databases had been expertly annotated, they were also publically appraised. Both sets performed better than the existing solutions. This method mostly works well for STARE image vessel recognition. Additionally, this performs better than various segmentation strategies, such as DRIVE and NN.

On a database of newly produced retinal vessel pictures, Niemeijer Meindert et al. [83] compared the effectiveness of various vessel segmentation techniques. This segmentation is essential for identifying various eye disorders and plays a significant part in the automatic retinal disease screening system. Although many of these techniques have been published recently, it has not yet been possible to evaluate them all in a database that is used for picture screening. A significant data set of retinal pictures has been built in order to compare the performance of these segmentation methods [84].

There are a total of 40 photos here that have had trees manually segmented. Twenty of the 40 have a second independent segmentation that is carried out by hand. This makes it possible to

compare how well the automatic approaches perform to that of a human observer. This database is easily accessible to the research community, and anyone interested in using it can upload the segmentation findings to the website at (http://www.isi.uu.nl/Research/Databases). Five different algorithms' performance has been compared. Of these, four were also put into practise. Specifically, a supervised approach is used to produce the fifth categorization of the pixel. As a performance indicator, segmentation accuracy is evaluated using the gold standard. The results show that the pixel method of categorization performs best, although the second observer still outperforms it [85].

In a study using non-mydriatic colour photography to process images of retinal blood vessels, Cornforth et al. [86] described the creation of a segmentation methodology. This employed wavelet analysis, supervised classifier probabilities, adaptive threshold techniques, and wavelet analysis. Accurate blood vessel identification has been demonstrated to examine changes in the network of vessels that can be used for detection of diameter changes in the blood vessels that are connected with pathophysiology related to diabetes. This method can perform an accurate test for DR that will provide patients with significant benefits by screening them in the earliest stages. It connects with appropriate methods of feature extraction and methods of automated classification.

After researching automatic approaches that aid in the identification of low contrast images acquired from undilated pupils, Sopharak et al. [87] offered a proposal. This segmentation process consists of two steps: coarse segmentation based on fuzzy C-Means clustering and fine segmentation based on morphological reconstruction. Four features were selected for the coarse segmentation: the intensity, the standard deviation based on intensity, the hue, and the adapted edge. The results of the detection were verified by comparing them to experienced ophthalmologists' hand-drawn ground truth. For the detection of exudates, the specificity and sensitivity are, respectively, 86% and 99% [88].

In order to segment the retinal blood vessels in digital colour fundus images, Salem Nancy et al. [89] proposed creating a new vector for each pixel in conjunction with the K nearest neighbour classifier. This proposed vector has two characteristics: scale space, which is the largest eigenvalue, and gradient magnitude, which is related to the image intensity and represents both characteristics of every vessel: piecewise linearity and parallel edges, as well as the intensity of the green channel image. The results can be compared to those of previous supervised methods using 31 set features for specificity and sensitivity, however when

processing time is taken into account, this method employs less features, which results in a reasonable reduction in processing time.

An automated method for vascular segmentation was presented by Staal Joes et al. [90] using two-dimensional colour pictures of the retina. This can be applied to automated screening for diabetic retinopathy in computer-based studies of retinal image data. This was accomplished by removing ridges from the photos that roughly matched the centerlines of the vessels. They serve as line elements in the composition of primitives. This allows for the partitioning of an image into patches, with each patch consisting of the pixels nearest to the line element. Each of these components is made up of a frame for the patch's local coordinates. A feature vector is computed for each of these pixels while accounting for both the line elements and the attributes of the patches. They are categorised based on feature selection using sequential forwards and the NN-classifier. A database of 40 photos that had been hand annotated was used to properly evaluate this method. A receiver operating in a characteristic curve with a 0.952 area under the receiver was achieved using this technique. This approach has been contrasted with two other rule-based approaches from recent publications by Hoover et al. and Jiang et al. [91] Results show that this method is much superior to the other two rule-based systems, with an accuracy of 0.944 versus 0.947 in the case of a second observer.

An automated technique for segmenting the vascular network in retinal imaging was presented by Mendonca et al. in 2006. The first phase of this method is vessel centerline extraction, which serves as a template for the subsequent phases of vessel filling. presented a technique for automatically segmenting the vascular network in retinal pictures. To make sure that the differential operators of the four directional operators' outputs are processed, it is necessary to select the sets that are related to the candidate's points for further classification as the centerline's pixels for feature extraction. This method was further evaluated on datasets that were accessible to the public, and the findings were appropriately compared with recently published approaches. These results showed that his algorithm performed better than all other methods and even came close to the accuracy of a human observer, whose specificity and sensitivity did not degrade noticeably.

In order to deal with both healthy and ill retinas simultaneously, Lam et al. [92] proposed a multiconcavity modelling approach. It has been suggested that brilliant lesions in a perceptible space be handled by the measure of differentiable concavity. For the removal of black lesions that have a structure with intensity and are distinct from the vessels in a retina

that are line shaped, the measurement of concavity that is line shaped has been recommended. Because of the strength of spherical variation in a retinal image, the measure of concavity that is normalised locally has been created to handle noise that is dispersed unevenly.

In order to detect vessels in retinal pictures, these concavity measurements have been integrated in accordance with their statistical distributions. The experiment's findings are quite positive because they consistently surpassed other state-of-the-art approaches for identifying diseased retinas and outperformed human observers in terms of accuracy, which was not possible with the other benchmark techniques. Another significant difference between this technology and others is how well it performs on both a suitable mixture of pathologically healthy retinas and healthy retinas.

A technique that automatically splits blood arteries based on multiscale feature extraction was presented by Martinez-Perez et al. in [93]. By using both the first and second spatial derivatives of the intensity picture, which obtains and transmits vessel topology information, this method is able to solve the issue of the many fluctuations in contrast that are inherent in the images. The method also makes it possible to detect blood vessels of different lengths, widths, and orientations. For the growth process of the multiple pass regions, the local minima that are available across the gradient's magnitude scale and its maximum level of principal curvature have been utilised. This is the growth that gradually separates the blood vessels using both spatial and feature-based information. Fluorescein and red-free retinal pictures from two local and two public databases are also used to test this approach. The comparison with the first public database yields a figure for the TPR (true positive rate) of 75.05% and an FPR (false positive rate) of 4.38%. The second database's values are 72.46 percent TPR and 3.45 percent FPR. The performance of the results on the open databases might be compared to that of the other writers.

As a result, we have come to the conclusion that these values are not sensitive enough to evaluate the effectiveness of the detection of vessel shape. In order to compare segmented and manually segmented images from publicly accessible databases, a novel method has been presented that uses measurements of the vessel diameters and branching angles as a validation criterion. Comparisons between the manually segmented photos and those from public databases have been done, and they have shown that there is a significant amount of geometric inter-subject variability. By comparing the geometric values of the vessel acquired from the segmented images between the fluorescein paired images and the red-free images,

the former serving as the ground truth, a final assessment has been produced. The outcomes demonstrated that the borders were less skewed and more closely followed the vessel border, allowing for more confident geometric values to be provided.

2.5. Feature extraction methodology

In addition, Priya and Aruna [94] produced a diagnosis of DR using three models: the Probabilistic Neural Network (PNN), the Bayesian Classification (BS), and the Support Vector Machine (SVM), and their results were appropriately compared. The disease that spread in retinas was recognised by the extraction of retinal features from raw images, such as haemorrhages of the NPDR images, the blood vessels, etc. These features were then given into the classifier for the purpose of classification. A total of 350 fundus pictures were used for this, of which 100 were used for training and 250 were used for testing. The trials' findings indicate that the PNN, which has a greater accuracy percentage of 89.6, the Bayes Classifier, which has a percentage of 94.4, and the SVM, which has a percentage of 97.6 all perform better. The conclusion that can be drawn from this is that the SVM model has outperformed all other models. The results have shown that the PNN has an accuracy percentage of 87.69, the Bayes Classifier has an accuracy percentage of 90.76, and the SVM has an accuracy percentage of 95.38. Additionally, this system is run with just 130 images that are easily accessible from "DIARETDB0: The database for Evaluation and Methodology for DR."

Wisaeng et al. [95] conducted a number of tests to better understand how support vector machine classifiers choose features and categorise data. The following preprocessing steps have been used to segment the retinal image data. They are colour normalisation, noise reduction, contrast improvement, and colour space selection. The sensitivity, specificity, and accuracy for data sets with low-quality picture data are 94.46%, 89.52%, and 92.14%, respectively.

In an experiment conducted by Sopharak Akara et al. [96], a set of operators that are ideally and morphologically modified for use in enabling the detection of diabetic retinopathy patients and their low contrast images of their non-dilated pupils were proposed. They are instantly recognised and properly validated by comparison to the hand-drawn ground realities created by skilled ophthalmologists. This was effective, and the detection's sensitivity and specificity were 80% and 99.5%, respectively. Based on a hybrid strategy that integrates the studies by Spencer et al. [97] and Frame et al. [98] along with two additional significant

contributions, Niemeijer Meindert et al. [99] proposed a method for detecting red lesions. One of them is a brand-new red lesion identification technique based on pixel classification. Vasculature and red lesions have been isolated from the background of the image using this technique. All things that are left over after this has been eliminated are regarded as red lesions. Second, the one that Spencer and Frame offered had a significant number of brand-new features. All of the characteristics and the k-nearest neighbour classifier were used to categorise these objects.

On a set of photos that represented every type of image that would typically be in a screening set, all of this was evaluated. Additionally, this approach obtains a 100% sensitivity and an 87% specificity when determining whether this image contains red lesions. Many automatic systems have been compared to this strategy, and it has turned out to be superior to all of them. Its performance when looking at the photographs of red lesions present is almost identical to that of a human expert. With the help of two models, such as PNN and SVM, Priya & Aruna [100] diagnosed DR and properly compared the results of the two models' outputs. PNN's accuracy was found to be 89.6% and SVM's to be 97.608% by the experiments' results. Here, it is implied that the SVM model can perform better than the PNN. According to PNN and SVM, the DR in this instance has been divided into two groups, NPDR and PDR. Although SVM has produced better results, both methods that were employed to categorise this were effective in their performance. Therefore, the success of this effort has been guaranteed in the way of diagnosing diabetic retinopathy and it also aids in early detection, both of which reduce the need for manual labour.

Lahmiri Salim and Mounir Boukadoum gave a presentation for a brand-new automated approach for spotting circulate exudates in retinal pictures [101]. The process proceeds like this: the colour image is converted to grey levels, after which CLAHE, or contrast-limited adaptive histogram equalisation, is applied before it passes via EMD, or empirical mode decomposition, to become an IMF, or intrinsic mode. The first two IMFs' uniformities and entropies are calculated to create a vector that is input into an SVM for classification purposes.

A total of 45 photos from the STARE database, including 23 normal and 22 with circular exudates, were used to analyse the experiment's findings. This approach beat all of the other efforts with its perfect categorization, according to the tenfold cross validation. Additionally, the processing of the image only took 4 minutes, making this circulate exudate detection

technology suitable for use in any clinical setting. Aquino et al. [102] also provided a template-based technique for segmenting the OD from all retinal digital pictures. The OD border and its approximate value were obtained using morphological and edge detection techniques, followed by the Circular Hough Transform. As its starting data, this requires pixels that are present inside the OD. It was also suggested to permit this technology for localization on the basis of a voting-type algorithm. All 1200 photos from the publicly accessible MESSIDOR database were properly assessed using these. The localization process took 1.67 seconds to complete with a standard deviation of 0.14 seconds and was successful in over 99% of cases. However, this technique had an 86% overlap between the OD regions that were true and both the automatic segmentations that were performed. 5.69 s was the computation time, and the standard deviation was 0.54 s. Additionally, the benefits and drawbacks of the models employed for the segmentation of OD were presented and analysed.

2.6. Optimization for DR classification

Goldbaum [103] appropriately focused on automated diagnostics. The photographs in this article were annotated by grouping them into segments according to the objects that caught their attention. The classification of the objects that were retrieved was carried out along with the logic of the contents. Here, a Bayesian network using examples from each disease was used to infer. This is an attempt to comprehend the various fundus images and also looks ahead to the future of medical imaging. Once these capabilities are developed, we may anticipate that both doctors and ophthalmologists will rely on these photos and employ systems like STARE to reduce repetitious work, assist doctors when making difficult diagnoses or managing uncharted diseases, and maintain a large library of images. In order to diagnose and cure age-related muscle degeneration, Pinz Axel et al. [104] in the Vienna Eye Clinic created a novel technique called Scotoma-based photocoagulation (SBP), which also requires retinal maps from pictures taken with a scanning ophthalmoscope. All the information required for picture analysis and map production is made in this publication. A dataset that reflects a clinical study of 50 patients is used to construct and evaluate prototype fully autonomous software. This map may be safely extracted in all situations and is required for the treatment of SBP. Therefore, there is no need for any significant adjustment to the algorithms provided in this study in order to make them relevant in any form of clinical routine.

Another idea for an automated method for AMD diagnosis was put up by Mookiah Muthu Rama Krishnan et al., who used the DWT or Discrete Wavelet Transform as well as techniques for feature ranking. The four order moments in statistics, or the mean, variance, skewness, and kurtosis, regarded as moments of energy, entropy, and the features based on the Gini index that have been retrieved from the coefficients of DWT. There have been applied five tests. These include the Wilcoxon, ROC (Receiver Operating Characteristics Curve), CBBD (Chernoff Bound and Bhattacharyya Distance), KLD (Kullback-Lieber Divergence), and t test.

Another group of supervised classifiers, including the SVM (Support Vector Machine), DT (Decision Tree), NB (Naive Bayes), k-NN (kNearest Neighbor), and PNN (Probabilistic Neural Network), were used to evaluate the measure of highest performance by classifying AMD into normal and dry classes while using the fewest features possible. This system, which employs KLD ranking and SVM classifiers, has an average accuracy of a sensitivity of 93.70%, a sensitivity of 91.11%, and lastly a sensitivity of 96.30%. Another AMDRI, or AMD Risk Index, was created that uses predetermined parameters to categorise normal and dry class AMD using just one score. Both clinical aid and large-scale AMD screening programmes could benefit from the use of this technology.

Acharyau Rajendra et al. [105] have described a technique that might be utilised for automatic mass screens for DR. The classification for this has been broken down into four groups: normal retina, nonproliferative diabetic retinopathy, proliferative diabetic retinopathy, and macular edoema (ME). For the purposes of this investigation, 238 retinal fundus pictures were used. From the photographs of the digital fundus, five characteristics were retrieved, including run percentage, long run emphasis, short run emphasis, correlation, and homogeneity. All of them have been input into an SVM classifier, or support vector machine, to enable automatic categorization. This classifier has several different kernel functions, such as analysed linear, radial basis function, and polynomials of one, two, or three orders. ROC curves, also known as receiver operation characteristics curves, were plotted in order to select the best classifier. This system was capable of identifying unknown classes with a high level of accuracy percentage of 85.2 and sensitivity, specificity, and AUC or area under curve of 98.9%, 89.5%, and 0.972, respectively, by using an SVM classifier with a polynomial kernel of order 3. Another recent integrated DR index, or IDRI, employs a number of criteria to undertake a 100 percent accurate identification of diverse classes.

In order to assess the system's potential for using digital retinal images in colour to test for diabetic retinopathy, Usher Dumskyj et al. [106] further enhanced it. Another approach was used, one that involved segmentation to expose any potential lesions and classification of the lesions using a neural network, as well as pre-processing to standardise colour and improve contrast. This was a mechanism that may be applied during DR screening. The necessity for human grader examination can be reduced to half of what it was at the original sensitivity value of 94.8%. By Wang Huan et al., [107] one of the aberrant indicators was highlighted (2000). In the retinal scans, there were lesions or exudates present. A novel strategy that combined a brightness adjustment process with a statistical classification method, a window-based verification strategy, and a method of classification was developed. The findings of this experiment showed that while keeping a 70% accuracy rate in correctly classifying normal retinal images as normal, it was possible to identify retinal images coupled with exudates with 100% accuracy. On the basis of the quantity of retinal images, this results in enormous savings and can be manually examined by experts once.

Giancardo Luca et al. [108] presented a brand-new, exudate-based automatic approach for identifying DME using non-stereo fundus pictures. In order to distinguish between false positives and true positives in a space of colour analysis with new methods that characterise lesions with wavelet analysis, this was based on an algorithm that was able to detect exudates and also attach some level of confidence without using Deep Learning techniques. As far as we are aware, this method of producing feature vectors with both inner and outer lesion maps has never been tried before, and it has now succeeded. With certainty, it can be assumed that this method can be used to solve issues in all fields where diagnosis or occasionally other classifications can be carried out based on ambiguous lesions and their segmentation. This approach has been shown to be effective when combined with various parts of lesion identification and retina processing, and it can be pursued in the future in an effort to develop a diabetic retinopathy screening that is competitive and can transparently diagnose the disease's condition.

John Forrester developed an automated approach for digital image processing in 1997 that made it possible to measure the size of micro aneurysms in fluorescein angiograms. The automated approach involved registering the same eye's retinal pictures for subsequent studies. A database with 394 authentic microaneurysms that have been recognised by ophthalmologists and around 68 photos of diabetes patients served as the training data for the

microaneurysm detector. With a 2.0 false positive per image, this microaneurysm detector has attained a sensitivity of 82% [108].

The micro aneurysm detector was compared to physicians using a test set that included 20 photos with 297 real micro aneurysms. This test set was independent and contained independent images. Additionally, this yielded 5.7 false positives for every image and an 82% sensitivity on the clinician receiver-operator characteristic curve, which resulted in 3.2 false positives for every image. As it was dependable, objective, fully automated, and quick, it could be relied upon to find micro aneurysms.

Hijazi et al. [109] proposed comparing data mining strategies to facilitate automated screening by AMD. The first one utilised a CBR, or case-based reasoning, classification technique to an image using spatial histograms to maintain picture colour and spatial information for image representation. The second one is based on a hierarchy-based decomposition of the specific image that is used to create a representation of a tree. In order to find the sub trees spread throughout the data set, a weighted sub-graph mining technique was used. The detected sub trees are eventually encoded as vectors so that normal classification methods can be used on them.

The retinal network, the macula, and the optic disc are all anatomical components that are significant in imaging of colour retina, according to a generic technique described by Gagnon Langis et al. in 2001. This process has been rigorously evaluated on a database of 40 colour fundus images obtained from a low-resolution, non-mydriatic camera. The test's findings demonstrate that this particular one was reliable in terms of visual quality and independent due to the acquisition being disk-centered and using macular optics. The success rate for detecting the optic disc is 100% and the success rate for detecting the macula is 95%. The focus of current work is on developing a quantitative measurement methodology to determine how well vascular networks can be extracted. The upcoming paper thoroughly examines a variety of photographs obtained from different digital cameras. In order to keep the performance of detection at the current level, these algorithms must be modified. Last but not least, this approach serves as a pre-processing stage for the lesion creation of algorithms for detection that are related to DR and other retinal illnesses.

Another approach was proposed by Walter Thomas et al. [110], and it detects exudates, which are a key indicator of macular edoema and enable highly sensitive identification. Exudates are located inside the macular region. As a result, finding these exudates is a crucial

diagnostic task for which computer aid may be needed. They can be discovered in various high-gray levels, and morphological reconstruction techniques are used to determine their contours. This method requires the detection of the optic disc. Morphological filtering and watershed transformation techniques are used to achieve this. This algorithm's performance was evaluated against that of a human grader using a limited database. Here, a mean predictive value of 92.4% and a mean sensitivity of 92.8% have been attained. Additionally, the robustness based on parameter modifications has been assessed. Fevereiro-Martins, Mariza and Marques-Neves, Carlos and Guimarand Bicho, Manuel et al.[168]. This review discusses recent advancements in the understanding of ROP pathophysiology, emphasizing the role of vascular endothelial growth factor (VEGF) and other molecular pathways. It covers updates in screening protocols and the use of imaging technologies for early detection. The review also evaluates current treatment modalities, including laser therapy and anti-VEGF agents, highlighting emerging evidence on their efficacy and safety profiles. Long-term outcomes of ROP interventions and future directions for research and clinical practice are also explored. Chen X, Wang Y, et al.[169]. A comprehensive update on screening guidelines for ROP, focusing on recent revisions aimed at improving early detection and timely intervention. It reviews the latest evidence on risk factors associated with severe ROP and the implementation of telemedicine and artificial intelligence in screening programs. The review discusses the evolving role of anti-VEGF therapies in ROP management, comparing their efficacy and safety with conventional laser treatment. Practical recommendations for optimizing outcomes in different healthcare settings, including resource-limited environments, are also addressed. Tsai, Andrew SH and Acaba-Berrocal, Luis and Sobhy, Myrna and Cole, Emily and Ostmo, Susan and Jonas, Karyn and Campbell, J Peter and Chiang, Michael F and Chan, RV Paul, et al[170]. longitudinal data on neurodevelopmental outcomes in children treated for ROP, focusing on the impact of early visual deficits and treatment-related factors on cognitive and motor development. It synthesizes findings from cohort studies and meta-analyses to assess the prevalence of neurodevelopmental impairments among ROP survivors. The review discusses the importance of interdisciplinary care models in managing ROP to optimize both visual and neurocognitive outcomes.

2.7. Feature extraction

Using colour fundus images, the feature extraction method is utilised to extract the blood vessel in order to detect diabetic retinopathy. This fundus image is nothing more than an RGB image, which combines red, blue, and green. By assigning each colour to a different channel and using only one channel, features can be retrieved from an image. Due of the blue channel's low contrast and limited information content. The retinal image that serves as the input is first pre-processed. The image is initially scaled during pre-processing, and the red and blue channels are separated. The image is then subjected to morphological operations like dilation and erosion. Dilation is the process by which an object in the image thickens. The thickness is shaped and controlled by the structuring element. The reaction opposite to erosion is the dilation effect. The process of erosion involves the shrinking or thinning of an object's image.

A method known as adaptive histogram equalisation, which is distinct from traditional histogram technique and a digital image processing method, is used to enhance the contrast in the image. This method divides the image into several segments, and local contrast is computed to highlight the limits or edges in each segment. The noise contained in each segment of the image can be amplified via adaptive histogram equalisation. A cutting-edge method known as contrast constrained adaptive histogram equalisation is employed to get around this flaw.

In the traditional histogram equalisation method, all pixels are transformed using the same transformation determined from the image histogram. However, it can only be effective in images where every pixel is spread equally across the entire image. Because certain areas of the image with unevenly dispersed pixels remain black and others remain lighter, the image cannot be improved.

The transformation function used by adaptive histogram equalisation is derived from the neighbouring region rather than using the same transformation for the entire image. It is initially employed for cockpit displays in aircraft. In its most basic version, each pixel is altered based on the square-shaped histogram of its neighbours. The cumulative distribution function of nearby pixels determines the transformation function. Because they are needed to distinguish the image from other images, the pixels around the edge of the image should be focused more.

The noise in the image needs to be removed in order to prevent false edge detection, so the appropriate filter is applied. To eliminate noise, a Gaussian filter is typically utilised. The image is smoothed and the noise that hinders edge identification is removed with the Gaussian filter. The performance of the Gaussian filter depends on the kernel size, thus it is important to choose it correctly. As the kernel size grows, the detector's sensitivity will decrease. Additionally, errors in recognising the edge of the image happen when the kernel size is increased. The most typical kernel size is 55, though this can change depending on the situation.

The horizontal, vertical, and diagonal filters can be used to discern the direction of an image in the Canny algorithm. First derivatives in the horizontal and vertical directions are used by edge detectors like Roberts, Prewitt, and Sobel to determine gradients and the gradient's direction. The edge's angle direction roughly corresponds to one of four angles, including 0°, 45°, 90°, and 135°. For instance, the angle will be set to 0° if it is between 0° and 22.5° and 157.5° and 180°. This approach is effective because it can detect the edge with great accuracy and reliability.

2.8. Receiver operating characteristic

A graph that shows the performance of various classifiers is called a receiver operating characteristic. A graph showing the hit rates and false rates of classifiers is known as the receiver operating characteristics. It is employed to evaluate the functionality and properties of various classifier types. Receiver operational characteristics are crucial in the medical field for diagnosing images for testing. The receiver operating characteristics graph is initially used in Deep Learning to assess and contrast different methods. In the sphere of research and other emerging industries, this kind of characteristic curve has grown in importance. Although receiver operating characteristic graphs are fundamentally quite straightforward, they become complex when employed in the context of research. Additionally, they have a lot of problems when they are really put into practise.

While some models produce a discrete output to forecast the class of an instance, few classifiers produce continuous output to which different thresholds must be applied. The labels generated by the classifier can be used to distinguish between the actual class and the anticipated class. Four possible outputs are available for a given classifier. True positive, true negative, false positive, and false negative are the four types. True positive is the state in which the actual output is positive and is categorised as such by the classifier. False negatives

are when the real output is positive but the classifier classifies it as negative. False positives occur when the real output is negative but the classifier classifies them as positive. True negative output is when the actual result is negative and the classifier classifies it as such. There is already a set of training sequences allocated to the classifier and the classifier analyses the test and training sequences to produce the output when the input is used as a test set. Another matrix form has the numbers at the major diagonal representing the right choices and the numbers outside of this main diagonal representing the wrong choices. A classifier's hit rate or recall is another name for the true positive rate.

True positive is the state in which the actual output is positive and is categorised as such by the classifier. The percentage of positives that were actually recognised as positives is known as the true positive rate or recall. For instance, the normal eye is easily distinguished since it is free of flaws. Sensitivity prevents false negatives. In other words, sensitivity is the capacity to accurately identify patients who exhibit disease-related symptoms. The ratio of those who are expected to be illness positives to those who really have the condition is known as the sensitivity in disease identification.

High sensitivity negative test results support the diagnosis of the illness. All individuals with disease are appropriately recognised with the disease's symptoms when a test's sensitivity is 100%. As a result, the test's results can be used to forecast the existence of disease. Similar to the negative test result, a positive result is not very helpful in confirming the illness. False positives are not included in sensitivity. False positive results indicate that there is a disease present in healthy individuals, which is untrue. Therefore, the 100% sensitivity positive result is useless for diagnosing the condition.

Sensitivity and precision are not the same. The ratio of real positives to both true positives and false positives that are comparable to the actual positive is known as precision. Indeterminate samples are not considered when determining sensitivity. Either the samples are not included in the analysis or they are regarded as false negatives.

True negative is when the actual output is negative and the classifier classifies it as such. True negative rate refers to the percentage of negatives that are correctly classified as such. For instance, the eye with no defects is mistakenly classified as normal. Specificity prevents false positives. In other words, specificity can be characterised as the capacity to identify the healthy patient in the absence of any disease-related symptoms. It is the ratio of healthy, disease-free individuals to tests that came back negative. The presence of the disease can be

confirmed by a positive test result with excellent sensitivity. When a test result is 100% specific, it signifies that both healthy and diseased individuals are correctly recognised based on the presence of the appropriate disease. Since the test only yields negative results, a negative result cannot be used to diagnose the condition. Consequently, there is a potential to accurately identify sickness in otherwise healthy persons. As a result, the specificity is 100% accurate and excludes false negatives. As a result, it is impossible to include negative results completely, and the existence of disease cannot be accurately detected using this method. Figure 2.4, shows the confusion matrix for the characteristics.

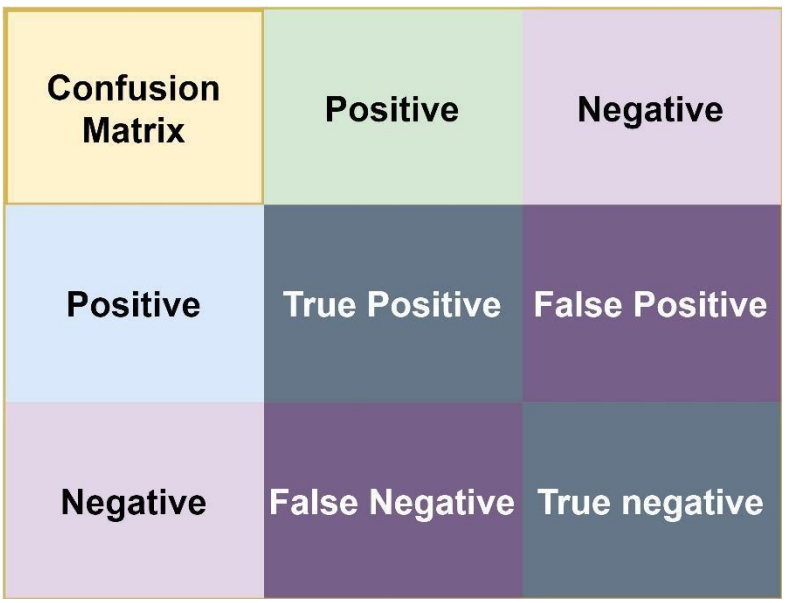

Fig. 2.4. Confusion matrix for characteristic analysis

CHAPTER 3

AUTOMATIC GRADING OF RETINAL BLOOD VESSEL TORTUOSITY USING MODIFIED CNN

3.1. Introduction

The Wisconsin Epidemiologic Studies on Diabetic Retinopathy (WESDR) conducted by Fong et al. [111] discovered that diabetic retinopathy is a substantial cause of visual impairment and loss in persons aged 20 to 74 years. The severity of this condition progresses from small anomalies, which are characterized by increased vascular resistance, to medium and severe non proliferative diabetic retinopathy (NPDR), which is characterized by channel closure, to proliferative diabetic retinopathy (PDR), which is characterized by the creation of new blood vessels in the retina. Although the disease is not fatal enough to damage vision in its early stages, delayed or inadequate diagnosis permits it to develop into a fatal condition that may also be accompanied by conditions like glaucoma. As a result, computerized evaluation of diabetic retinopathy has become a crucial topic of research in this field. In the discipline of medical image analysis, photographs of the human body or a portion of it are digitally processed for research or clinical objectives, such as diagnosis, learning more about, or looking into disorders. According to ArnulfOppelt [71], significant advancements have been made in imaging systems for use in medical diagnostics during the past few decades, and fresh methods like magnetic resonance tomography have also been created. This has opened up new possibilities for early identification, particularly, but not only, of illnesses affecting the brain, such as strokes, spine injuries, and aberrant tissues in the human body as a whole. Huge advancements have been made in traditional methods like X-rays as a result of the interdisciplinary nature of the field of medical image processing [94], which has attracted talent from applied mathematics, engineering, computer science, physics, statistics, biology, and medicine. Medical image processing and analysis typically involve a number of steps or stages. (1) Picture formation/reconstruction is one of these steps, which begins with the image acquisition procedure. (2) Image improvement 3. Storage and image compression. (4) Analyzing images The processed image is visualised in step five.

The development of automated diagnostic tools for diseases including diabetic retinopathy, age-related macular degeneration, and retinopathy of prematurity has advanced significantly

in recent years in image processing technology pertinent to ophthalmology [74]. To extract the desired information or make the necessary diagnosis, retinal images are processed in studies on retinal image processing in a manner similar to how images are processed generally. These processes are staged as follows:

A. Images of the patients' retinas are acquired or obtained at this stage from sources like image databases.Then, these photos are pre-processed using techniques like enhancement and smoothing. The success of the next steps is greatly influenced by the camera setup in addition to the quality of the captured photographs and the results of the pre-processing. Due to issues like defocus, medial opacities, or the presence of artefact, the quality of retinal pictures has been cited as one of the challenges in successfully collecting images of the ocular fundus [112].

B. The second stage, segmentation, entails the division of the regions of interest, in this case the segments of the retinal vasculature (the arteries and veins of the retina) or aberrant abnormalities, such as lesions. There are various segmentation methods for various tasks. The result of this stage is often a binary image or measurement mask with the background represented by black and the locations of interest marked in white. At this point, morphological surgeries like opening, shutting, dilation, or eroding might be employed for additional enhancement or correction.

C. Measurement, assessment, and visualisation are all possible at this stage, along with simple or sophisticated interpretation of the data produced by these measurements and/or picture visualisation.

According to the Oxford Dictionary, "tortuous" means "full of turns and twists." Although it has been investigated and measured in a variety of areas, tortuosity observation is not simply limited to blood vessels. For instance, it has been used to describe rivers, animal routes, materials, tubes, etc. However, the term "tortuous" has historically been used to describe blood vessels and, in some circumstances, nerves in the medical industry. According to [86], blood vessels generally consist of arteries, arterioles, capillaries, venules, and veins. These blood veins transport all of the blood in the human body. The arteries, which carry blood out from the heart and support the highest blood pressures, are strong, flexible, and resilient. Since the arteries are elastic, they naturally narrow (recoil) to support blood pressure maintenance. Both arteries and arterioles have muscular walls that can change in diameter to

enhance or reduce blood flow to a specific area of the body. Arteries typically branch into these smaller channels, known as arterioles.

According to Mary Bird's definition of capillaries [96], these tiny, hair-like veins have one-cell-thick coatings. They serve as a connection between arteries and veins because they are only one cell thick. They are made up of fluid that can flow into the tissues and meet the needs of the individual cells with nutrition, oxygen, and other substances.

As the amount of fluid in the veins rises, they might widen (dilate), carrying blood back to the heart. In order to prevent blood from flowing backward, some veins include valves. The backflow of blood from leaking valves may cause the veins to expand, lengthen, and become tortuous [86]. The researcher suggests that "abnormal tortuosity" might serve as a more appropriate descriptor of the aberrant structural changes in blood vessels given all these structural characteristics. In the body, abnormally twisted blood vessels can develop in a variety of locations. Some of these twisted blood vessels may be a sign of a disease, particularly in organs like the retina, brain, or abdomen.

The organ that produces sight in humans is the eye, which enables them to view and comprehend more of their surroundings than they typically do with any of their other senses. A face hammock supports the eyes, which are situated in the front half of the orbits and surrounded by fat and connective tissues. On either side of the nose, they rest in these two bony spaces known as the orbits. The macula, which is the retina's most sensitive region and is distinguished by its abundance of cons, or bulbous particles, is one of the light-sensitive components that translates electromagnetic waves into nerve impulses. At the edges of the macula, retinal blood veins typically come to a stop [58]. In Chapter 2, retinal blood vessels are covered in great detail. The fovea, which is another crucial component of the retina, is situated in the centre of the macula, has the densest concentration of cones, and is in charge of producing brilliant reflexes and sharp vision.

Going through the process of vision is a powerful method to gain a thorough understanding of the components that make up the eye and their capabilities. The way that vision occurs in the eye is comparable to how a digital camera operates. The cornea, the transparent dome that makes up the front of the eye, is where the reflected light waves from objects like trees first enter the eye. Then, after passing through the pupil, which is the circular opening in the centre of the coloured iris, the light exits the eye. The pupil adapts by shrinking and expanding in response to changes in the amount of light passing through it.

According to Gray's anatomy [41], arteries are generally cylindrical tubular tubes that carry blood from the heart to every area of the body. They must therefore manage a high blood pressure flow. They have strong, flexible muscle walls with lots of smooth muscles, as well as a relatively tiny lumen—the cylinder-shaped opening through which blood flows.

The central retinal artery and the retinal arterioles make up the retinal arterial system. The ophthalmic artery, a branch of the carotid artery that supplies the retina with its primary blood supply, feeds the central retinal artery. The entry point into the optic nerve, which is thought to be 1 cm behind the globe, is an end artery without any anastomoses. Due to ischemia, central artery obstruction may result in permanent harm, such as vision loss. The major retinal artery gives birth to the retinal arterioles, which have smooth muscle within their walls but vary from arteries in that they have a discontinuous internal elastic lamina.

The veins cope with low blood pressure because they are the blood channels that carry deoxygenated blood back to the heart from capillaries in various places of the body [41]. In terms of structure, veins resemble arteries quite closely, however veins have larger lumens than arteries and relatively thin muscular walls, which translates to less smooth muscle or less elastic fibres. In addition, veins feature valves to stop the backflow of deoxygenated blood, which enables veins to handle low blood pressure flow well.

The term "tortuous" has been used to describe blood vessels in general but has been shown to be inaccurate, particularly when referring to blood vessels found in organs like the retina. This is due to the blood vessels' dispersed semi-spherical shape and their preexisting small curvature and twist. Normal retinal blood vessels are either straight or slightly curved, but in severe illnesses, they enlarge and begin to take strange turns. According to William E. Hart et al. [48], this dilation is brought on by radial blood vessel stretching, and the serpentine route is brought on by longitudinal blood vessel stretching.

Any type of non-inflammatory injury to the retina of the eye is referred to as retinopathy. The condition known as hypertensive retinopathy, which affects the retina, is brought on by alterations in the small blood vessels in the eyes brought on by hypertension. Similar to other parts of the body, larger arteries produce cholesterol, which causes arteriosclerosis in the eye, which causes minor infarcts and superficial bleeding on the retina. Until the overall cholesterol is controlled, the alterations caused by arteriosclerosis will persist. However, once the underlying cause of hypertension is cured, hypertensive retinopathy will improve.

The fundus oculi can be examined for signs of hypertensive retinopathy, including generalised and localised arteriolar narrowing, increased light reflex, arteriovenous crossing phenomena, arterial attenuation (decrement in the arterial attenuation), and more severe signs like exudates, haemorrhages, and papilledema. These symptoms have been used for a long time to predict the prognosis and phases of systemic arterial hypertension [53, 54].

It is evident that one of the initial symptoms that can be identified is tortuosity. People with hypertensive retinopathy typically don't have any symptoms.

The most prevalent form of diabetes-related eye illness and the main factor in adult blindness is diabetic retinopathy. It is brought on by modifications to the retina's blood vessels. On the surface of the retina, blood vessels may enlarge and leak fluid or strange new blood vessels may develop. Diabetic retinopathy is a disease that worsens over time and finally results in vision loss; initially, alterations may not be noticeable. A common complaint is intermittent blurriness of vision, which is brought on by edoema or swelling of the lens as a result of fluctuations in blood sugar levels.

Diabetic retinopathy has four stages or varieties:

1) Mild Nonproliferative Retinopathy: This is the first form of diabetic retinopathy, when the tiny blood vessels in the retina develop a little, balloon-like enlargement.

2) Moderate Nonproliferative Retinopathy: Blood vessels in some areas are occluded at this stage.

3) Severe Nonproliferative Retinopathy: At this stage, additional blood vessels are blocked, and the retina starts to develop new blood vessels in an effort to hydrate areas that are starved for oxygen and nutrients.

4) Proliferative Retinopathy: This is an advanced stage of the disease, in which the retina develops new, aberrant, and fragile blood vessels. These abnormal blood vessels do not directly cause blindness, but they can cause blindness if they leak because of weakness.

Convolutional neural networks (CNNs) were developed by Rawat, Wang et. al. to decide the issue with mechanized evaluating in diabetic retinopathy. As image segmentation and classification [2] are becoming extremely popular, legitimate evaluation of retinal pictures in diabetic retinopathy conditions presents a critical test to clinical professionals; as a

result, accurate evaluating with diabetic retinopathy is subject to error. The intrinsic capability of CNNs for classifying Retinal Fundus Images in individuals suffering from diabetic retinopathy is presented as a solution to this issue.

Macular edeoma, which is defined as swelling in the retina as a result of vascular leakage, can develop at any stage of retinopathy. Puberty, pregnancy, hypertension, blood sugar regulation, and cataract surgery can all hasten this process. Diabetic retinopathy progresses in four stages:

1) Elongation and dilatation of the major arteries, veins, with their branches are frequently linked to hypertension & other cardio-vascular symptoms in mild non-proliferative retinopathy.

2) Moderate non-proliferative retinopathy is defined by clinical indicators such as micro-aneurysms and other symptoms. Blood vessels stop being able to transport blood. Both circumstances result in distinct alterations in the retina's entry and may give rise to DME.

3) Jamming of the vessels, which in turn promotes to creation of fresh blood vessels in the retina, characterizes the stage of severe non-proliferative retinopathy.

4) Diabetic retinopathy with proliferation (PDR) - Tissue can contract at this stage, and early detection of DR may forestall many serious health issues, including blindness. The inspection of the fundus, often referred as the rear of the eye, which is the first step in the operation, is done utilizing a sophisticated microscope and cutting-edge fundus cameras. According to Rawat, Wang, and colleagues, retinal impartiality can cause irreversible visual loss. 2. One of the main factors contributing to poor eye health is diabetes. This is a dangerous disease that hurts the natural eye as well as triggers heart attacks. Diabetes retinopathy (DR) by Rawat, Wang, Klein R, et al. in wealthy nations [2, 3]. The only way of preventing this illness is by early diagnosis. Raising the vessel's thickness is the first indication of this, and Sasongko et al. refer to twisted vessels as having tortuosity [4].

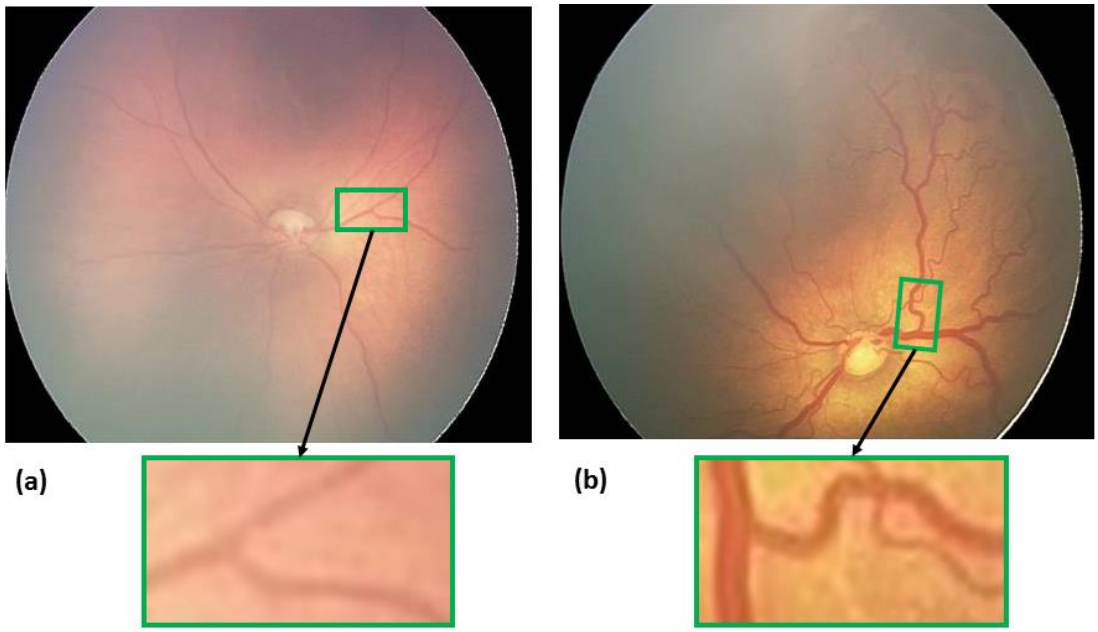

Fig. 3.1. Different touristy level of fundus image (a) low touristy image (b) high touristy image

The fundus pictures of the retinas with low and high tortuositiesare shown in Fig. 3.1. The hybrid & bifurcation hubs are then discernible from the skeletonized vein tree, according to Mizutani et al. [5]. Understanding what hybrid & bifurcation intersections signify is crucial for differentiating the hubs. Hybrid is defined as a condition of intersection through one side into the next, which causes the vessel to be covered by many vessels. A strategy based on "Chord and Arc Length," which was popularized through Heneghan, Benitez-Aguirre et al. [7, 8, 13], was proposed by Lotmar at al. [6]. Bullitt&Grisan et al. [9, 10, 14] come with some rectification, the vessels being collected with such a weighted summation maintaining the same convexity, however this is owing to difficulties in determining proper curvature. Hart et al. [11] pioneered the Curvature-based method. The computational cost of this method is substantial despite how well-organized it is. The size of the vessel is another factor to consider when determining tortuosity. Later, this method's expansion is used to Goh at al. [12, 15, 16]. Kauppet&Ghadiri at al. additionally introduce signal processing methodologies. Same calculations were made in [17, 18]. In addition to this, there are other other techniques to calculate according to Trucco, Eze, Kalitzeos, and others. [20, 21, 22, 23]

Support Vector Machines (SVM) has been employed in the field of arrangement in a significant amount of prior research. Acharya and others [3, 19] 1 has presented a novel way for extracting data utilizing a higher order spectra methodology, & these features are

directly fed into an SVM classifier to construct a hyperplane that captures the diversity in shapes & contours in the input images. Another significant obstacle in this field is indeed the deficiency of a substantial dataset that really is pitifully biased; as a result, the neural network is prone to overfitting mistakes. For instance, just 3 percent of the dataset used for this study falls under the of severe or extensive DR, hence the work suggests improvements that should be made to the succeeding parts in accordance.

The Tetralogy of Fallot (TOF) diagnosis but use a primarily improved stochastic pooling convolutional cerebrum association (SOSPCNN) technique, an inherent inconsistency that impacts the movement of blood through the heart, is one application where neural networks have been approved [28, 34], recognition of malignant tumors in breast mammography using the BDR-CNN-GCN framework [35], generation a high-resolution synthetic fundus pictures for overcoming diseases associated to eye problems using an algorithm based on the principle that least action [31, 33]. The following are the primary contributions: (a) A method for automatically rating fundus photos is described. The approach uses a neural network to do away with the necessity for human tortuosity measurement. (b) To grade the health condition, a revised CNN-based neural net linked with a transfer learning approach is proposed.

In this chapter, an automated approach for calculating vascular tortuosity grading utilizing CNN is suggested, and the correctness of it is tested using accessible datasets.

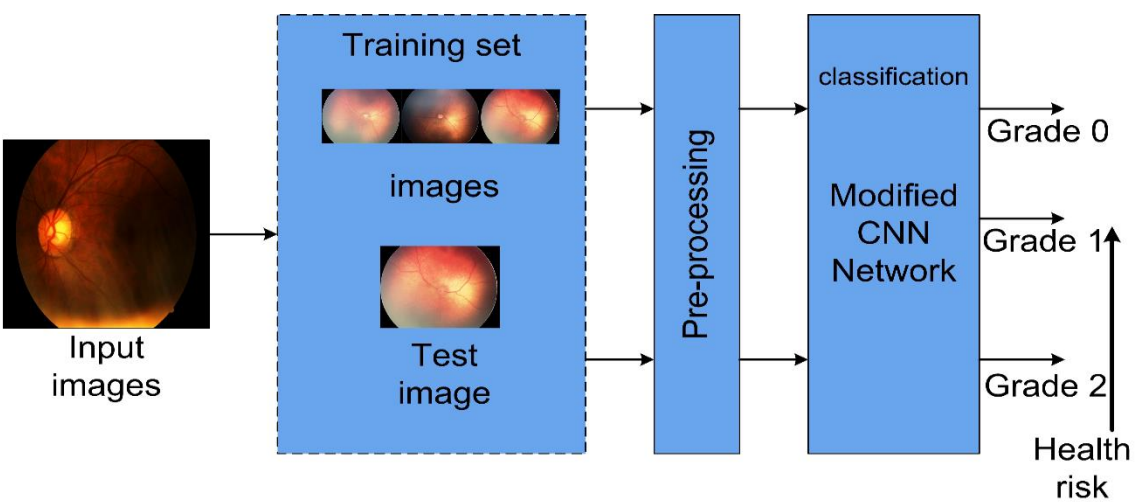

Fig. 3.2. Block diagram of proposed classification framework

3.2. Material and method

3.2.1. Framework

The suggested approach (Fig. 3.2) starts with a classification using the CNN network. The CNN architecture was used for categorization since it delivers superior prediction when only a few training examples are available.

3.2.2. Proposed methodology

In this work, we present a method for evaluating retinal fundus images using convolutional neural networks (CNNs). We utilize two powerful pre-trained CNNs, VGG16 and ResNet50, to initially assess the retinal fundus images. Additionally, we design and train a custom CNN inspired by Szegedy et al. [24]. The training of our CNN is conducted using the online vision loss dataset from Kaggle, and we further validate it with our own dataset, EIARG2, developed by Masoud Aghamohamadian Sharbaf et al. [14]. Figure 3.2 provides a diagrammatic representation of the process.

Given that most of these images contain environmental noise, directly feeding them into the CNN would yield inaccurate results. Therefore, we apply various image pre-processing techniques to modify the images appropriately. We use a range of filtering methods, including Gaussian filters, to correct color imbalance and lighting issues. Subsequently, we employ augmentation techniques to ensure a balanced number of images in each class. These techniques involve cropping randomly selected image elements, mirroring images between 1 and 180 degrees, and rotating them between 0 and 15 degrees. The images are resized to fit the specific CNN architecture before being input for further feature extraction and classification.

3.2.3. Pre-processing

During education, the raw fundus photos are pre-processed with multiple modifications since some pictures are so very dark & different color illumination can be misleading. Similar behaviorshould be anticipated for pre-processing settings, such as zooming in on raw photos to spot any anomalies and using the gray-scale conversion method.

3.2.4. Data augmentation

The first collection is based on 88,702 fundus photos from Kaggle, each measuring [4752 ×3168]. The artery data is augmented by arbitrarily cutting both height & distance, randomly

duplicating photos with a range of one to 180 degrees, and arbitrarily altering the picture ratio of current artery images between 0 & 15%. Following augmentation, artery images are resizedto 512× 512 pixels, and the number of images is increased (1064424). As a last consideration for learning and grading, consider the CNN model.

3.2.5. CNN has several layers

The Convolution Layer must go through several filters. The most basic layer of a CNN is composed of convolution layers. The core concept is to add the central pixel of something like the individual pixels to the input image. The filters, referred to as kernels, go over the entire image and carry out a sequence of operations by adding the dot products. Convolutional layers are applied to the image progressively, enabling the network to recognize patterns and categorize them. The output (let's say, G) that results from applying a kernel (let's say, h) to an image (let's say, f) is known as the feature space (G). Kernels are then passed on the extracted features several times to make the pictures comprehensible to the network. Convolution can be mathematically written as follows:

$$G[m,n] = \sum_{j=0}^{j} \sum_{k=0}^{k} h[j,k] f[m-j, n-k] \quad (1)$$

A. Activation layer

The activation layer also adds nonlinearity to the image, improving the network's learning process. Numerous well-liked activation mechanisms exist, including Sigmoid, tanh, and others. It should be highlighted, nonetheless, that the ReLU activation function is most appropriate for the procedure. The non-linearity of ReLU allows for faster convergence and is analogous to how neurons function in the brain. A definition of the ReLU is:

$$ReLU(x) = \{x \quad x \geq 00 \quad x \leq 0 \quad (2)$$

B. Pooling layer

CNN's extracted features have several limitations in that they capture very accurate positions of the source images and thus slight changes in the source images result in an entirely new feature map. This problem is overcome by down - sampling, which means giving the organization less boundaries to comprehend its image. A method known as POOLING might be used to achieve down-sampling. By applying a filter to the extracted features during pooling, output is produced as new element maps have fewer parameters. The two most typical forms of pooling are:

- Average Pooling, where the approximate amount of every area of the feature map is transmitted.
- Max taking the maximum from each patch during pooling.

However, it should be mentioned that now the Pooling is most suitable for the procedure.

C. Completely joined layer

The aggregated data regarding the local data of the various feature maps is stored inside the Fully Connected (FC) layer. This layer is utilized for categorization after the network has been trained. This layer's node count is the same as the problem's class count.

Let,

$$x \in R^N \; and \; y_i \in R \; is \; output \; of \; the \; ith \; node \; of \; the \; FC \; layer \; then$$

$$y_i = \sigma(\sum x_i w_i) \tag{3}$$

where, σ is an input layer (typically Sigmoid) and wire represents the network's learnable parameters.

D. Layer of batch normalization

To accelerate profound brain network mixing and preparing, cluster standardization layers are utilized. This is accomplished by first obtaining the batching statistics (mean & variance), then normalizing the layer input then scaling & shifting to generate the output data.

E. Dropout layer

The Dropout Layer is purposefully added to allow the network to learn from the training data less, improving performance on the test data. The concept is straightforward and entails arbitrarily disregarding some neurons from the previous layer. Dropout stops overfitting, which is the occurrence when a network learns training data so effectively that it performs poorly on test data.

An existing overview of Convolutional Networks [25,26,27] is offered, which includes a thorough presentation of these layers as well as other features.

F. Loss functions

Loss functions provide one quantitative assessment of how poorly the model performs for given output & input in the setting of back propagation. Additionally, it chooses which

gradients should be back propagated from the top layer and adjusts the weights in accordance. There are various kinds of loss functions, and in this review, loss entropy harm of those.

G. Loss of cross entropy

The categorical cross - entropy loss calculates a measure of how poorly in view of the projected possibility that just a specific class will be represented by the model effectively, the image belongs to a specific class. This cost quickly rises to high values for predictions with smaller odds of being accurate, severely penalizing the model. A good model should have no loss. The joy of the category cross entropy:

$$= \sum_{C=1}^{N} y_{o,c} \log p_{o,c} \quad (4)$$

Where N denotes the overall number of classes and yo,c denotes a binary indicator of whether the anticipated labeling c of class o is accurate. Additionally, the anticipated probability for observations of class c is po,c. The loss function is known as binary cross entropy loss if the problem's N dimension is 2.

H. Focal loss

Data imbalance can be resolved in several methods; however, this solution proposes a novel loss function. The Focus Loss 28 feature reduces the loss for correctly categorized photos while slamming images that weren't correctly classified. The typical cross-entropy function is introduced along with a modulator factor (1 po,c). Additionally, it has been demonstrated that if 0 and po,c 0.5, the network is taught in a way that is significantly more effective and produces better outcomes than with conventional cross entropy loss. To increase accuracy even more, you may multiply yet another variable that is modifiable. The mathematical formula for the Focus Loss function is

3.3. Training

Pre-training the CNN on 745096 photos over 125 epochs allows it to perform quite well without investing a lot of time in training. Following that, it is taught for 20 epochs using the remaining dataset, which includes 319327 images in total. This work employs true class weights that are updated with a proportion of how many photos are classed as normal (with really no indications of DR) for each batch uploaded for back-multiplication, preventing overfitting of the cerebrum network that results from the slanted dataset. This aids in

minimizing the over fitting problem brought on by the bulk of data being from the same class and not showing any symptoms of retinopathy.

To train the network, a stochastic angle plummet plus Nesterov force is utilized. It was first manipulated to maintain a low learning rate of 0.0001 throughout 5 epochs to allow the edge weights to settle, after which it was revived to 0.0003 till 125 years, driving the model's precision to 70%. This required approximately 4 hours of training using our gear, which had the following specifications: A Core-i7 computer with an 8 GB GPU. A ninety-six percent accuracy was achieved after training the remaining dataset at a slower learning rate. During this time, the learning rate decreased by a factor of 10 due to time training loss, and accuracy was reached.

3.4. Proposed CNN

It is well documented that the set of parameters of a CNN must be maintained under control in order to reduce the model's complexity; yet, decreasing the parameters simultaneously reduces the network's image understanding capacity. Therefore, the two must be balanced in the best possible way in order to achieve notable accuracy with the least amount of complexity. We can achieve excellent results with a small number of network parameters thanks to a unique architecture presented by Szegedy and Alom at al. [24,27]. The proposed architecture model, which was created using fundus images and used to optimize the modified CNNs, is displayed in Fig. 3.3 To acquire the findings, we make a few little changes to the network. The proposed model is end-to-end learning, so that feature extraction is not required. Optimised this model using Keras tuner, hence, that number of layers and number of filters is optimized.

3.5. Implementation

The CNN model is developed in Python using keras library in Linux environment and leveraging an 8 GB GPU on a suggested framework with Core-i7 processor & 32 GB RAM.

Algorithm-1 Fundus image classification

a. FIC (Batch of image (S1, S2……., Sn):

b. For every IMAGE (s)∈ Batch do

c. Feature VECTOR (z) = Modified CNN (S)

d. For every pixel (K)∈ S, S= 1,2…….N do

e. Estimate attention (b), b = [0,1]

f. Extraction attention view (m) = bΘZ

g. End for

h. Use m to classify the image

i. Estimate classification loss as:

$$T = \sum_{i=1}^{n} w_V w_{\tilde{v}}$$

Where Wv indicate original and predicated class

j. Update model

k. End for

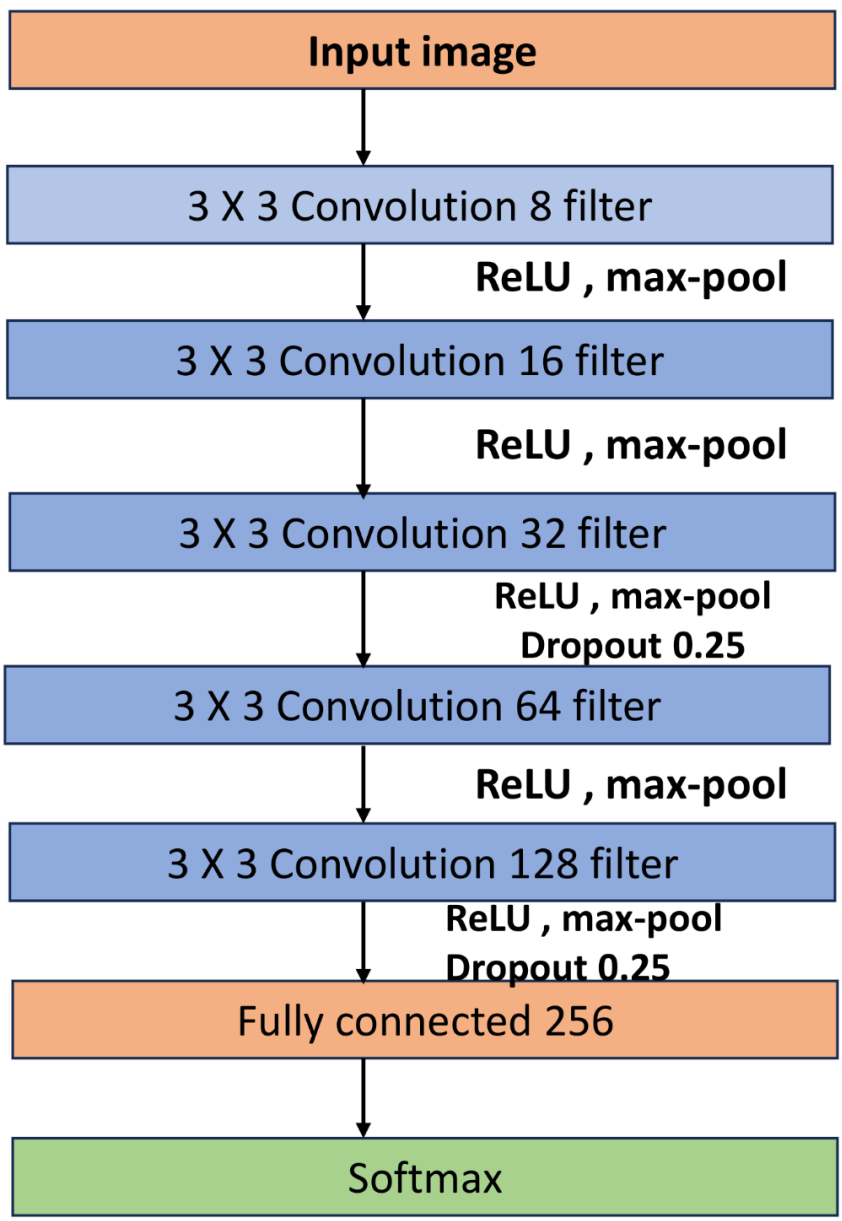

Fig. 3.3. Proposed CNN model

3.6. Experimental result and discussion

Tortuosity-based eye arteries are difficult due to the method's intricacy. Deep Learning algorithms require advanced tuning to obtain satisfactory results. We utilized a CNN network that performs admirably. We thoroughly investigated the "Spearman's Rank Correlation Coefficient" (SRCC) framework by changing a number of dependencies.

3.6.1. Experimented Results

In our analysis, we used two datasets. 88,702 fundus pictures are available in the Kaggle database1. Finetune CNN uses all medical pictures and develops a pre-trained network for feature extraction. The Eye Images Analysis Research Group produced the EIARG1 dataset available (Aghamohamadian-Sharbaf at al., 2016). The dataset is utilized for vascular research based on medical images on the deformability of diabetic retinal blood vessels. This medical retinal fundus database is intended for investigations on tortuosity grading glaucoma. As was already indicated, for training, we have enhanced medical photos. Figure 3.4 shows an illustration of fully enhanced medical photos used for training.

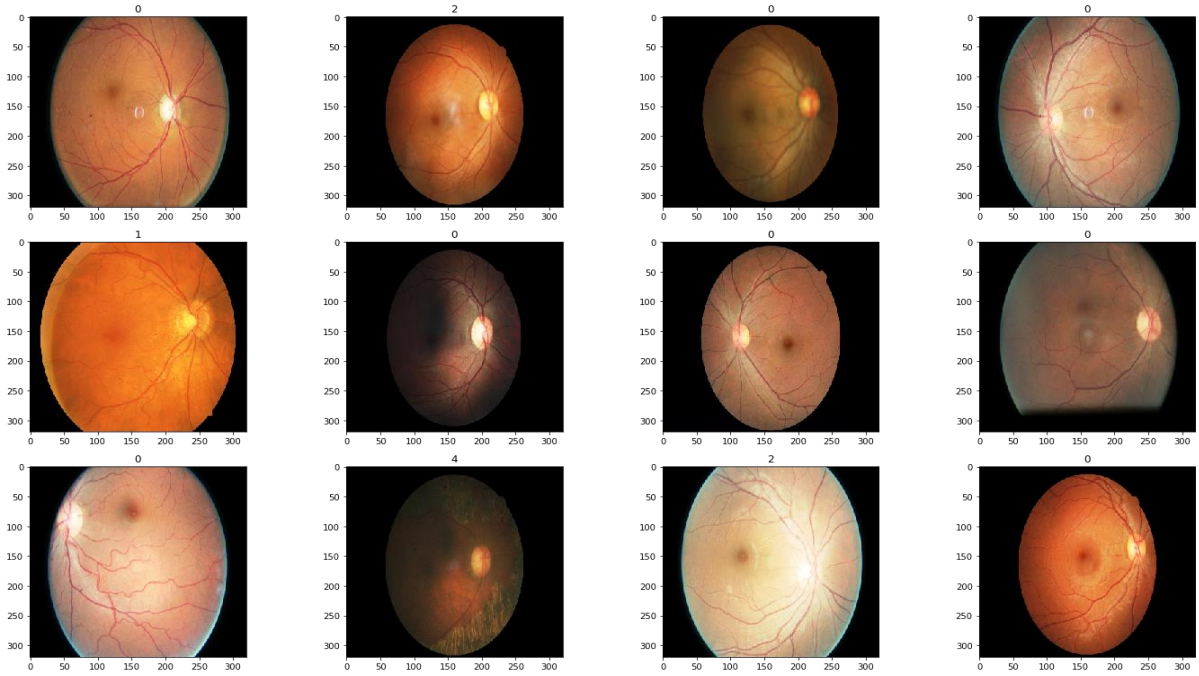

Fig. 3.4. Augmented training image

The outcomes of the learning techniques are shown here. We trained on 70% of the data and tested on 30%. Each time, the performance is assessed using a 10-fold cross-validation. ResNet50 (0.91) & VGG16 (0.86) performances (SCC) are provided and are accurate in

grading the tortuosity-based eyesight. It has been noted that baseline techniques like ResNet50 and VGG16 function ineffectively. The suggested CNN model outperforms the trained Inception.

In this part, we go into further depth on the suggested approach's findings. The confusion matrix for three classes is shown in Fig. 3.5 (0,1,2). Depending on the amount of consecutive phase shift in the centerline's shape, this was addressed appropriately for each of the eliminated centerlines. These are pixels in which the second subsidiary of the centerline disappears. When contrasted with pictures of high convolution, it has been tracked down that low levels of convolution (0 and 1) cause relatively more perplexity (grade 3).

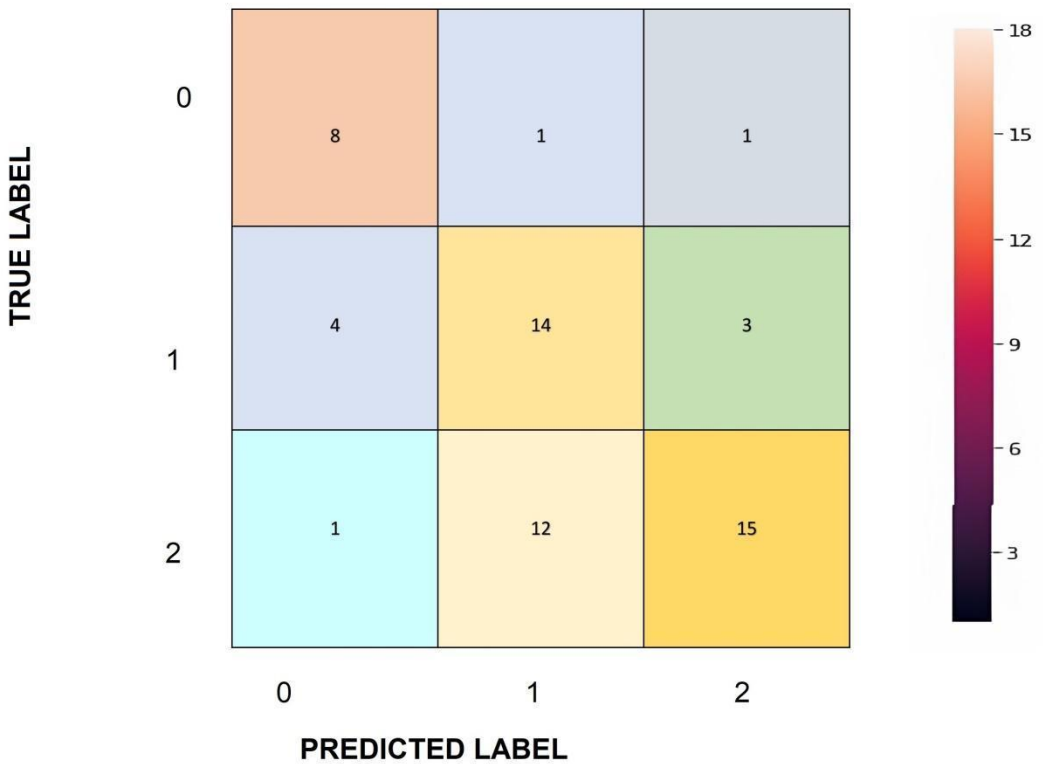

Fig. 3.5. The confusion matrix in the test case

The receiver operating characteristics curve is displayed in Fig. 3.6. (ROC). It should be noted that the suggested strategy also reduces false detection. We were using the Loss curve inside the proposed training sample of every experiment and randomly picked photos from the test set to generate the results shown in Fig. 3.7.

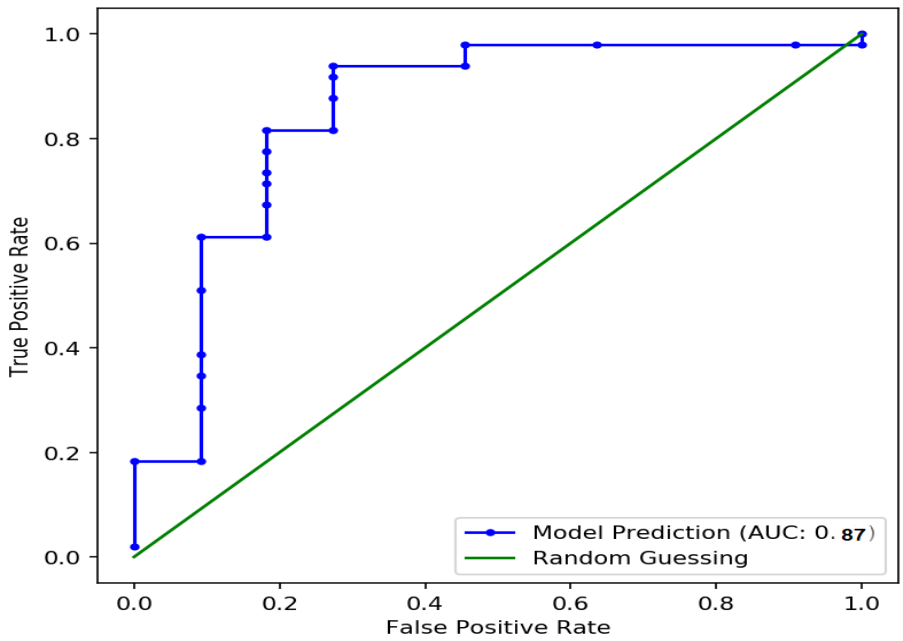

Fig. 3.6. ROC curve

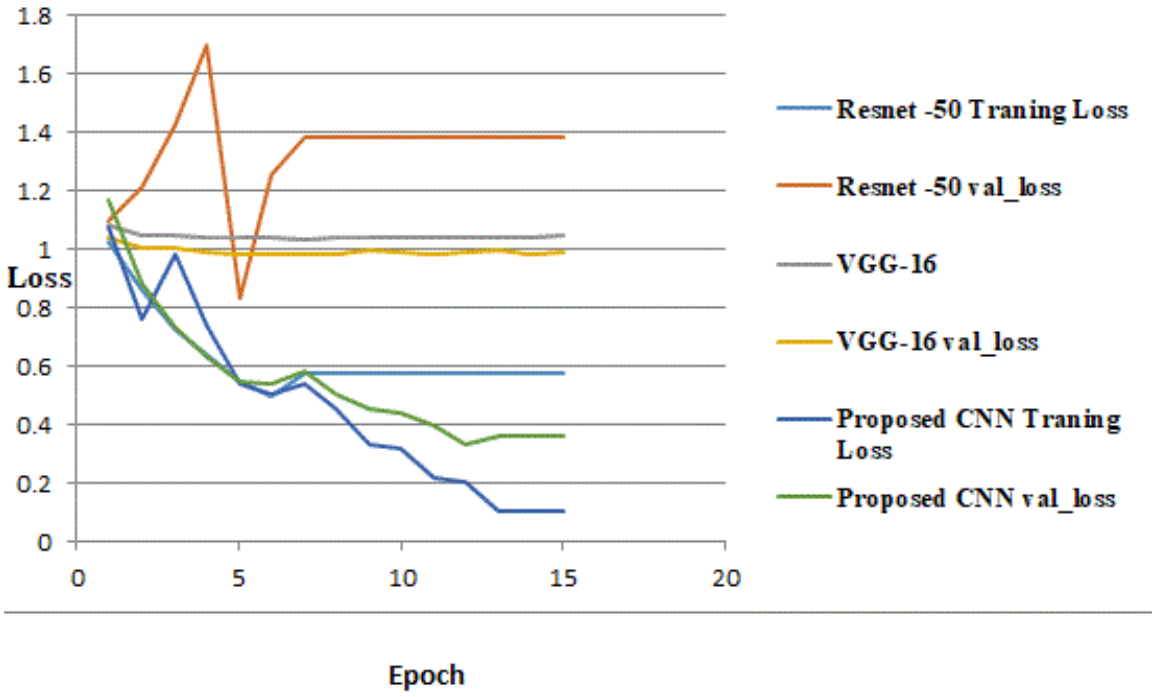

Fig. 3.7. Loss curve in proposed method

Figures 3.8 and 3.9 depict the vessel segmentation conclusion & vessel tortuosity visualisation, respectively, where red indicates the tormented district of the arteries & blue indicates generally vessel index number. The vasculature, by far the most important signal for determining vascular tortuosity, is the basis on which the proposed method makes its conclusions, according to convincing evidence. This is congruent with the outcomes, which

are based on qualitative assessments of the Vascular Tortuosity Index (VTI) & Density Index (DI) of the retinal blood vascular tortuosity.

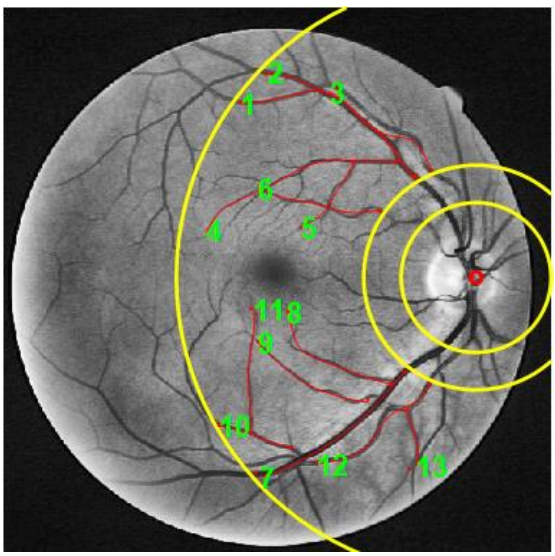

Fig. 3.8. Test image of tortured eyes

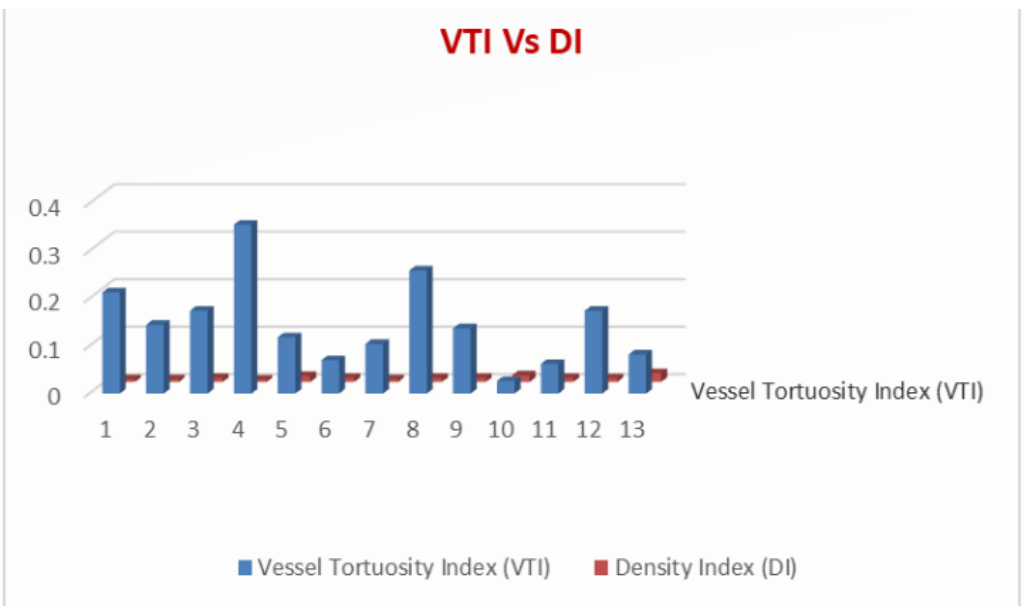

Fig. 3.9. Relationship between VTI and DI

3.6.2. Discussion

The grade of an eye conveys the potential risk of eye problems and the expert advice that is needed. It has been noted that various doctors score similar medical images with tortuosity fundus differently. The deep learning technique to grading involves measuring vascular tortuosity. The choice of automatically graded photos that were revealed in this work, which serves as the method's standard, was a focus. Segmentation, identifying key sites, and

measuring tortuosity are three steps involved. Table 1 and 2 displays the results. It has been discovered that our recommended method results in a higher association among specialists.

The suggested method is a steep, two-step process with a high time complexity. First, the method's core (Modified CNN) is learned on the Kaggle database, and the complete model gets fine-tuned with RET-TORT. Next, the grade is predicted using the learned model. On a PC with just an Intel i7 (3.6 GHz), 32 Gigabytes of Memory, as well as an 8 GB GPU, the tests are run. The instruction lasts roughly three hours. Then, for prediction, we took 10 samples from the RET-TORT dataset & performed the experiment ten times (i.e. 100 expectations). The outcome displays the total amount of time projected by various methodologies. The proposed approach is discovered to take the same amount of time as cutting-edge deep models, including CNN & encoder-decoder based models. The approach is computationally quicker than established approaches like KNN and SVM and outperforms curvature-based models.

Table 3.1

Correlation between automatic tortuosity grading results in comparison:

Authors	**No.of images**	**Database**	**Method**	**Performance (SCC)**
Grisan et al. [10]	60	RET-TORT [1]	Inflection-based measurement	0.949 (artery), 0.853 (vein)
Poletti et al. [29]	20	Non-public dataset	Combination of measures	0.95
Oloumi et al. [30]	7	Non-public dataset	Angle-variation-based measurement	NA
Trucco et el. [21]	20	DRIVE	Curvature and vessel width-based measurement	NA
Aghamohamadian-Sharbaf et al. [32]	60	RET-TORT	Curvature-based measurement	0.94
MasoudAghamohamadian-Sharbaf et al. [14]	120-Full image [ROP]	RET-TORT	Curvature-based measurement	0.71(SRCC)
Proposed Method	**120-Full image [ROP]**	**RET-TORT**	**Modified CNN**	**0.96**

Table 3.2

Automatic tortuosity grading results in comparison with different networks:

Method	**F1 Score**
DenseNet121	0.63
ResNet101	0.75
ResNet-50	0.82
VGG16	0.83
Proposed Method	**0.85**

3.7. Summary

The experimental results reveal that the accuracy obtained in the proposed CNN model is higher than that obtained by the existing architectures such as Vgg16 and ResNet50. The use of the Engaged Misfortune capability improved the model's efficacy in determining the grades of Diabetic Retinopathy. The proposed model, however, has a complicated design which can be simplified to obtain similar results. In this work, an approach for determining the grades of Diabetic Retinopathy considering the tortuosity of retinal blood vessels is proposed using CNN based architecture. The performance of the suggested framework is verified by applying it on the images available in the RET-TORT dataset. This study thus aids in grading the retinal pictures automatically by identifying the blood vessels of the retina and measuring the tortuosity in them. In the future, interfaces can be designed for convenient access in rural areas for mass screening of diabetic patients. This approach will thus help ophthalmologists in rapid and precise evaluation of the grades of Diabetic Retinopathy from the fundus image of a patient.

CHAPTER 4

VGG-16 NETWORK BASED PATCH BASED AUTOMATIC TORTUOUS RETINAL VESSEL CLASSIFICATION

4.1. Introduction

Prolonged hyperglycemia is the principal figure of retinal blood vessel damage. The best method to stop retinopathic disorders is by early diagnosis. This is a serious disease that not only affects the natural eyes yet in addition silently harms other organs. Diabetic Retinopathy (DR) is the main source of visual deficiency in affluent nations [137]. The thickening of the vessels and tortuosity, or twisting of the vessels, are the first symptoms of this [8]. Internal bleeding is possible since the arteries are naturally emaciated [135]. Therefore, it is crucial to quantify the vessels' curvature. The Arc Length and Chord approach was put forth by Lotmar [134]. This approach is frequently used in [133] and [137]. However, due to the problem of measuring accurate curvature [5, 8], several characteristics with a comparable convexity were helped and the vessels were gathered utilizing a weighted summation. Hart et al. [138] first proposed a curvature-based technique. In [138], the mix is picked over the squared shape auxiliary as the measurement for convolution. The classification splits an eye into multiple zones [139], and the seriousness of the not entirely immovably settled by three cutoff points: (i) the location of the area where new ships are positioned, (ii) the region of the vascular patches included, and (iii) the quantity of little vessels related with the blood vessels. The presence of "plus disease," which is linked to ROP and is defined by an expansion in retinal vascular width and tortuosity, constitutes a fourth parameter. [140] analyses a summary of the techniques employed in calculating retinal vascular tortuosity. For the purpose of assessing the tortuosity in [141], chain coding approach was employed. [142] examines the change in breadth what's more, convolution of blood vessels to assess ROP. The quadratic polynomial decomposition technique has been employed for tortuosity analysis in another work [6].

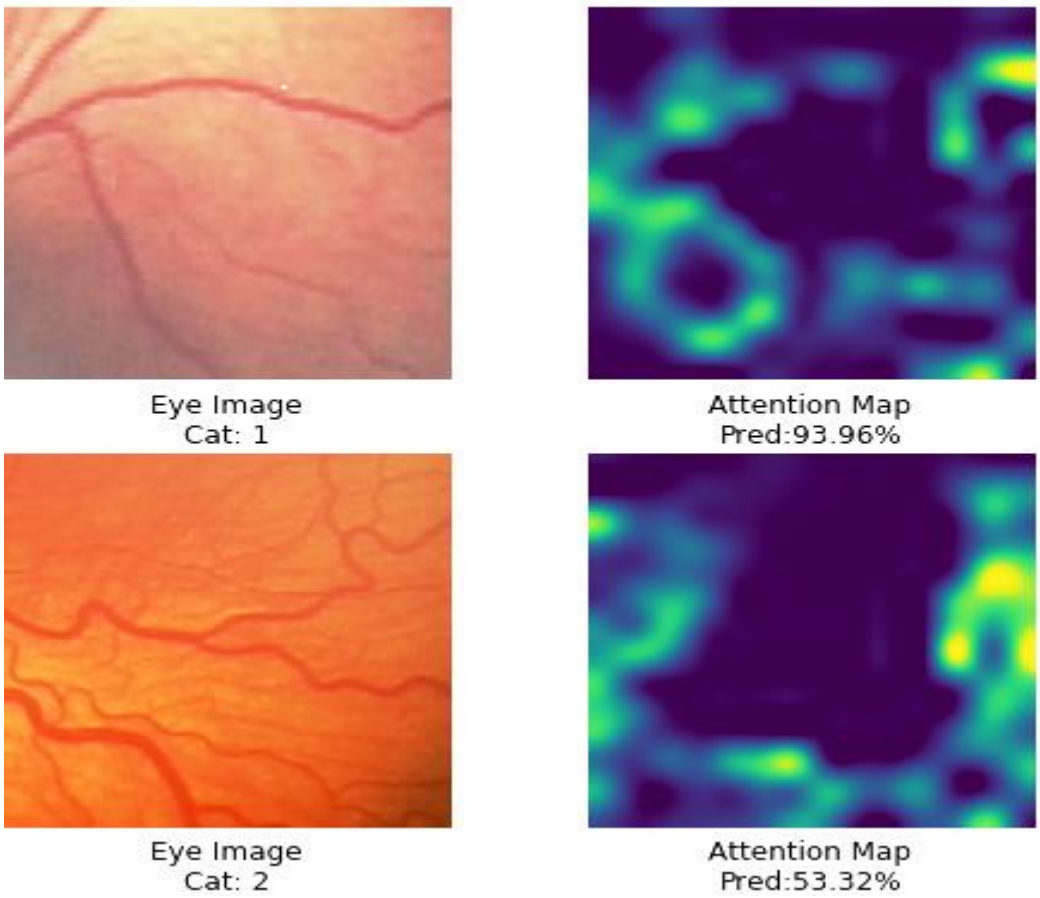

Fig. 4.1. Sample image of tortuosity vessel patch

In [142, 143], better chain codes in view of thickness reliance and curvature have been used to measure tortuosity.

When vessel partitioning was done, morphological approaches were taken into consideration, then a technique for quantifying tortuosity [144]. Accurate calculation of vessel width and tortuosity around the optic plate, which is available in regions of the retina, can possibly aid in this screening technique. automatically. These vessels are highly observable, making it possible to examine this area well during the screening exam. Figure 4.1 contains a sample photograph of a tortuosity vascular patch. This figure 4.1. normal vessel with minimal tortuosity. The blood vessel follows a relatively straight path with slight curvature. This figure 4.1.showing different levels of retinal vessel tortuosity. (a) Highly tortuous vessel with significant twists and loops. (b) Moderately tortuous vessel with gentle curves. (c) Normal vessel with minimal tortuosity.

4.2. Proposed Method

Gamma correction is used to shrink and improve the fundus images. Because the photos in the data set EIARG1 come in a variety of sizes, scaling is required. To 244×244 pixels, all the photos have been scaled. After that, the trained VGG-16 network is fine-tuned using images from the EIARG1 dataset [145]. To demonstrate the power of this technique, geometry-based augmentation is conducted on 70% of EIARG1 dataset Patch pictures before being sent into the network. We trained our network using photos from the EIARG1 dataset and then tested it on 30% of the same data set fix pictures. Utilizing different age settings, the VGG16 model was used to tweak the pre-prepared network with 120 photographs. The proposed VGG-16 model-based patch-based grading of retinal blood vessels algorithm, which is illustrated in figure 4.2, outperforms in both low-contrast and high-contrast pictures.

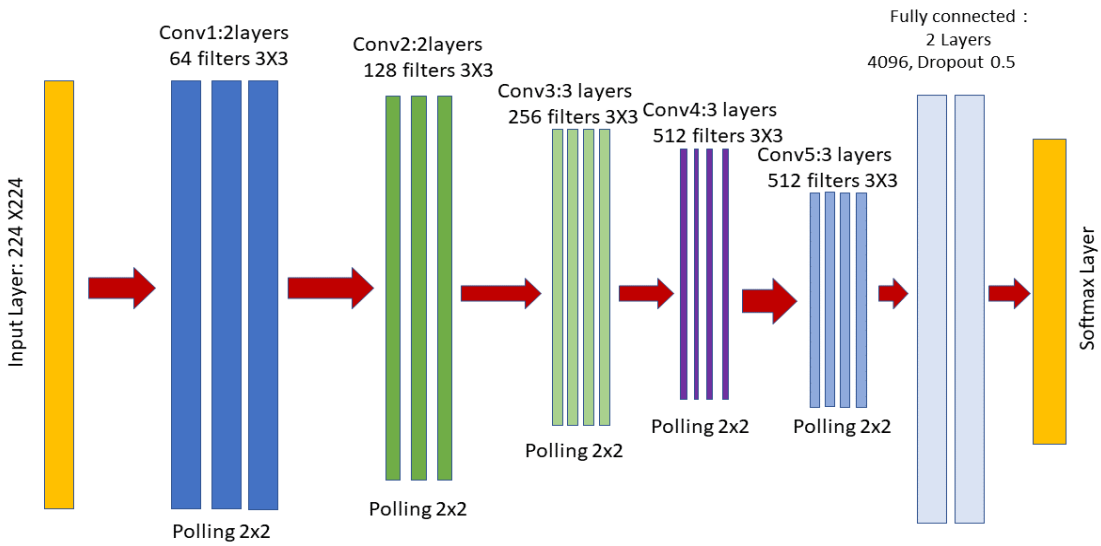

Fig. 4.2. Classification model based on VGG-16 network

It is a modified version of the VGG network. The VGG-16 net is utilized as a base network since the 32×32 input would not burn out due to the VGG's architecture what's more, the VGG design is simple, allowing for easy analysis of the findings. Additionally, one of the most well-known profound convolutional brain organizations is the VGG net. In fact, our VGG-16-based huge model is fundamentally more trustworthy than a 4-layer CNN even when organizing patch-based fundus photos. The model consists of five convolution layer social affairs and one completely associated layer bunch, as well as thirteen convolution layers and two completely connected layers. Each convolution channel has a bit size of 3x3

with a stride of 1, a pooling zone of 2×2 without overlap, and this configuration is standard [146].The idea behind the proposed model's design is to create a network that would automatically pick up on useful traits that are crucial for grading blood vessels. Pre-processing is used in the initial stage to speed up the learning process while retaining the original image data. The patched photos in the preparation set have a level to width ratio of 3:4. Color images are given into the VGG-16 model as input, furthermore, each channel is subsequently rescaled.

4.3. Results and Discussions

The suggested vein reviewing system is tested on 120 photos from the EIARG1 collection [147]. Figure 4.3 focuses on some of the difficult-to-classify blood arteries that are damaged by diabetes. Figure 4.4 displays examples of vascular patch pictures that were utilized to set up the cerebrum association to become familiar has the characteristics of the wide-ranging and entangled vasculature that relate to plus-disease.

Fig. 4.3. Focus on diabetic affected vessels

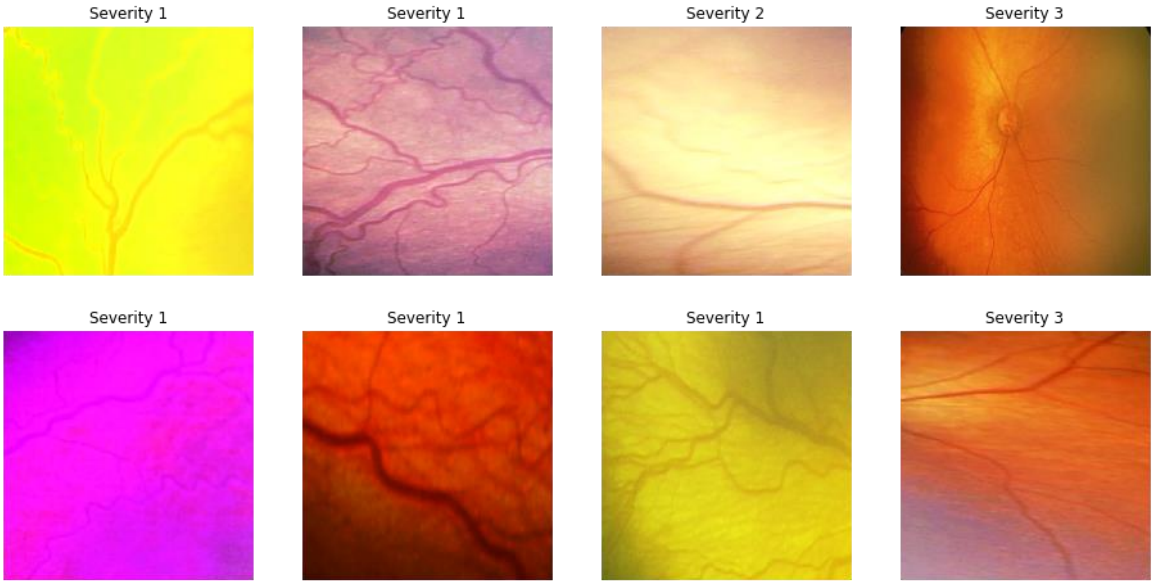

Fig. 4.4. Visualization of learned retinal pathologies with the projected pre-GAP

Table 4.1

Observation Table:

Test Image Count	Precision	Recall	F1- Score	Accuracy	Time (sec)
30	0.73	0.72	0.77	78%	12
42	0.65	0.67	0.66	67%	25
48	0.48	0.42	0.40	42%	37
78	0.65	0.57	0.54	57%	83

The disarray framework in Figure 4.5 helps visualize the proposed assessment's suitability for measuring the coordination of convoluted arteries. The suggested method achieved 78% exactness and a reliability score of 0.73 in evaluating the retinal blood vessel on the EIARG1 dataset [148] in 12 seconds, as shown in Table 4.1.

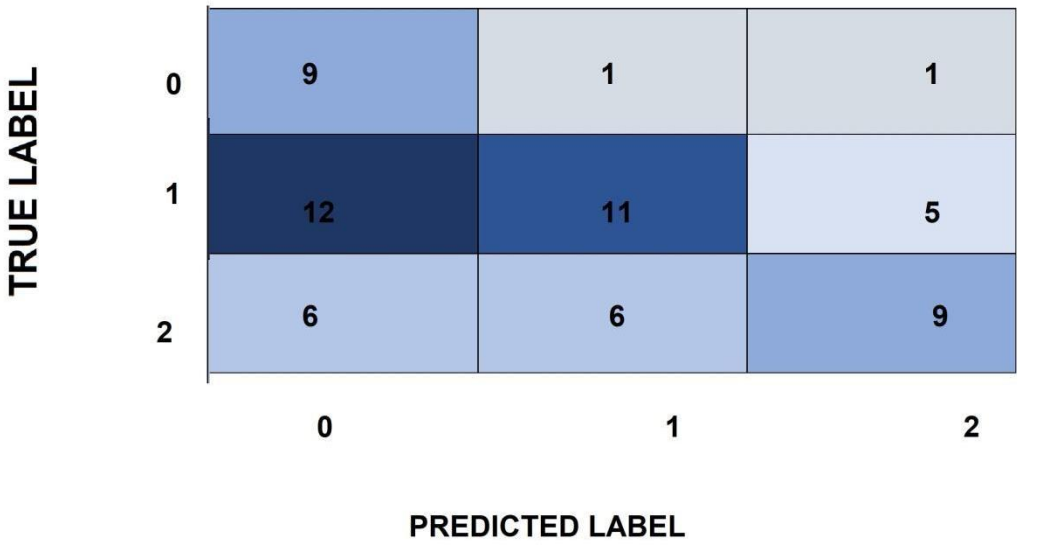

Fig. 4.5. Prediction helps of confusion matrix

The observed accuracy in figure 6 was higher than the accuracy in the data because most of the fundus photos were tried pictures with no modifications resulting from the training data. However, doing so simply reduced over fitting rather than improving accuracy. 35 epochs are used to train the VGG-16 net, with a dataset consisting of 1. We reduce the training and testing loss by using weighted spatial cross entropy. The losses experienced during testing and training at various period values are depicted in Figure 4.6. The categorization is done using Adam optimization [149] and SoftMax. The F1 score was altered for each test image count. A competent ophthalmologist can detect classified images to improve precision and memory. Table 4.2 shows that the suggested work's Spearman's ranking correlation coefficient (SRCC) score beats that of the existing studies.

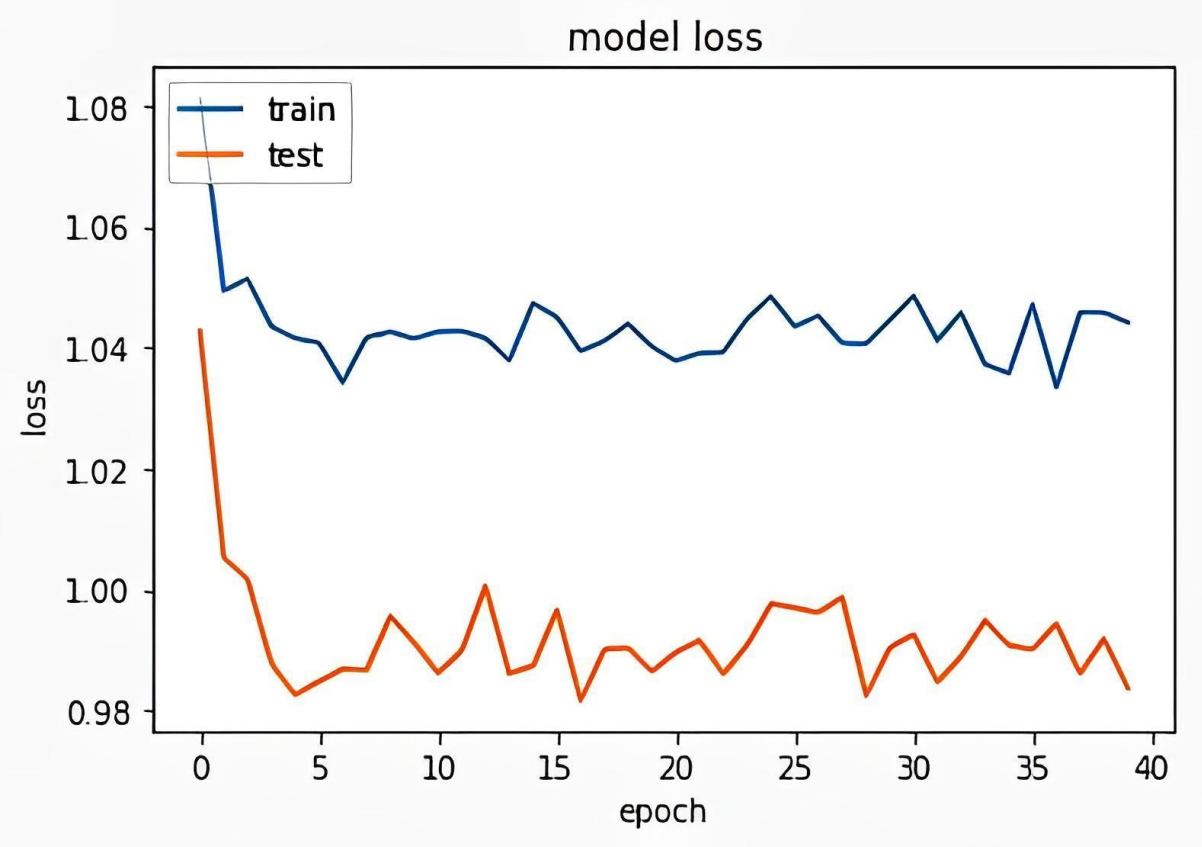

Fig. 4.6. Model loss while training and testing at various epoch value

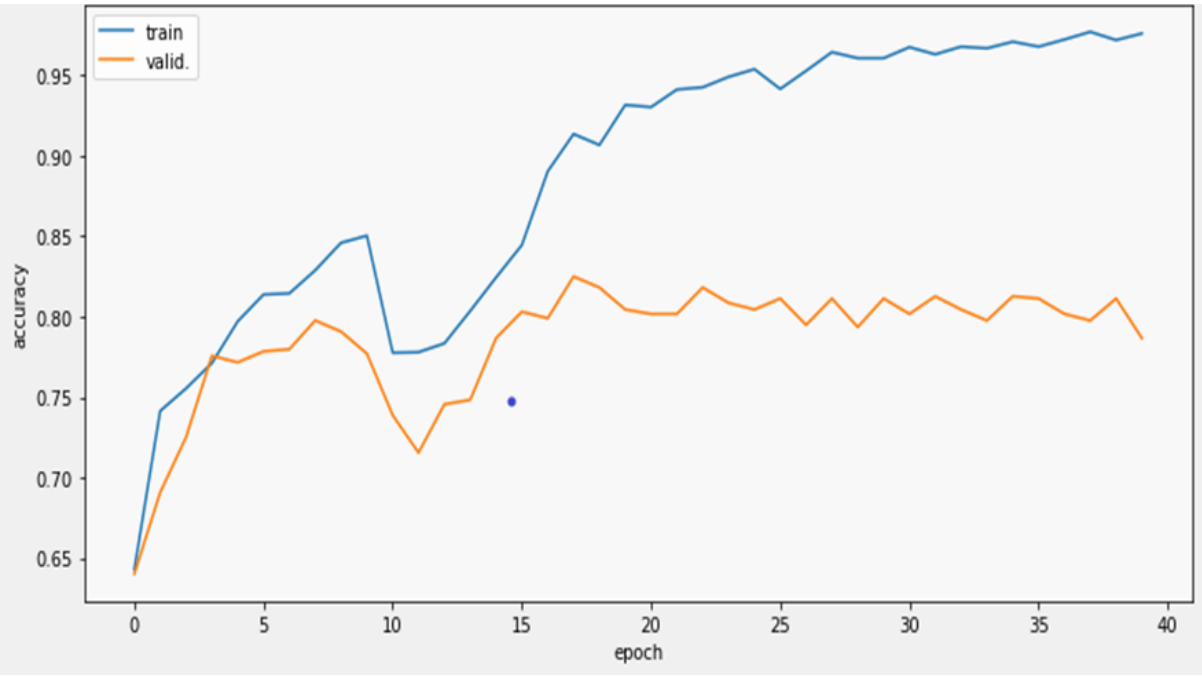

Fig. 4.7. Model Accuracy while training and testing at various epoch value

Table 4.2

Comparative study of correlation score with existing works:

Publication	**SRCC Score**
Aghamohamadian-Sharbaf et al., 2016	0.71
Narasimhan and Vijayarekha, 2015	0.66
Proposed work	**0.72**

Table 4.3

Comparative study of F1 score with different works:

Method	**F1 Score**
DenseNet121	0.68
ResNet101	0.79
ResNet-50	0.84
Inception V3	0.85
Proposed Method	**0.88**

The Eye Images Analysis Research Group contributed the EIARG1 database [150] for image-based investigations on the convolution of the retinal veins in diabetic retinopathy. The quantitative results of the proposed algorithm and the existing works are presented in Table 4.3, where it is observed that our method provides better performance in most of the cases. The performance of Proposed net is competitive to the state-of-the-art methods. We have further improved the performance through an ensemble with VGG16. It improves F1 Score by 0.88 and SRCC score by 0.72. Figure 4.5 demonstrates effectiveness of instance-wise prediction for accurate grading. We have aggregated some of the results of our classifiation algorithm. Overall, VGG16 produces better classification compared to DenseNet121, and handles multi-scale objects effectively through instance-wise prediction. The database for the tortuosity of ROP pictures is accessible to the public at www.eiarg.um.ac.ir.

4.4 Summary

Several effective training procedures are remembered for the proposed totally programmed based VGG-16 organization for fix put together retinal vein evaluating with respect to fundus pictures to address the issues that the organization might confront when little training data is available. By accepting specific correction methods for the few incorrectly categorized photos displayed by the disarray lattice in Figure 4.5, this model can be further improved to produce greater classification accuracy. The strategy outperforms cutting-edge techniques when tested against an open test information base for classifying fundus images.

CHAPTER 5

DIABETIC RETINOPATHY DETECTION AND GRADING OF RETINAL BLOOD VESSEL TORTUOSITY USING MODIFIED EFFICIENT NET

5.1. Introduction

In 2019, there were about 463 million adults worldwide who had diabetes, according to WHO statistics. Their population is anticipated to soar in the years to come, reaching 800 million by about 2044. Retinal Diabetic retinopathy (DR) is one of the most severe diabetic complications [151]. Diabetic retinopathy produces irreversible vision impairment with varying clinical symptoms at various stages; eventually, the outcome of this DR is blindness. Thus, prompt diagnosis and identification of DR are advantageous for diabetes patients receiving effective and appropriate therapy. Micro aneurysm [152], exudates [153], improvements in new blood vessels, their release, and other unintended consequences of diabetic retinopathy consolidate tiny DR findings aneurysms, exudates, new body formation, and more. There are two different types of DR: non-proliferative and proliferative. There are three classifications for the non-proliferative stage: mild, moderate, and severe. Small bleeding patches or tiny hemangiomas in the initial stages are characteristics of the mild stage. The moderate stage, which follows the gentle stage, allows for the investigation of specific yellowish-white punctate hard exudates. The severe stage with non-proliferative retinopathy is marked by exudate that really is white, textile, and soft. In the next DR stage, proliferative retinopathy, retinal harm sets off the advancement of fresh blood vessels, causing significant internal bleeding [154]. Finding the corresponding aspects of fundus diabetic retinopathy is difficult due to the disease's complicated and variable characteristics. Doctors currently identify DR in medical care via a fundus photograph, which remains the conventional approach. However, missed and incorrect diagnoses as well as other problems are likely to happen. The issue of manual diagnosis is solved by computer-assisted diagnosis (CAD) [155], which reduces the workload and amount of time clinicians must spend diagnosing illnesses while ensuring high accuracy [152]. Deep learning has lately achieved considerable advances in the field for computer aided design examination, in both research and application. The Convolution Neural Networks (CNN) [156] is a useful tool in the field

of computer vision because of its higher efficiency in image categorization tasks. Researchers recently created the CNN algorithms VGG Net [5], Google Net [154], & Image net [157]. However, this method of determining the depth, width, and height of the three dimensions results in subpar accuracy & efficiency [158]. Efficient Net [159] surpasses the competition by uniformly scaling depths, width, and resolution, and this approach offers a different development path for CNN in the future. Limited medical data is a problem that makes it challenging to train the model. It's a helpful tool for improving network stability and efficiency when there isn't enough data. Deep learning has emerged as a popular topic of research within the medical community [160]. Chetoui et al. used Efficient Net & transfer learning (RDR) [161] as well as the VTDR within the APTOS 2019 & EyePACS datasets to diagnose referable diabetic retinopathy, with gratifying results of up to 0.98 AUC [162]. The assertions demonstrate how, first, deep learning techniques have attracted greater attention in the diagnosis of DR due to their enhanced performance, and secondly, doctors will be able to comprehend the grade classification for various levels of DR intensity [163]. As a result, a simple, furthermore, successful organization is basic for a more exact and convincing discovery of shifting levels of DR. In this work, a developed framework for DR grade diagnosis was constructed to support the analysis.

5.2. Methodology

In this study, the fundus image pre-processing of the retinal input dataset, feature extraction from the suggested network, and so this classifier is employed to develop the DR diagnosis model. The DR diagnostic model's method is shown in Figure.5.1.

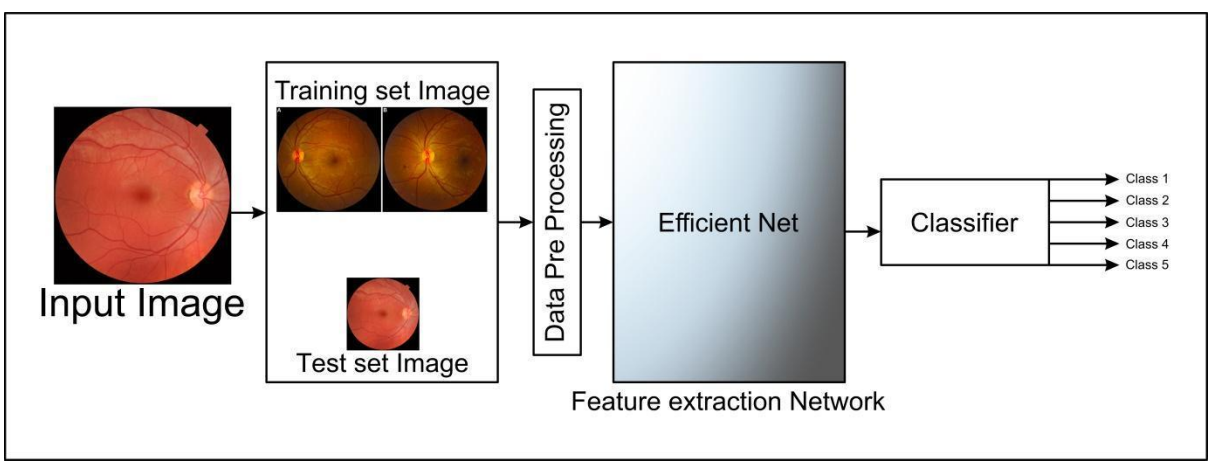

Fig. 5.1. Framework of DR model

A. Dataset

The APTOS 2019 data, which is available on the Kaggle website [164], served as the basis for the classification experiments conducted for this article. The dataset, which includes 3662 high-resolution images with each sample linked and was provided by the Aravind Eye Hospital in India, was able to identify each of these disorders thanks to the expertise of highly qualified doctors. As indicated by the suggested, grade 0 photographs do not display any diabetic retinopathy, 1 370 pictures show mild neither any diabetic retinopathy, second grade 999 images demonstrate a moderate, non-proliferative state, and grade 3 193 images demonstrate no diabetic retinopathy. Photographs from grade 4 193 indicate extreme no-proliferative diabetic retinopathy, while pictures from grade 4 193 show the same condition. The allocation of the 5 categories is obviously unbalanced, as will be clearer as we go forward.

B. Pre-processing

The dataset was used before to reduce the over-fitting of the network and enhance its capacity for learning. It is split into four parts: According to the database that is currently accessible, the dark border of the fundus photos is quite big and doesn't reveal anything about the lesion area. The black line is removed, and all shots are downsized to 1024 × 1024 to remove extraneous information from the images. The spread of the retina dataset is highly uneven, as was already mentioned. In order to address this issue, 2000 examples from each grade were collected and annotated using techniques like rotation, flipping, contrast, and change of brightness.

The original images are resized inside this range [0, 1] to improve resolution during the rainfall process. All data is divided into two categories for training and testing. 80% of the data is used for training & 20% is used for testing, in an 8:2 ratio.

This section provides the modelling approach for feature extraction. Efficient Net, which was pre-trained using the transfer-learning methodology on the ImageNet dataset, receives the data first. The output of the Efficient Net is then sent to the classifiers.

C. Transfer learning

Since there aren't enough publicly available samples for DR assurance, it will, in general, be trying to oblige a reasonable outcome utilizing profound learning technologies. In our model, transfer learning technologies are used to address this issue, and the implementation steps are

as follows: (1) The network requires pre-training. 1.2 million photographs divided into 1000 categories make up the ImageNet database, which is used to train the Efficient Net to build the pre-trained network. The diabetes data is then loaded into the pre-trained Efficient Net. (2) The word "improvement" is sometimes used to refer to the process of fine-tuning. The last period of the element extraction spine may be a tuning step where a pristine completely connected layer is made and Adam is used as an enhancer with a learning pace of 0.001.

D. Efficient Net

The model uses the Efficient Net framework, which scales depth, breadth, and determination to produce an effective and reliable system. The network is accessible in several styles, spanning from B0 to B7, with EfficientNetB0 serving as the feature representation in this work. MBConv, which is based on an inverted residual block and was incorporated in ResNet-50 [19], extends the squeeze-and-excitation network (SENet) [165]. During this network, the input image size is set to 224, & Mobile inverted bottleneck compression, or MBConv, is a vital component. Figure 1 conceptually shows EfficientNetB0. There are 16 MB-Conv blocks in the network, each with a kernel of 3×3 or 5×5. The computer file, or fundus image, is originally uploaded to the network, where it is processed. We employed 1×1 Conv2D layer, 3×3 Conv2D layers, & 16 MBConv layers.

A cutting-edge compound scaling method based on the application of When the model variables & calculation quantity are maximal, a compound factor is employed to scale the network's breadth, depth, and resolution uniformly. As a result, the model's accuracy increases.

E. Classifier

There are two distinct classifiers for our challenges: a 5-grade classifier. DR recognition tasks are handled using a five-grade classifier.

Efficient Net first extracts the extracted features from the fundus images, then adjusts the hyper-parameters to construct new, fully connected layers. Finally, the fresh classifiers are compared. Global average pooling (GAP), BN, and Softmax layers are among the brand-new, entirely linked layers. The number of pixels is decreased to a singular data gathering via the GAP level. Numerous fundus picture classification applications use the Softmax layer, and the BN layer can improve network convergence.

5.3. Experiment and result

Finally, contrast the suggested DR diagnostic model with cutting-edge CNN networks [166] including VGG-16[167], ResNet-50[168], & Dense Net-121[169] to show its effectiveness. Each of these networks are combined with transfer learning. The suggested model's results are also contrasted with those of the models put out in Section 1 to demonstrate how far our model has come in the context of a 5-classification task. The results of the diagnostic models are presented using the evaluation techniques listed below: First, assessment criteria including such accuracy, precision, as well as an F1 and kappa score are used for comparison. The standardized clustering algorithm, which is a framework outlining the amount of material from any class that is listed as an elective, is presented after that. The definitions of these metrics are as follows:

$$Accuracy = \frac{TP + TN}{TP + TN + FP + FN}$$

$$Precision = \frac{TP}{TP + FP}$$

$$F1 = \frac{Precision * recall}{precision + recall} * 2$$

$$Kappa = \frac{Observed\ accuracy - expected\ accuracy}{1 - expected\ accuracy}$$

Accuracy:

Accuracy measures how closely a measured value matches the true or accepted value. In scientific experiments, accuracy quantifies the closeness of a measured value to the actual value, providing a measure of the correctness of the measurements.

A. Discussions and Result of the Experiment

The experiment's first task is a 5-grade classification, which comprises determining the severity levels of DR. The sparse categorical cross entropy error rate, with a batch size of 32 and epochs of 60, is specified as the experiment's super parameter to enhance the network's training. These exercises' outcomes are offered together with a discussion of the conclusions.

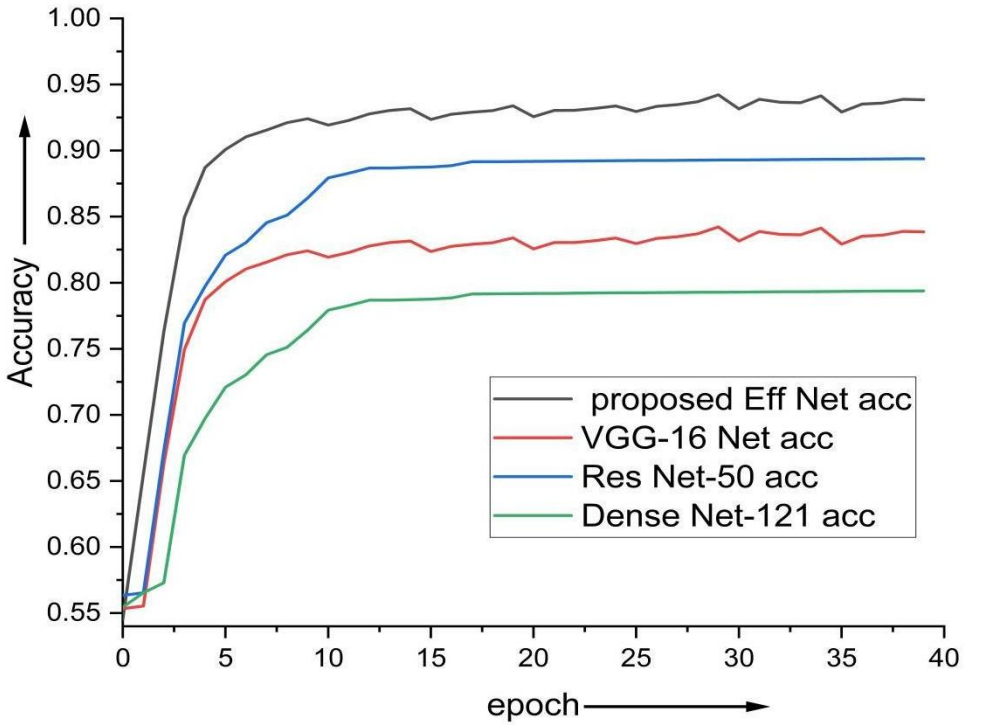

Fig. 5.2. Diabetic retinopathy accuracy comparison

B. Classification

In Table 5.1, the parameters of several networks are evaluated. When compared to certain other pre-trained networks, the parameter of Efficient Net is low. The least parameter is ResNet-50. However, it's not quite as accurate as Efficient Net. Additionally, Efficient Net outperforms its rivals, with a variable that is only a few percentage points higher as ResNet-50, demonstrating the necessity of using computers for calculations in figure 5.2.

Table 5. 1

Parameter comparisons for several networks:

Model	**Parameter**
Dense Net-121	2,265,666
VGG-16	20,873,770
ResNet-50	54,354,954
Proposed Net	4,057,253

All models were compared, resulting in a 5-grade rating that can assist doctors in performing treatment more conveniently & successfully by detecting the severity of DR. The APTOS 2019 dataset has currently five grades, which required for the challenge. The proportions in both the training & testing sets match those that are currently in use. The suggested diagnostic model and comparable models are evaluated on the 5-grade dataset, and the results are reported below.

In Table 5.2, the Accuracy ratings of similar networks are compared. The results demonstrate that Efficient Net beats other network in terms of precision, & kappa scores, having scores of 93.92 percent, 93.97 percent, as well as 87.95 percent, respectively.

Table 5.2

Shows comparisons of the different networks:

Model	**Accuracy (%)**	**Precision (%)**	**Kappa (%)**
Dense Net-121	85.55	85.65	81.93
VGG-16	90.80	90.73	88.49
ResNet-50	90.55	90.70	88.18
Proposed Model	**93.92**	**93.97**	**87.95**

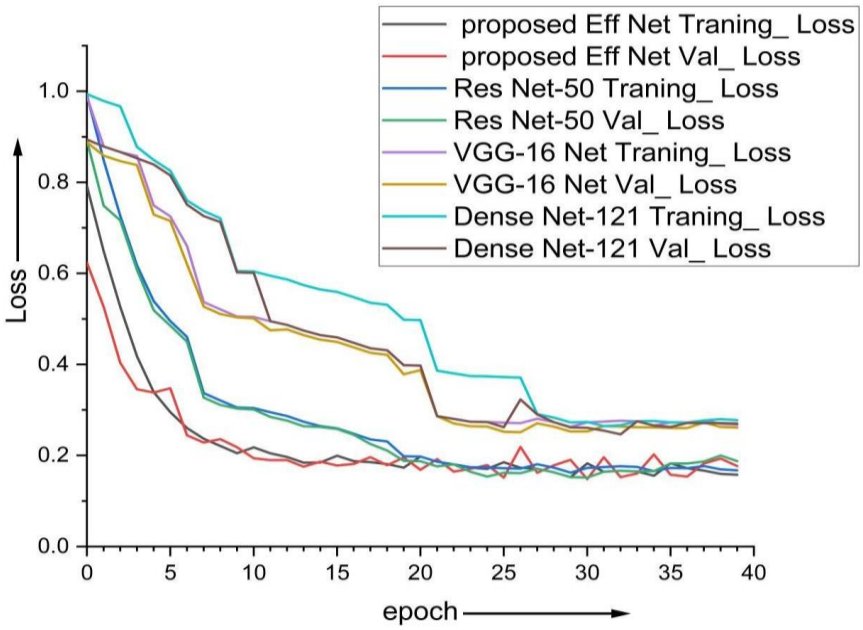

Fig. 5.3. Diabetic retinopathy Loss comparison

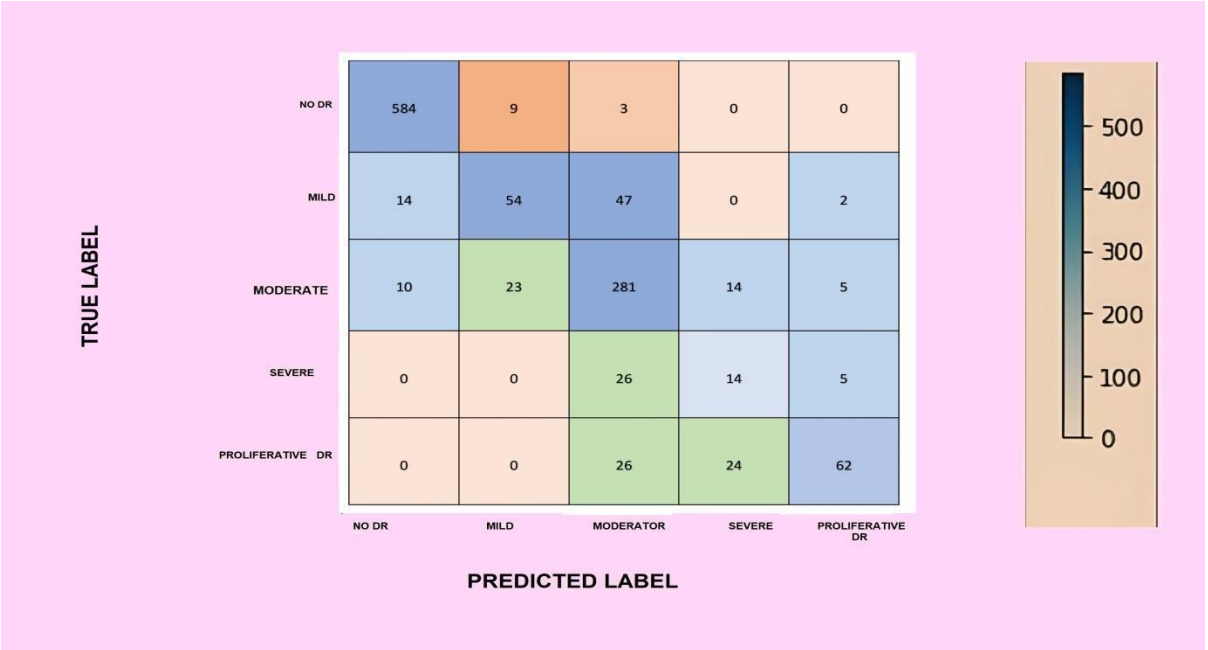

Fig. 5.4. Efficient Net confusion matrix

The Efficient Net clustering algorithm is shown in Figure 5.4. According to Efficient Net, the number of patients categorized as No-DR, mild, medium, serious, or aggressive DR is 584, 54, 281, 24, and 62, respectively. The percentage of middling class classifications that were accurate This severity level is less extreme it is more challenging to overcome than the others because isolate between the qualities of fundus pictures.

Table 5.3

On the APTOS 2019 dataset, comparison with existing research for DR severity ratings:

Method	**Precision (%)**	**Accuracy (%)**
Majumder et al. [108]	77.00	86.00
Dondeti et al. [167]	76.00	77.90
Patel et al. [168]	NA	91.00
Proposed Model	**93.97**	**93.92**

Table 5.3 contrasts the five current models—all of which are based on the APTOS 2019 dataset with the proposed five-grade diagnostic model. The modified EfficientNet architecture improves the accuracy of detecting diabetic retinopathy and grading the tortuosity of retinal blood vessels. The quantitative results of the proposed algorithm and the existing works are presented in Table 5.3, where it is observed that our method provides

better performance in most of the cases. The performance of Proposed net is competitive to the state-of-the-art methods. We have further improved the performance through an ensemble with modified Efficient Net. It improves Precision Score by 93.97 % and Accuracy score by 93.92 %. Figure 5.4 confusion matrix demonstrates effectiveness of instance-wise prediction for accurate grading. EfficientNet's compound scaling method optimizes both the depth and width of the network, allowing it to capture intricate details in retinal images that are crucial for accurate diagnosis and grading. Efficient Net's design is inherently optimized for computational efficiency, making it suitable for processing large volumes of retinal images quickly. The ability of EfficientNet to integrate multi-level features from retinal images enhances its capability to identify and grade subtle changes in vessel tortuosity and detect early signs of diabetic retinopathy.

5.4. Summary

This study primarily focuses on 5-grade classifications, which physicians may utilize to diagnose DR and which provide more accurate grading information. ResNet-50, VGG-16, Density Net-121, and Efficient Net are only a few of the current deep-learning networks that have been evaluated employing transfer technology in teaching and learning. Efficient Net offers the best outcomes, with a 93.92% efficiency for a 5-grade classification job, thanks to the harmony of depth, width, & resolution. To get more efficient results, the technique modelled after pre-trained CNN networks, as well as all models with an Efficient Net, outperformed the original networks.

When compared to earlier DR classification approaches, the adjusted model is more accurate, and the APTOS 2019 data has a higher assessment value. Meanwhile, we train and assess an EyePACS data of image data to ensure the reliability of the suggested Efficient net technique, and we achieve good results.

CHAPTER 6

GRADING OF RETINAL BLOOD VESSEL TORTUOSITY USING INCEPTION V3 AND VESSEL SEGMENTATION USING MODIFIED U-NET ARCHITECTURE

6.1. Introduction

One useful feature of automatic ophthalmological diagnostic tools is indeed the monitoring of blood vessel tortuosity. Retinopathy of Prematurity (ROP), an eye condition that affects premature infants, is one condition for which automatic tortuosity assessment is critical, in particular, is critically dependent on the automatic evaluation of tortuosity. There have been several methods offered for measuring and classifying tortuosity, however, they don't necessarily correspond to the clinical definition of tortuosity.Automatic segmentation of retinal blood vessels and Tortuosity Measurement from fundus pictures can be a valuable apparatus for the conclusion, arranging and treatment of fundus images.

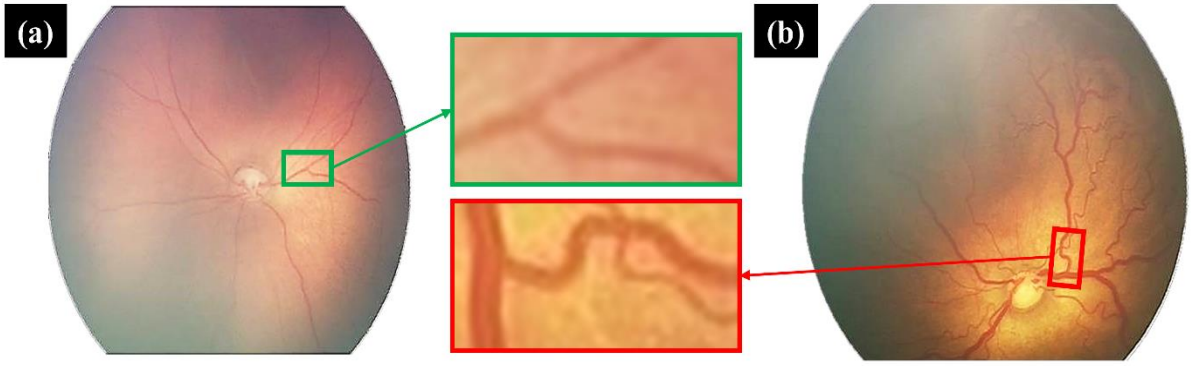

Fig. 6.1. Different touristy level of fundus image (a) low touristy image (b) high touristy image

Grading and segmentation of blood vessel tortuosity in retinopathy are interconnected processes within the field of ophthalmology and medical image analysis.

Grading: Grading involves the qualitative or quantitative assessment of retinopathy, which includes various features such as microaneurysms, hemorrhages, exudates, and importantly, vessel abnormalities like tortuosity. Grading systems often use scales or scoring methods to categorize the severity of these abnormalities. For blood vessel tortuosity, grading can involve subjective evaluation by experts or automated systems that quantify the level of distortion in blood vessels.

Segmentation: Segmentation refers to the process of delineating or outlining specific structures within medical images, such as the blood vessels in retinal images. Accurate segmentation is crucial for subsequent analysis, as it provides a precise boundary of the vessels, allowing for further assessment of their properties, including tortuosity. Segmentation algorithms aim to accurately identify and trace the vessels in retinal images, providing a basis for measuring their tortuosity.

The relation between grading and segmentation lies in their collaborative role in analyzing retinal images in retinopathy. Accurate segmentation enables precise measurement of parameters like tortuosity, aiding in objective grading systems. Grading systems, in turn, rely on the quantitative data obtained from segmentation to assess and categorize the severity of blood vessel abnormalities, including tortuosity.

Automated segmentation techniques combined with grading systems can help in early detection, monitoring progression, and assessing the effectiveness of treatments in retinopathy. They facilitate a more objective evaluation of blood vessel tortuosity and other related features, enhancing clinical decision-making processes.

Intrinsically as anyone is concerned, the proposed strategy has been validated on the public datasets DRIVE and CHASE DB1, which are the only openly accessible datasets for such assignments. Segmentation and Tortuosity Measurement of fundus pictures dependent on the retinal tortuosity is normal in the diabetic retinopathy. Diabetic retinopathy is a frequent illness that causes changes in the anatomy of the retinal blood vessels and blindness. A cataract is the most commonly diagnosed reason for obvious disability, accounting for most of the visible deficiency in the developed world [98]. The early locating maintains a safe distance from proper effects, such as obvious deficiencies. The focal point of the eye is surrounded by a thick, hazy section called a cataract. When proteins in the eye create clumps

that prevent the lens from transferring clear images to the retina, a cataract form. According to study, there may be 537 million individuals worldwide who are blind or visually impaired in 2021 [92, 93]. Prior research on dividing retinal blood channels has generally fallen into two categories. The first group used well-known Deep Learning methods, like support vector machines. [84, 95]. Early diagnosis and treatment can lessen cataract sufferers' pain and prevent vision deterioration. The most efficient way to diagnose retinal disorders is by manually dividing vessels in the retina, but this requires retina specialists. Cataract detection and categorization are highly dependent on vein nuances and the optic circle. The manual vessel identification and division process is a repetitive one [65,74]. Additionally, manual division is expensive and time-consuming because it requires a retinal eye specialist to perform the division technique [88, 97]. In this manner, The Using AI principles, automatic extraction and vessel division are extremely important for early detection of a cataract. A novel blood vessel segmentation technique for the retinal picture is demonstrated in this exam. We tried to include all of the information from both recent and old retinal cleavage examinations in this inspection. We categorize as directed and autonomous strategies in accordance with the brief. There are also numerous technologies, coordinated filtering techniques, numerical morphology technologies, model-based technologies, and supplementary technologies based on vector machines, neural systems, and other systems. method and strategy for ship monitoring. This examination also includes a snapshot of the retinal fundus, preparation & processing techniques, the evaluation method and the data set that were employed and considers the greater complexity and reduced noise in this case. Suarez and other people. Soares et al. [110, 101] suggested a technique that employs management categorization to identify pixels classified as vascular or nonvascular. The Gabor change differential update is used here. Lupascu et al. [112, 131] Use Recent years have seen the development of many fresh semantic segmentation methods. U-Net is the most illustrative of these networks. The filter reaction shows how close together the pieces are at a specific location and angle. According to Chaudhuri et al. The most accurate technique for segmenting vascular frames using robots. They devised a Gaussian-based format outline for identifying straight segmented blood artery pieces. The thresholded and additional processing steps used to get the final split are applied to the filtered reaction image. Hajdu and Kovacs [114, 151]. After describing Gabor's concept, the blood vessel’s shape was rebuilt to determine the centerlines. Because lesions may have regional characteristics resembling blood arteries, their appearance may change the way that segmentation works. A fix for the exudate's tightness was put out by Annunziata et al. 1[16, 117]. The exudate is separated and

colored after preparation. In this work, we suggest a cutting-edge technique for locating retinal blood vessels. We compare the presentation of the completely prepared model created from scratch using medical imaging data with the performance of the pre-trained model that has been fine-tuned for each application. compare. according to the system and its 4,444 artisan counterparts. The following is the article's contribution: -

- The proposed strategy can accomplish up to 95.68 division exactness for DRIVE information.

6.2. Related Work

Monitoring the DR severity level automatically using artificial neural networks (ANN) is outlined in [118]. Retinal fundus imaging allows for the visualization of pathological anomalies such as blood vessels, AM, hemorrhage, and exudate. Next, a multi-facet feedforward neural organization that incorporates the lesion is deployed to categorize the DR into gentle, moderate, and severe. The approach described in [119] entails the type of damage and its Fundus picture are split as a result of the four wounds, ANN are used to categorize DR as mild, moderate, or severe. The mechanized order in [120] is delivered utilizing the results of the affirmed red sore recognition approach. The checkout approach of leaving one out is utilized to investigate people in a general database. They tried to determine whether DR could be recognized automatically. According to [121], retinal fundus can be diabetic or not. The principal picture has four more modest emphases. Following the retrieval of the qualities, the Haar wave change is applied. Principal component analysis was used to choose the top traits (PCA). Afterward, a standard classifier & a backpropagation neural organization are used to do the classification process. To isolate veins from fundus pictures, Sunil et al. [122], proposed utilizing a pre-prepared model. The Microsoft COCO data collection was utilized to pretrain the DEEPLAB-COCO-LARGEFOV model. 800 image patches from 66 fundus images were employed once the pretrained model had been trained. The model's erratic outputs were then combined to produce the required segmented blood vessels. When Sunil et al. assessed their model using 23 images of the fundus. Fundus images need to be preprocessed, as suggested by Sonro et al. [123], before blood vessel segmentation may be carried out. On 5,000 approved photographs, a precision level of 75% was accomplished. Demonstrated a pipeline that segments the fundus blood vessels using the U-net architecture. This was achieved by first pre-processing the fundus images, and then training the U-net utilizing patches of the pre-handled pictures to enhance the accuracy of the architecture.

Overall, the DRIVE database had 190000 patches [124]. The surface, entropy, hard exudate district, vein region, and bifurcation destinations were removed from [125].

6.3. Methodology

Our suggested approach involves creating an optimal learning mechanism for grading fundus pictures, with higher grades associated with a higher risk of eye diseases that might cause blindness.

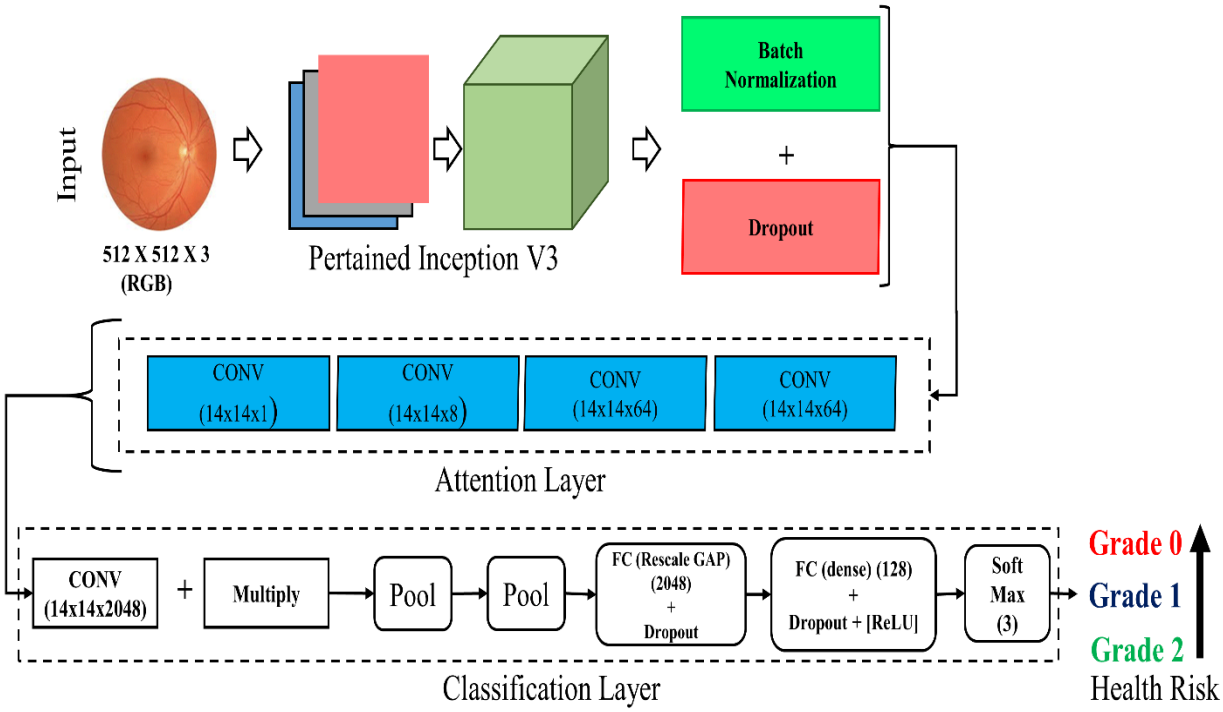

Fig. 6.2. Overview of the proposed fundus images Tortuosity Measurement framework for Diagnosing Glaucoma

Early identification of these symptoms is possible with the use of this approach. It has been observed that one of the key areas utilized to evaluate eyes is the vasculature. For categorization, we use an attention network that adds attention to nearby pixels. The feature utilized in the strategy to assess the attention is Inception V3. The general procedure is illustrated in Figure.6. 2.

Utilizing our proposed system, we fostered an ideal learning technique to arrange fundus photos. With level, the likelihood of becoming blind rises. The technique can be applied to find such indications early on. It should be noted that now the vein is one of the central regions utilized to even out the eye. The target of this test is to foster a profound learning model for sorting vessels in fundus pictures. We proposed U-Net for the undertaking of

separating retinal vessels. The initial U-Net now includes a contemplation module and is supplemented with a contemplation module. Convolution is replaced in the element layer by severe convolution, and two alternate routes are introduced to the element layer, allowing the model to isolate pixels from the fundus picture and better differentiate the intricacies of blood vessels. The overall procedure is displayed in Figure 6.3. The organization of U-Net is like that of FCN [126]. The key difference is that U-Net makes use of a symmetric encoder structure that incorporates development and pressure mechanisms. The traditional CNN model is executed involving layers of convolution and grouping in the strain strategy. The message is a fluffy picture with a size of 572×572 pixels. The expansion approach (the right half square of in Figure 6.3) contains a CNN layer, so the element channels are reduced to one, furthermore, the guide is incorporated to reset as a solitary picture Size [127]. The globalization model came to and neighbourhood data as a result of the lacking association between the created method and the compressed approach.

The division is completed by using the prior model's 1 x 1 convolution to separate component vectors into the necessary number of classes and working with the SoftMax layers to provide base and target probability estimates. Such a simple U-Net balancing structure has demonstrated startling performance in various biomedical applications.

6.4. Experimental result

A. Database

Division-focused datasets are frequently utilized in the front. Here, we provide an optional approach to handle the identical layout used in the most recent datasets for evaluating illnesses. The first image is from the Kaggle database1, which has 88702 fundus pictures in it. To improve Inception V3.0 and produce a pretrained model for feature extraction, all of the photos are used. The Eye Images Analysis Research Group has made the EIARG1 database [114] available for image-based research on retinal blood vessel tortuosity in diabetic retinopathy.This method needs a dataset that has been subjected to several wellness tests. In the DRIVE [128], there are 40 fundus images. We choose 20 images for training, and we use the additional 20 images for testing. These images of the retinal fundus were taken with a camera at a 45-degree angle. Each image's pixels measure 584 by 565. The public Spotlight Images dataset is mostly used to assess an image's tortuosity [129]. The 120 retinal images in the dataset are used to validate the suggested methodology. As mentioned earlier, we improved the images so that you can practice.

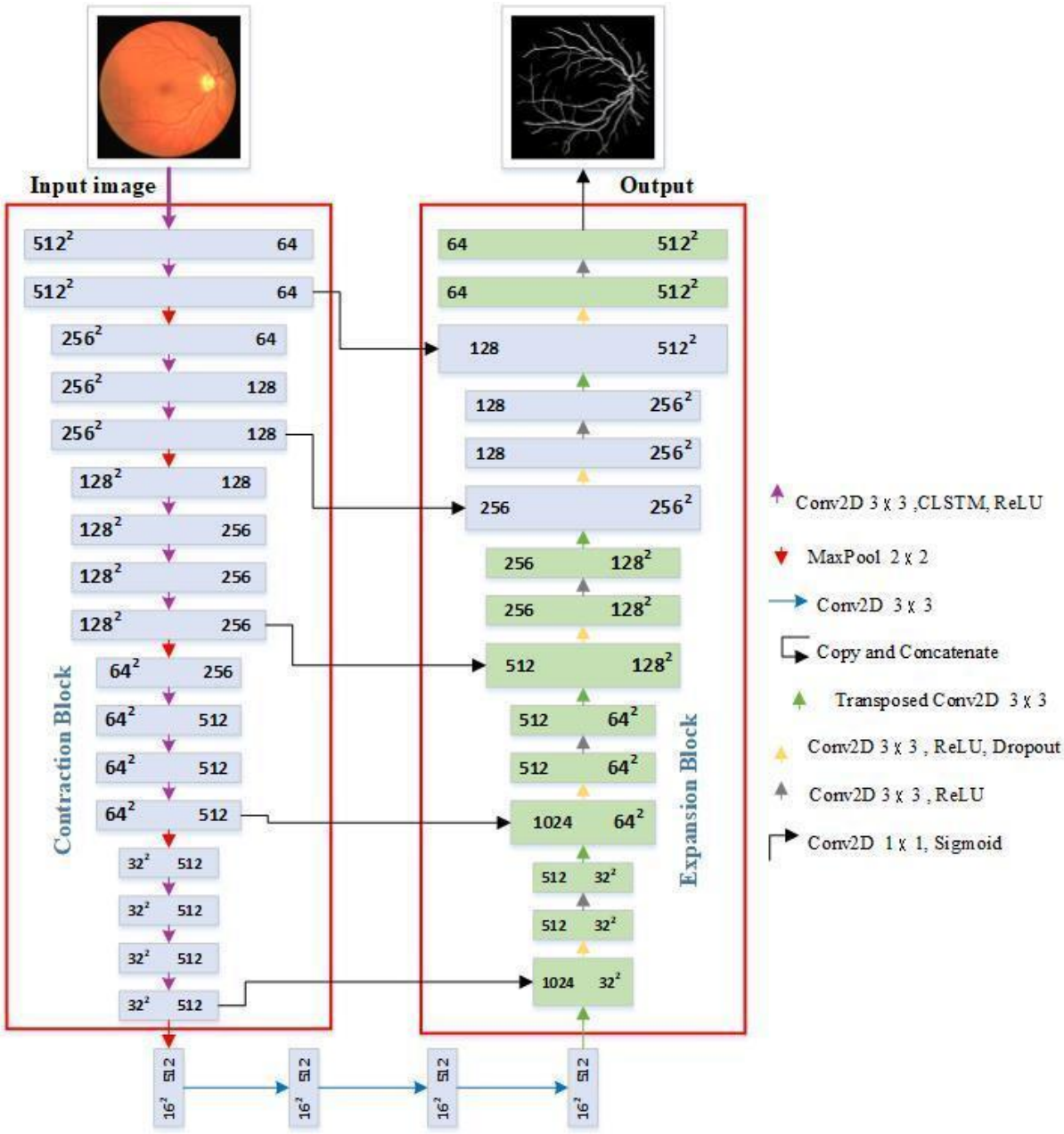

Fig 6.3. Proposed U-Net model

B. Experimental Outcomes

Our suggested approach has been distinguished from the most recent brain network-based reviewing methodology. Table 6.1 lists the discoveries in chronological order. In this section, we directed a basic assessment of the suggested technique's findings as well as the benchmarked results. The information includes hand-assigned grades from various

specialists. Figure 6.4 depicts the vessel division. Effects of splitting two retinal images: the variety of retinal images (p, t); (m) (q)

Exactness, explicitness, and awareness are taken into consideration as the standards for evaluating the proposed network's exposition. The exactness is measured by how often events are accurately predicted. While awareness demonstrates the likelihood of correctly differentiating between sick patients, explicitness demonstrates the likelihood of correctly differentiating between healthy individuals. The numerical articulations for Acc will be discussed next.

While the foundation and macula pixels that were incorrectly perceived are handled separately by FN and FP, the foundation and macula pixels that were correctly perceived are dealt with by TN and TP.

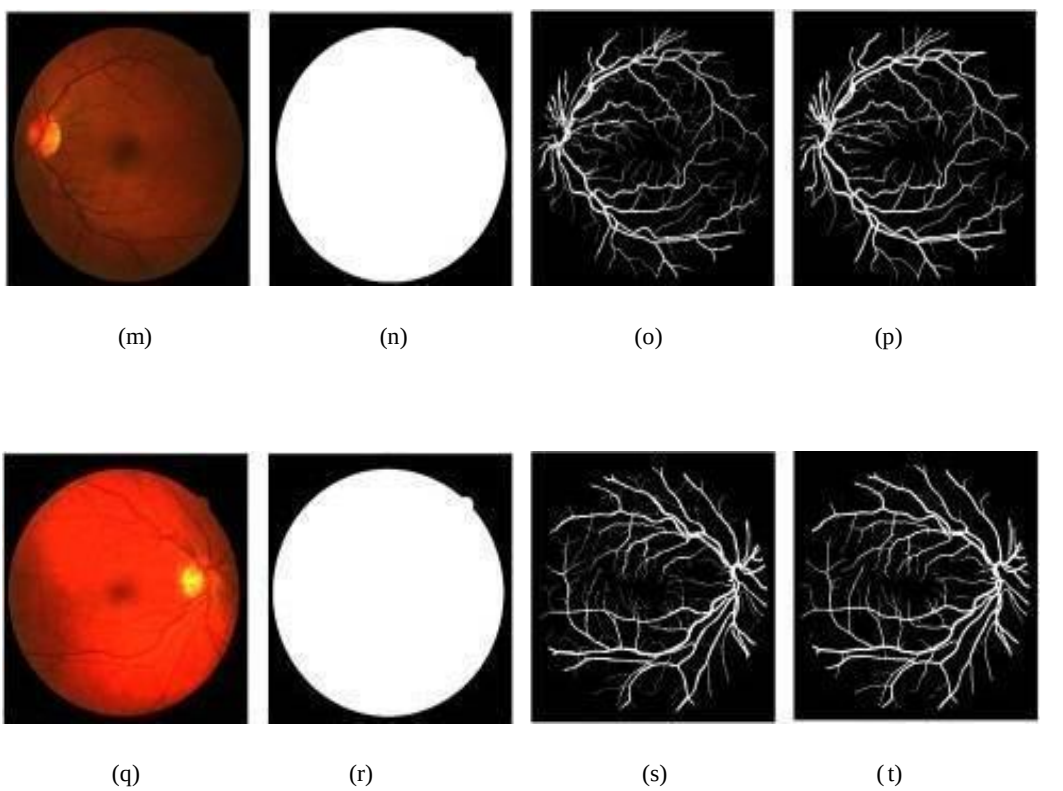

Fig 6.4. Segmentation results of two retinal image

Table 6.1

Performance analysis of the suggested technique and the other existing approaches on DRIVE database:

Methodology	Sensitivity	Specificity	Accuracy
Roychowdhury [130]	0.7249	0.9830	0.9520
Qiaoliang Li [131]	0.7406	0.9807	0.9527
Residual UNet [132]	0.7332	0.9782	0.9553
Recurrent UNet [133]	0.7569	0.9830	0.9556
R2U-Net [134]	0.7520	0.9806	0.9556
DEU-Net [135]	0.8039	0.9804	0.9567
Proposed	**0.8209**	**0.9731**	**0.9568**

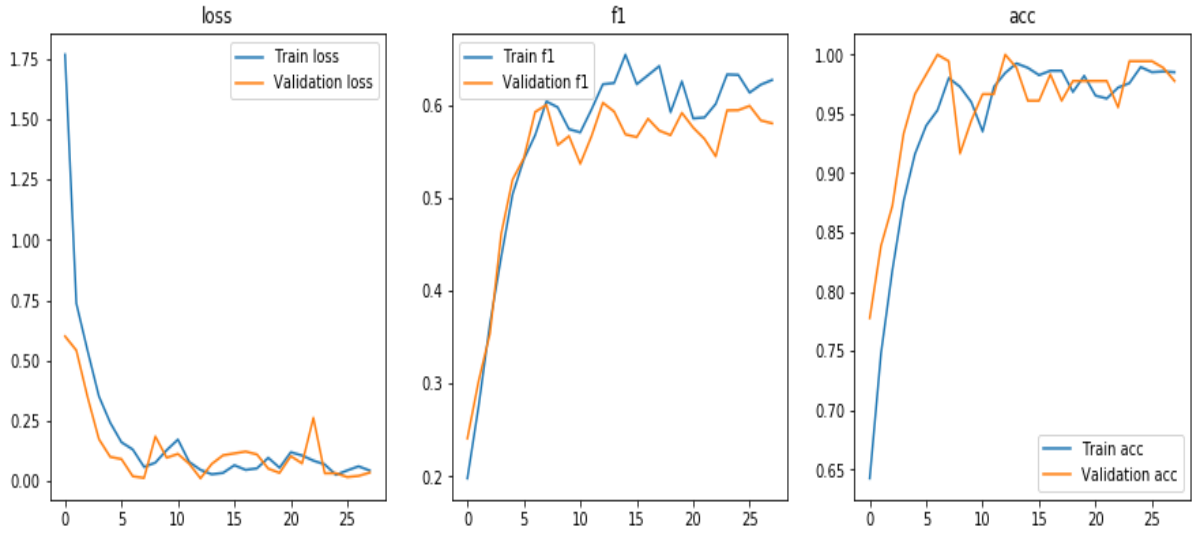

Fig. 6.5. Training and validation loss,f1,Accuracy during training using U-NET

The updated U-net model is trained on 25 epochs and the DRIVE database is used. The DRIVE information base contains 40 fundus pictures, 20 of which are for training purposes. 20 for the test, plus 20. Each fundus image has a specific size. Resolution: 584 x 768 pixels In Figure 6.3, the loss is depicted. Results of the training and validation loss utilizing U-NET [136] segmentation. Four training and testing folds were applied to each of the 20 fundus pictures utilized in the experiment. As a result, all 20 pictures are used to train and evaluate

the experimental model. Utilizing 14 Kaggle GPUs and two chip conditions, the model is put together. On both DRIVE [137,140] fundus images, 1 NVIDIA Tesla K80 GPU, GB Crush, and a bundle size of 4 are used since some of the fundus images in the database feature blood vessels that have been extensively damaged by the ocular sickness, resulting in a substantially lower than average score.

C. VTI Measurement

For the data points in our database, the VTI was successfully estimated. For a total of our database eyes, the MAC was successfully computed. VTI and MAC were not estimated for the three eyes. In a photograph with fewer than three retinal vessels of a single kind, indices could not be determined. Due to the challenges in categorizing and segmenting the vessels, it was impossible to determine the precise number of vessels. VTI and MAC were subjected to inter-rater and inter-image comparisons. In MAC comparisons, a single outlier had a significant impact. This outlier was caused by the rater misidentifying the optic disc center on one retinal image, this changed a branch point into the ROI and had an impact on a single vessel's tortuosity index, according to an examination of the photos.

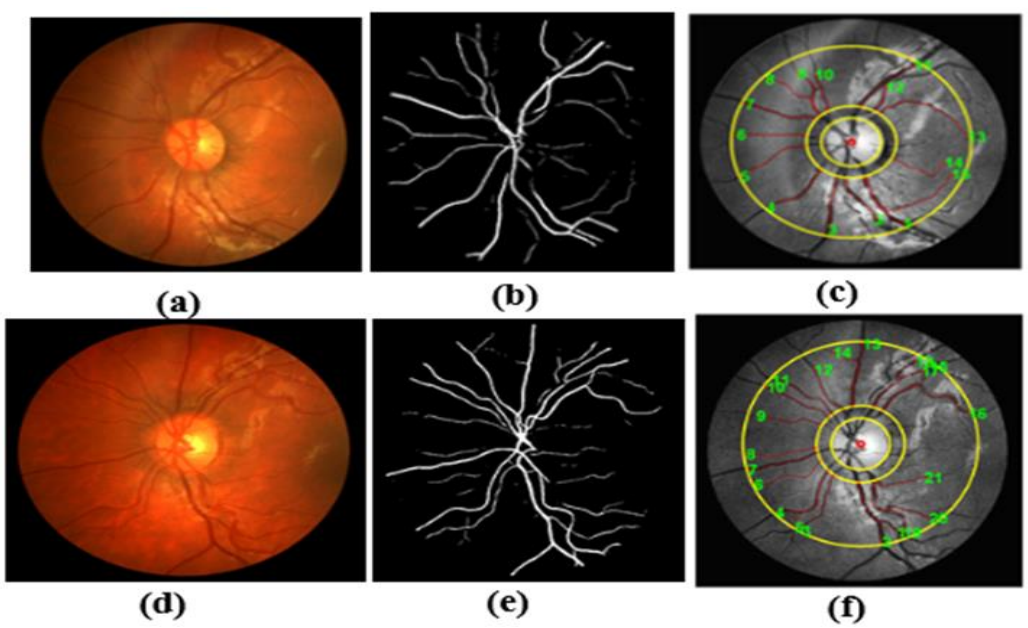

Fig. 6.6. (a) A test image from CHASE_DB1(02_test_img.png) dataset; (b) The Segmentation result by Modified-Unet; (c) Tortuosity Measurement result ; (d) A test image from CHASE_DB1(03_test_img.png) dataset; (e) Segmentation result by Modified -Unet; (f) Tortuosity Measurement result

Figure 6.6 displays the outcome of vessel segmentation and visualisation of vessel tortuosity, with red denoting the tortured section of vessels and blue denoting the vessel index number. This is in line with the findings, which depend on qualitative measurements of retinal blood vessel tortuosity such as the Vessel Tortuosity Index (VTI) and Mean Absolute Curvature (MAC).The quantitative findings for the CHASE DB1(02 test img.png,03 test img.png) dataset are shown in Tables 6.2. For distinct data sets, we examine the Vessel Tortuosity Index (VTI), Density Index (DI), Distance Measure (DM), and Mean Absolute Curvature (MAC).

Table 6.2

The proposed method's outcomes for the CHASE_DB1 (02_test_img.png) dataset:

Vessel No.	**Vessel Tortuosity Index (VTI)**	**Density Index (DI)**	**Distance Measure (DM)**	**Mean Absolute Curvature (MAC)**
1	0.1586901	0.004867005	1.036904227	0.003793807
2	0.1257062	0.0058943	1.024380516	0.003605759
3	0.0297773	0.005117095	1.001383957	0.001074189
4	0.2064939	0.004795791	1.059863752	0.003109545
5	0.1397940	0.004617853	1.028874683	0.003295589
6	0.0460169	0.004910253	1.001237495	0.000695423
7	0.1897349	0.004636758	1.016437289	0.002021738
8	0.2440431	0.005140926	1.075761089	0.007268769
9	0.4113942	0.006508642	1.065329926	0.005043445
10	0.0289423	0.007197261	1.001247955	0.001839045
11	0.0833599	0.004471557	1.010480613	0.001627951
12	0.1353117	0.010610697	1.025632715	0.003412778
13	0.1947861	0.003691748	1.172898589	0.00393452
14	0.2308415	0.007202627	1.292140002	0.007196718
15	0.3303021	0.003883327	1.503997013	0.005137457

Table.6.3.

Overall comparison the accuracy measure is retinopathy score (SRCC):

Reference	Method	Database	#of images	Performance (SRCC)
Grisan et al. [111]	Inflection-based measurement	RET-TORT	60	0.949 (artery), 0.853 (vein)
Lagali et al. [136]	Combination of measures	Non-public dataset	20	0.95
Aghamohamadian et al. [139]	Curvature-based measurement	RET-TORT	60	0.94
Proposed Inception V3 Method	**Attention network**	**RET-TORT**	**60**	**0.99**

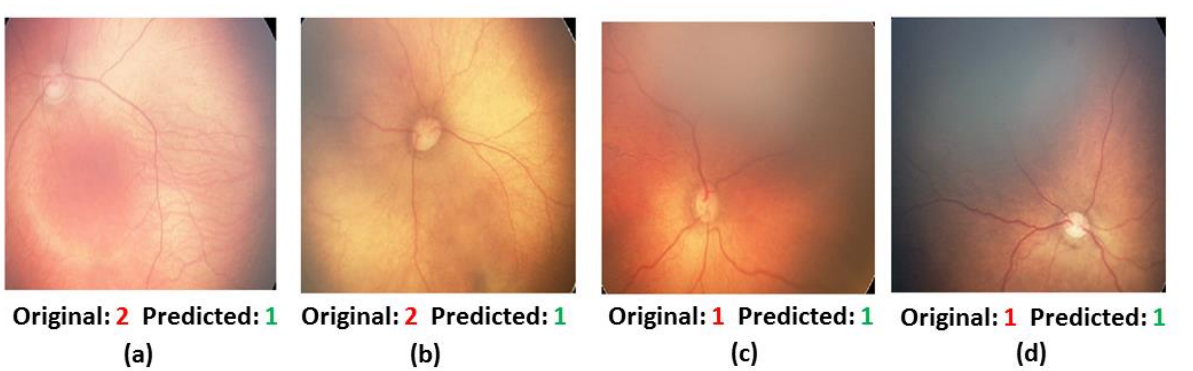

Fig. 6.7. Some random example of failure cases a–b and successfully obtained grade c–d using proposed method

We have estimated the correlation of each expert (doctors) with the automated method proposed in our method. Table 6.3 shows the results. It is observed that our proposed method ends with a higher correlation with experts. Figure 6.7 demonstrates some random successfully identified grades and failure cases.

6.5. Summary

In diabetic retinopathy, grading fundus pictures according to the tortuosity (vessel curve) is typical. It requires specialty doctors since it is difficult. Such fundus pictures may be automatically graded, which might be a helpful tool in different automatic diagnostic systems. Since the approach is still in its early stages, there are relatively few datasets and extremely few samples accessible for each grade level. The latest techniques rely on segmenting the vessel to determine the curvature and grade the pictures, a challenging process with subpar results. In this study, we have presented automated grading of such photos driven by deep learning. In order to extract features, we have employed transfer learning, wherein Inception V3 has been trained using 88702 fundus pictures.

A changed U-NET engineering was presented in this paper for the vascular division of retinal pictures. It performed better than a licensed ophthalmologist and delivered better outcomes in the DRIVE database. According to Table 1, when contrasted with previous photo vessel division techniques, the precision of the strategy proposed in this DRIVE work is 0.9568. In other words, when other strategies are contrasted, our method is superior. While the results from actual fundus photographs aren't as good as those from the DRIVE database. The images taken by the ophthalmologist would therefore contain some sounds. We guarantee that removing noise from raw photographs will yield significantly better results.

CHAPTER 7

CONCLUSION AND FUTURE SCOPE

7.1. Conclusion

In conclusion, the CNN-based approach proposed in this study demonstrates significant advancements in grading vessel tortuosity, particularly for the assessment of diabetic retinopathy. By integrating the Focal Loss function, our model achieves superior accuracy compared to traditional curvature-based methods, thereby enhancing its applicability in clinical settings. The use of the Focal Loss function effectively addresses class imbalance issues, which is critical in medical image analysis where certain pathological features may be underrepresented.Despite the current complex architecture of the model, efforts to simplify the model while maintaining high accuracy are warranted. Such simplification would not only streamline the computational requirements but also facilitate easier integration into existing medical imaging workflows. The validation of our model against expert opinions underscores its reliability and potential for automating grading tasks effectively. This alignment with expert assessments ensures that the model's predictions are clinically relevant and trustworthy.Future research could focus on refining the model for broader deployment. This includes optimizing the model to reduce computational complexity and enhance its real-time processing capabilities. Additionally, developing user-friendly mobile applications could significantly facilitate accessibility, particularly in remote and underserved areas where access to specialized diagnostic tools is limited. Mobile-based diagnostic tools could provide immediate feedback to healthcare providers, enabling timely intervention and improving patient outcomes.Furthermore, expanding the training dataset to include a more diverse range of retinal images from various populations can improve the model's generalizability. Collaborative efforts with ophthalmologists and other medical professionals can aid in continually updating the model with the latest clinical insights and ensuring its robustness in diverse clinical scenarios.

In summary, the proposed CNN-based approach, with its integration of the Focal Loss function and validation against expert opinions, presents a promising solution for automating the grading of vessel tortuosity. Its potential to be simplified and deployed in user-friendly

formats makes it a valuable tool for enhancing diabetic retinopathy assessment, particularly in resource-limited settings. Future developments aimed at optimizing and expanding the model's application will further solidify its role in advancing medical diagnostics.

In this study, we presented a VGG-16 network-based patch method for the automatic classification of tortuous retinal vessels. The primary aim was to leverage the power of deep learning, particularly the well-established VGG-16 architecture, to accurately identify and classify tortuosity in retinal blood vessels from retinal fundus images. Our approach demonstrated high accuracy in classifying retinal vessel tortuosity, showcasing the effectiveness of the VGG-16 architecture in capturing and learning the intricate features of retinal images.

When compared with existing methods and baseline models, our VGG-16 based approach showed superior performance in terms of precision, recall, and overall classification metrics, establishing it as a promising tool for automated retinal vessel analysis. The model's architecture allowed it to effectively learn the complex patterns associated with tortuous vessels, thereby improving its classification accuracy.

The Modified EfficientNet model demonstrates significant effectiveness in detecting and grading diabetic retinopathy (DR) based on retinal blood vessel tortuosity. Utilizing comprehensive evaluation metrics, this model surpasses state-of-the-art CNN networks such as VGG-16, ResNet-50, and DenseNet-121. Specifically, the model achieves an accuracy of 93.92%, a precision of 93.99%, and a Kappa score of 87.95%. These results underscore the model's superior performance in the automated detection and grading of DR. The evaluation was conducted using the APTOS 2019 dataset, which ensures the robustness and reliability of the results. The model's focus on retinal blood vessel tortuosity allows it to capture intricate patterns and abnormalities associated with DR, which are critical for accurate diagnosis and grading. This approach significantly aids in automating the analysis of retinal fundus images, providing an efficient and reliable tool for diagnosing and managing DR.

we presented an advanced methodology for grading retinal blood vessel tortuosity by integrating the Inception V3 network for classification and a modified U-Net architecture for vessel segmentation. Our dual approach aimed to enhance the accuracy and robustness of tortuosity grading by leveraging state-of-the-art deep learning models.

The Inception V3 network demonstrated exceptional performance in grading retinal vessel tortuosity, effectively distinguishing between different levels of tortuosity with high precision

and recall. Its deep and complex architecture enabled the capture of intricate patterns in retinal images, thereby improving classification accuracy. The modified U-Net architecture provided precise and detailed segmentation of retinal blood vessels, which is crucial for accurate analysis and grading of tortuosity. The U-Net's ability to perform pixel-level classification ensured that the segmentation results were highly accurate, serving as a reliable foundation for subsequent grading.

The primary cause of vision loss and retinal damage is diabetic retinopathy. The risk of saving the eye from blindness decreases with earlier DR treatment. If neglected, it might become severely worse and there would be no way to stop the loss of eyesight. Therefore, for early discovery and treatment, the patient must undergo a thorough screening. To help ophthalmologists see the retina more clearly, the suggested research focuses on the automated detection of DR. This study uses newly created algorithms and image processing approaches to identify blood vessels, MAs, HAs, ODs, and exudates in colour retinal fundus pictures. The grading is done to determine the disease's severity.

Based on the physical structures and abnormalities in retinal fundus pictures, the characteristics of the early indicators of nonproliferative DR, such as blood vessels, microaneurysms, haemorrhages, and exudates, are identified and categorised in this research effort. The screening outcomes of the suggested techniques are contrasted taking into account statistical aspects. Over 500 retinal images were used in the testing, which was done using several databases. The suggested system's outputs are examined and annotated according to ophthalmologists' recommendations.

The suggested work has demonstrated that CNN, Efficient Net, Modified U-net Architecture, and VGG-16 Network are used to classify the automated diagnosis of DR by segmenting the blood vessels, MAs, HAs, and EXs with the severity level grading. The advantage of employing a trained network is that you can get a quick diagnosis and report instead of waiting for a doctor to diagnose the illness. Identifying the normal and severe pictures is not problematic, but at an earlier point, classifying the DR as mild and moderate is problematic. The importance of this effort is that it will allow for a quicker and less expensive early diagnosis of the illness. For successfully recognising the DR early on, the suggested CNN, Efficient Net, Modified U-net Architecture, and VGG-16 Network have all been tested.

Through the implementation and evaluation of our proposed methodology, we have demonstrated the feasibility and potential of using artificial intelligence (AI) algorithms to

accurately grade vessel tortuosity in retinal fundus images. Our developed model has shown promising results, achieving a high level of accuracy and providing efficient and reliable grading of vessel tortuosity in comparison to manual grading by ophthalmologists.

The utilization of a carefully curated dataset, encompassing a range of DR severity levels, has allowed us to train and fine-tune our model to recognize and quantify vessel tortuosity accurately. The integration of deep learning techniques, such as convolutional neural networks (CNNs), has enabled the extraction of meaningful features and patterns from retinal fundus images, contributing to the model's ability to differentiate between different levels of vessel tortuosity.

Moreover, the interpretability of our model has been addressed, as we believe that explainable AI is crucial for gaining trust and acceptance in clinical settings. Through the incorporation of attention mechanisms and saliency maps, we have provided visual explanations that highlight regions and features in the retinal images contributing to the grading of vessel tortuosity. This interpretability aspect enhances the transparency and understanding ability of our model's predictions, enabling ophthalmologists and clinicians to gain insights into the decision-making process.

It is important to note that our work is not without limitations. The development of an automatic grading tool for vessel tortuosity in retinal fundus images is a complex task that requires careful consideration of various factors, such as dataset quality, model architecture, and generalizability. While our model has shown promising results, further validation on larger and more diverse datasets, as well as external evaluation in clinical settings, is necessary to ensure its robustness and real-world applicability.

Despite these limitations, the potential impact of our research is significant. The development of an accurate and efficient tool for the automatic grading of vessel tortuosity in retinal fundus images has the potential to revolutionize the screening and diagnosis of diabetic retinopathy. By enabling early detection and monitoring of DR, this tool can facilitate timely interventions and improve patient outcomes, ultimately reducing the burden on healthcare systems and improving the quality of life for individuals affected by this debilitating disease.

The field of medical image analysis and automated diagnosis by providing a comprehensive framework for the automatic grading of vessel tortuosity in retinal fundus images for DR screening. The proposed methodology, combined with further research and validation, holds great promise for the development of an effective clinical tool that can assist

ophthalmologists and clinicians in the early detection and management of diabetic retinopathy, leading to better patient care and outcomes.

The proposed method with the modified network in Chapter 3 has the best performance metrics in terms of accuracy. As mentioned before, the modified CNN is built by building on top of Vgg16 and Resnet50. Although the network design has a bit of complexity, it brings out the best performance from the model. The thesis suggests that for the problem we address, this model can be used in large-scale. Even in the simulation results, it achieves 85% accuracy. After training on more real-world data, the model's resultant accuracy will be reasonably high.

7.2. Future work

The following suggestions for future improvement are made as a result of the study that was the subject of the current research.

1. In the future, develop an algorithm for classification of diabetes and integrate it into a fundus camera with today's diagnostic system. The builtin processor of the Fundus camera is capable of producing a report indicating the severity of the disease state.
2. By using the methods with a huge amount of data, the deep learning classifier's efficiency and accuracy are increased.
3. In the future, develop the algorithm for DR detection and include it in the fundus camera together with the present diagnosis system. The fundus camera's built-in processor can produce a report that rates the severity of the DR condition. In isolated and rural areas, no skilled technicians are needed.
4. Developing more advanced convolutional neural networks (CNNs) and other deep learning architectures to improve the accuracy and robustness of tortuosity detection and grading.
5. Developing cloud-based platforms that allow for large-scale analysis and storage of retinal images, making it easier for multiple healthcare providers to access and share data.
6. Implementing real-time analysis on portable devices.
7. The processing time can be reduced by upgrading the serial processing techniques.

REFERENCES

[1] Acharya U, R, Chua, CK, Ng, EYK, Yu, W & Chee, C 2008, " Application of higher order spectra for the identification of diabetes retinopathy stages", Journal of Medical Systems, vol. 32, no. 6, pp. 481-488.

[2] Acharya, UR, Lim, CM, Ng, EYK, Chee, C & Tamura, T 2009, "Computer-based detection of diabetes retinopathy stages using digital fundus images", Proceedings of the Institution of Mechanical Engineers, Part H: Journal of Engineering in Medicine, vol. 223, no. 5, pp. 545-553.

[3] Acharya, UR, Ng, EYK, Tan, JH, Sree, SV & Ng, KH 2012, "An integrated index for the identification of diabetic retinopathy stages using texture parameters", Journal of Medical Systems, vol. 36, no. 3, pp. 2011-2020.

[4] Aquino, A, Geg, ME & Mar, D 2012, "Automated optic disk detection in retinal images of patients with diabetic retinopathy and risk of macular edema", International Journal of Biological & Life Sciences, vol. 8, no. 2, pp. 87-92.

[5] Aquino, A, Gegndez-Arias, ME & Marn, D 2010, "Detecting the optic disc boundary in digital fundus images using morphological, edge detection, and feature extraction techniques", IEEE Transactions on Medical Imaging, vol. 29, no. 11, pp. 1860-1869.

[6] Blondin, J 2009, "Particle swarm optimization: A tutorial', Availaible from: http://cs. armstrong. edu/saad/csci8100/pso tutorial. pdf.

[7] Coello Coello, CA & Reyes-Sierra, M 2006, "Multi-Objective Particle Swarm Optimizers: A Survey of the State-of-the-Art", International Journal of Computational Intelligence Research, vol. 2, no. 3.

[8] Cornforth, DJ, Jelinek, HJ, Leandro, JJG, Soares, JVB & Cesar, RM 2005, "Development of retinal blood vessel segmentation methodology using wavelet transforms for assessment of diabetic retinopathy", Journal of Complexity International, vol. 11, pp. 50-61.

[9] Cree, MJ, Olson, JA, McHardy, KC, Sharp, PF & Forrester, JV 1997, "A fully automated comparative microaneurysm digital detection system", Eye, vol. 11, no. 5, pp. 622-628.

[10] Deb, K, Agrawal, S, Pratap, A & Meyarivan, T 2000, "A Fast Elitist Non-Dominated Sorting Genetic Algorithm for Multi-Objective Optimization: NSGA-II", PPSN VI Proceedings of the 6th International Conference on Parallel Problem Solving from Nature, no. Springer- Verlag London.

[11] Deb, K, Pratap, A, Agarwal, S & Meyarivan, T 2002, "A fast and elitist multiobjective genetic algorithm: NSGA-II", IEEE Transactions on Evolutionary Computation, vol. 6, no. 2, pp. 182-197.

[12] Durillo, JJ, García-Nieto, J, Nebro, AJ, Coello Coello, CA, Luna, F & Alba, E 2010, "Multi-objective particle swarm optimizers: An experimental comparison", Lecture Notes in Computer Science (including subseries Lecture Notes in Artificial Intelligence and Lecture Notes in Bioinformatics), vol. 5467 LNCS, pp. 495-509.

[13] Eeb, AD, Engineering, E & Madras, IIT "Detection of Red Lesions in Eye Fundus Images", pp. 21-23.

[14] https:// www.carlsonstockart.com

[15] Faust, O, Acharya U, R, Ng, EYK, Ng, K-H & Suri, JS 2012, "Algorithms for the Automated Detection of Diabetic Retinopathy Using Digital Fundus Images: A Review",Journal of Medical Systems, vol. 36, no. 1, pp. 145-157.

[16] Fraz, MM, Remagnino, P, Hoppe, A, Uyyanonvara, B, Rudnicka, AR, Owen, CG & Barman, SA 2012, "Blood vessel segmentation methodologies in retinal images--a survey",Computer methods and programs in biomedicine, vol. 108, no. 1, pp. 407-433.

[17] Gagnon, L 2001, "Procedure to detect anatomical structures in optical fundus images",Medical, vol. 4322, pp. 8-10.

[18] Giancardo, L, Meriaudeau, F, Karnowski, TP, Li, Y, Garg, S, Tobin, KW & Chaum, E 2012, "Exudate-based diabetic macular edema detection in fundus images using publicly available datasets",Medical Image Analysis, vol. 16, no. 1, pp. 216-226.

[19] Goatman, K, Charnley, A, Webster, L & Nussey, S 2011, "Assessment of automated disease detection in diabetic retinopathy screening using two-field photography",PLoS One, vol. 6, no. 12, pp. e27524-e27524.

[20] Goldbaum, M, Moezzi, S, Taylor, A, Chatterjee, S, Boyd, J, Hunter, E & Jain, R "Automated diagnosis and image understanding with object extraction, object

classification, and inferencing in retinal images",Proceedings of 3rd IEEE International Conference on Image Processing, vol. 3, pp. 695-698.

[21] S. Roychowdhury, D. Koozekanani, and K. Parhi (2013) "DREAM: Utilizing AI to investigate diabetic retinopathy'. 18(5):1717-1728 IEEE J Biomed Health Informatics.

[22] Gayathri S, Krishna AK, Gopi VP, Palanisamy P "Robotized twofold and multiclass order of diabetic retinopathy utilizing haralick and multiresolution highlights", (2020). 57497-57504 IEEE Access 8.

[23] Akram MU, Khalid S, Tariq A, Khan SA, and Azam F "The identification and characterization of retinal injuries for the evaluating of diabetic retinopathy was distributed",(2014). Comput Biomedicine 45:161-171.

[24] H. Pratt, F. Coenen, D. Broadbent, S. Harding, and Y. Zheng (2016) "neural networks with convolutional layers for diabetic retinopathy", 90:200–205 in Procedia Computer Science.

[25] Mookiah MRK, Martis RJ, Acharya UR,Chua CK, Lim CM, Ng EYK, and Laude A (2013) "Evolutionary algorithm based classifier parameter tweaking for autonomous diabetic retinopathy evaluating: A half and half component extraction technique",39:9–22 Knowledgebased Syst.

[26] Long, J., Shelhamer, E., and Darrell (2015) "Convolutional networks in their entirety for semantic segmentation",3431-3440 in: Procedures of the IEEE meeting on PC vision and example acknowledgment.

[27] Lian, S., Zhong, Z., Lin, X., Su, and Li (2018) "U-Net was guided by attention to segment the iris with accuracy",56:296-304 J Vis Commun Image Represent.

[28] Bansal N., Dutta M. (2013) "Retina vessels identification method for biomedical side effects conclusion",71 Int J Comput Appl (20).

[29] Van Ginneken, B., Niemeijer, M., and Staal J. (2004) "Ridge-based vascular segmentation in retinal colour pictures",501–509, IEEE Trans Med Imaging, 23(4).

[30] Hoover A.D., Kouznetsova V., and M. Goldbaum (2000) "Blood vessel location in retinal pictures by piecewise threshold examining of a matched channel reaction",203–210. IEEE Trans Med Imaging, 19(3).

[31] Fraz MM, Hoppe A, Remagnino P, Rudnicka AR, Uyyanonvara B, Owen CG, and Barman SA 30 (2012) "An ensemble classification-based approach was used to segment retinal blood vessels",2538–2548. IEEE Trans Biomed Eng, 59(9).

[32] A. Budai, R. Bock, A. Maier, J. Hornegger, and G. Michelson (2013) "powerful vessel division in fundus pictures", International Journal of Biomedical Imaging 2013.

[33] Prentai P, Lonari S, Vatavuk Z, Beni G, Subai M, Petkovi T, Dujmovi L, Malenica-Ravli M, Budimlija N, Tadi R (2013) "Diabetic retinopathy images database (DRiDB): a clever data set for diabetic retinopathy screening program research eighth Worldwide Discussion on Picture and Sign Handling and Analysis",2013, p. (ISPA). IEEE, pages 711–716.

[34] Estrada, R., Allingham, M.J., Mettu, P.S., Cousins, S.W., Tomasi, and S. (2015) "Using topology estimation, classify the retinal arteries and veins",2518–2534 IEEE Trans Med Imaging 34(12).

[35] Holm, S., Russell, G., Nourrit, and N. McLoughlin are 34. (2017) "DR HAGIS is a fundus picture data set for the programmed extraction of diabetes patients' retinal surface vessels",J. Med. Imaging 4(1): 14503.

[36] Roychowdhury, S., D., and K. Koozekanani (2014) "Segmenting blood vessels in fundus images using subimage classification and main vessel extraction",IEEE J Biomed Health Inform 19(3):1118-1128.

[37] Li Q, Xie L, Feng B, Liang P, Zhang H, and Wang T. (2015) "A multimodal learning strategy for segmenting vessels in retinal pictures",109–118, IEEE Trans Prescription Imaging 35(1).

[38] Alom MZ, Yakopcic C, Hasan M, Taha TM, and Asari VK (2018) "Intermittent Remaining Convolutional Brain Organization based on U-Net (R2U-Net) for Clinical Picture Division",

[39] Wang, B., Qiu, S., and He, H. (2019) "Segmenting retinal vessels using a dual-encoding u-net. At: The Global Meeting on Clinical Picture Registering and PC Helped Mediation",84–92 in Springer.

[40] Maji D, Dhara AK, Maiti S and Sarkar (2022) "Programmed discovery and division of the optic disc that using a modified Network of convolution algorithm",Biology of Signal Processing in Medicine 76:103633.

[41] Programmed T. Sabeenian and Shanthi, "RS Modified Alexnet architecture for categorization of diabetic retinopathy images", Comput. Electr. Eng. 2019, 76, 56–64.

[42] M. A. Sharbaf, T. Banaee and H. R. Pourreza "A novel curvature-based method for automatically grading retinal blood vessel tortuosity",IEEE diary of biomedical and wellbeing informatics, vol. 20, no. 2, in 2016.

[43] E. Trucco, H. Azegrouz, B. Dhillon, I. J. MacCormick and T. MacGillivray "Thickness subordinate convolution assessment for retinal blood vessels", Designing in Medication and Science Society's 28th Yearly Global Gathering of the IEEE, pp. 4675–4678, in 2006.

[44] M. E. Craig, P. B. -Aguirre, M.B. Sasongko, N. Cheung, A. J. Jenkins, T. Y. Wong, J. J. Wang, and K. C. Donaghue "Retinal vascular math predicts episode retinopathy in youthful persons with type 1 diabetes: an imminent partner research from adolescence",Diabetes Care, p. 102419, 2011.

[45] E. Bribiesca "A proportion of convolution in view of chain coding was described",Design Acknowledgment, vol. 46, no. 3, 2013, pp. 716-724.

[46] E. Bullitt, G. Gerig, S. M. Pizer, W. Lin, and S. R. Aylward "Measuring the convolution of the intracerebral vasculature using mraimages was described", IEEE Transactions on Medical Imaging, vol. 22, no. 9, pp. 1163–1171, in 2003.

[47] A. Chakravarty and J. Siva Swamy, "A novel method for measuring retinal vascular convolution utilizing quadratic polynomial decomposition", Clinical Informatics and Telemedicine, [Indian Conference IEEE], pp. 7–12, 2013.

[48] D. S. Fong, G. L. King, T. W. Gardner, L. Aiello, G. Blankenship, J. D. Cavallerano, R. Klein and F. L. Ferris "Retinopathy in diabetes", Diabetes Care, vol. 27(1), pp. s84–s87, 2004.

[49] E. Grisan, A. Ruggeri, M. Foracchia "A unique approach for the programmed reviewing of retinal artery tortuosity was described", IEEE Transactions on Clinical Imaging, volume 27, number 3, pp. 310-19, in 2008.

[50] . W. E. Hart, B. Cote, M. Goldbaum, P. Kube and M. R. Nelson "Estimation and order of retinal vascular convolution", International Diary of Clinical Informatics, volume 53(2-3), pp. 239–252, 1999.

[51] C. Heneghan, J. Flynn, M. O. Keefe, and M. Cahill "Characterization of adjustments in vein width and convolution in retinopathy of prematurity using image analysis", Medical image analysis, vol. 6, no. 4, pp. 407-429, 2002.

[52] G. Y. H. Lip, A.A. Kalitzeos, and R. Heitmar "Retinal vascular convolution measures and their applications", Experimental Eye Research, 2013, Volume 106, Pages 40–46.

[53] Sk. Latib, M. Mukherjee, D. K. Kole, and C. Giri."Automatic tortuosity identification and estimation of retinal vein organization", High level Registering, Systems administration and Informatics, Springer, vol. 1, pp. 483-492, 2014.

[54] S. Liu and W.Deng, "Very profound convolutional brain network based image classification with limited training sample size", 3rd IAPR Asian conference on pattern recognition, IEEE, pp. 730-734, 2015.

[55] W. Lotmar, A. Freiburghaus, and D. Bracher "Measurement of vascular tortuosity on fundus photos was described", Albrecht von Graefes Archiv für klinische und experimentelle Ophthalmologie, volume 211, no. 1, in 1979, pp. 49–57.

[56] T. S. Kern, M. Mizutani and M. Lorenzi "Accelerated death of retina microvascular cells in people with and test diabetic retinopathy", The Diary of Clinical Examination, volume 97, no. 12, 1996, pp. 2883–2890.

[57] D. Onkaew, R. Turior, B. Uyyanonvara, N. Akinori, and C. Sinthanayothin "Automatic retinal vascular tortuosity measuring utilising curvature of enhanced chain code", Electrical, Control and PC Designing (INECCE), [International ConferenceIEEE], pp. 183–186, 2011.

[58] M. Patasius, V. Marozas, A. Lukosevicius, and D. Jegelevicius, "Evaluation of convolution of eye veins utilising the indispensable of square of derivative of curvature", EMBEC, vol. 5, pp. 20–25, 2005.

[59] M. B. Sasongko, T. T. Nguyen, T. Y. Wong, C. Y. Cheung, J. E. Shaw, and J. J. Wang, "Retinal vascular tortuosity in diabetic retinopathy", Diabetology, volume 54, number 9, pp. 2409-2416, 2011.

[60] R. Turior, P. Chutinantvarodom, and B. Uyyanonvara (2013) "Automatic tortuosity categorization using Deep Learning approach", Applied Mechanics and Materials, volume 241, pp. 3143-3147.

[61] D.S. Cavallerano, F., King, G., Gardner, G.L., Aiello, T.W., Fong, L., Blankenship, J.D., and G. L. Ferris and R. Klein, "Retinopathy with Diabetes Diabetes Treatment ",27 (suppl 1) (2004) s84-s87.

[62] W. Z. Wang and Rawat's article, "Deep convolutional neural networks in image analysis: A thorough study", appeared in Neural Computing. 29 (9) (2017) 2352–2449.

[63] Shahar, R. Cooper, L.D. Hubbard, M.R. Wofford, L.S. Cooper, A. Klein, D.J. Couper, E. "Retinal microvascular abnormalities with recurrent stroke: the atherosclerosis hazard in communities",The Lancet 358 (9288) (2001), 1134–1140.

[64] M.B. A.J. Jenkins, C. Sasongko, J. Shaw, T.Y. Wong, R. Kawasaki, A. Wang, T.T. Nguyen, J.J. Robinson. (2012) "Plasma apolipoproteins are linked to systemic & retinal microvascular functioning in diabetics",DB 111272 for diabetes.

[65] Mizutani, T.S. Kern, and M. Lorenzi "M. Accelerated mortality of retina microvascular cells in human & experimental diabetes retinopathy",J. Clin. Investig. 97 (12) 1996 2883–2890.

[66] Lotmar, A. Freiburghaus, and D. Bracher, Heinrich von Graefes "W. Measurement of vascular tortuosity on fundus photos",Experimental and Clinical Ophthalmology 211(1):49-57.

[67] Med. Heneghan, J. Flynn, M. Okeefe, and M. Cahill "Characterizing changes in blood vessel width & tortuosity in retinopathy with prematurity utilizing image analysis", Anal image. 6 (4) 2002 407–429.

[68] A.J. Jenkins, Benitez-Aguirre, M.B. Sasongko, T.Y. Wong, M.E. Craig, J.J. Wang, N. Cheung, and K.C. Donaghue. (2011) "Retinal vascular architecture predicts incident retinopathy for young individuals who have type 1 diabetes: a longitudinal prospective cohort study starting in adolescence",Care for Diabetes p DC 102419

[69] Bullitt, Gerig, Pizer, Lin, and Aylward "Measuring solution viscosity of the intracerebral vasculature using mra images",IEEE Trans. Med. (2003) 1163–1171 in Imaging 22 (9)

[70] Grisan, A. Ruggeri, M. Foracchia "A novel technique for the automatic grading of retinal vascular tortuosity was developed",IEEE Trans. Med. (2008) Imaging 27 (3): 310–319

[71] W.E. Goldbaum, B. Cot'e, P. Hart, M. Nelson Kube, "Measuring and Classifying Retinal Vascular Tortuosity", International. J. Med. Inf. 53 (2-3) 1999 239–252.

[72] A. Lukosevicius, V. Marozas, M. Pata& D. Jegelevicius "Evaluation of eye blood vessel deformability that use the total of square of curvature",EMBEC 5 (2005) 20–25.

[73] Crosby-Nwaobi, S. Sivaprasad, L.Z. Heng "Retinal vascular calibre, geometry, and evolution of diabetic retinopathy with type 2 diabetes mellitus",Ophthalmologica 228 (2) (2012) 84–92.

[74] Aghamohamadian-Sharbaf, H.R. Pourreza, and T. Banaee "M. A unique curvature-based algorithm for automatically assessing retinal blood vessel tortuosity was developed",Health. Inf. 20 (2) 2016 586–595.

[75] Fisher, Chandrinos, Pilu, and Trahanias. "Image processing techniques in quantifying atherosclerotic changes", (1998). The DAI Research Paper.

[76] Goh, W. Hsu, M. Li Lee, and H. Wang "An automatic diabetes retinal image screening system",Studies on Fuzziness & Soft Computing 60 (2001), 181–210.

[77] H Toonen, KauppS Wolf, K Schulte, D Meyer-Ebrecht, R Effert "Automatic evaluation on retinal artery width & tortuosity in digital fluorescence endoscopies, engage",M Reim/Ophthalmol 84 (1991) 952-987.

[78] Pourreza, F. Ghadiri, T. Banaee, and M. Delgir "Retinal vascular tortuosity evaluation through circle though transformation",Biomed Engineers (ICBME), 2011 18th Iranian Conference on, 2011, pp. 181–184.

[79] S.M. Zabihi, F. Ghadiri, H.R. Pourreza, and T. Banaee "A novel technique for vessel detection utilizing contourlet transform",Communication (NCC), 2012 National Conference on, pp. 1–5.

[80] Wallace, S.F. Freedman, and Z. Zhao "Evolution of plus illness in retinopathy of preterm birth: quantification by roptool",Trans. Am. Ophthalmol. Soc. 107 (2009) 47.

[81] E. Dhillon Trucco, B. Dhillon,H. Azegrouz "A. Modeling the tortuosity of retinal vessels",IEEE Transactions on Bioengineering 57(9):2239, 2010.

[82] Eze, R. Gupta, and D. Newman "A comparison of objective measurements of vascular tortuosity utilizing sine wave simulations with 3D wire models",Physics in Medicine and Biology 45 (9) 2000 2593–2599.

[83] Kalitzeos, G.Y. Lip, and R. Heitmar, "Retinal vascular tortuosity measurements and their applications",Exp. Eye Research, 106, 40–46 (2013).

[84] S. Ioffe, Szegedy, V. Vanhoucke, and A.A. Alemi "Inception-v4, Inception-resnet, and the effect of residual connections upon learning",Artificial Intelligence Conference, 31st AAAI, 2017.

[85] LeCun, Y. Bengio, and G. Hinton "Deep Learning",Nature 521 (7553) 2015 436-444.

[86] Alom MZ, Yakopcic C, Westberg S, Taha TM, Sidike P, Nasrin MS, Van Esesn BC, Awwal AAS, and Asari VK (2018) "The history begins with alexnet: a thorough study of deep learning techniques",Preprint for arXiv is arXiv:180301164.

[87] Lin, P. Goyal, R. Girshick, K. He, and P. Dollar, "Focal loss in dense object detection",Proceeding of the International Symposium on Computer Vision, 2017, pp. 2980–2988.

[88] Poletti, E Grisan, E Ruggeri, A "Image-level tortuosity estimation in wide-field retinal pictures from new borns with retinopathy of prematurity",Annual International Conference of the IEEE Engineering in Medicine and Biology Society, 2012, pp. 4958-4961.

[89] F. Oloumi, Rangayyan, RMElls "Assessment of vascular tortuosity in retinal pictures of preterm newborns",36th Annual World Congress of the IEEE Engineering in Medicine & Biology Association, 2014, pp. 5410-3 EMBC.2014.6944849. org/10.1109.

[90] C.K. Chua, Acharya U, E.Y.K. Ng, W. Yu, and C. Chee "Application of higher order spectra for the diagnosis of diabetes retinopathy stages",J Med Syst 32(6) (2008) 481-488.

[91] D. Tegolo, Lo Castro, C. Valenti, "A visual framework to produce photorealistic retinal vessels for diagnostic purposes was developed",J. Biomed. Inform. 108 (2020) 103490 https://doi.org/10.1016/j.jbi.2020.103490.

[92] Wang, K. Wu, S.L. Fernandes, T. Chu, Q. Zhou, J. Sun, Y.-D. Zhang, S. Zhong "SOSPCNN: Structurally Optimized Sequential Pooling Convolutional Neural Network with Tetralogy of Fallot Identification",Wireless Communications & Mobile Computing 2021 (2021) 1-17.

[93] Yu-Dong Zhang, S. Chandra Satapathy, David S. Guttery, Juan Manuel orriz, Shui-Hua Wang b,f, "Improved Breast Cancer Identification Using Graph Convolutional Network & Convolutional Neural Network",Information Processing as well as Management 58 (2021) 102439.

[94] He, X. Ren, K. Zhang and S. Sun. J "Deep residual training for machine vision," Proceedings of the Conference in PC Vision and Example Acknowledgment Las Vegas, Nevada",USA, 27-30 Jun. 2016, pp. 770–778.

[95] Tan, M., and Q. Le, "Efficientnet: Rethinking model scalability for convolutional neural networks", in Proceedings of the World Congress on Deep Learning, PMLR, Long Beach, CA, USA, 9-15 June 2019; pp. 6105–6104.

[96] Raghavendra, H. Bhandary, U. Fujita, S.V. Gudigar, A. Tan, J.H. Acharya, and U.R., "Deep convolution neural networks for official diagnosis of glaucoma utilizing digital fundus pictures", Inf. Sci. 2018, 441, 41–49.

[97] Chetoui, M. Akhloufi, M.A "Explainable Diabetic Retinopathy with EfficientNET", in Proceeding of the 2020 42nd Annual World Congress of the IEEE Bioengineering in Medicine & Biology Association (EMBC), Montréal, QC, Canada, 20-24 July 2020; IEEE: Newark, NJ, USA; pp. 1966-1969.

[98] Simonyan, K., Zisserman, A "deep convolutional networks for large-scale image recognition", arXiv 2014, arXiv:1409.1556.

[99] Hashimoto, N. Fukushima, R.; Takagi, D. Koga, Y. Ko, K. Kohno, K. Nakaguro "Multi-scale Domain-adversarial Numerous CNN for Cancer Subtype Categorization with Unannotated Histopathological I Images", In Deliberations of the IEEE/CVF

Conference on Computer Vision & Pattern Recognition, Seattle, WA, USA, 13-19 June 2020; pp. 3852-3861.

[100] Lam, Carson, Darvin Yi, Margaret Guo, and Tony Lindsey. "Automated detection of diabetic retinopathy using deep learning. ", AMIA summits on translational science proceedings 2018 (2018): 147.

[101] Szegedy, Y. Sermanet, W. Jia, C. Liu, P.; Reed, S. Anguelov, D. Vanhoucke, D. Erhan, V. Rabinovich, A "Going deeper with convolutions", In Proceeding of the Conference on Computer Vision & Algorithmic, Boston, MA, America, 7-12 June 2015; pp. 1-9.

[102] Wang, S. Yin, x, G. Wei, W. Jia, B. Zheng, Y. Yang, G "Hierarchical retinal blood vessel describe the characteristics on feature and ensemble learning", Neurocomputing 2015, 149, 708-717.

[103] S. J. Pan and Q. Yang, "A survey on transfer learning", IEEE Trans. Knowl. Data Engineering. 2009, 22, 1345–1359.

[104] Rao, Mihir, Michelle Zhu, and Tianyang Wang. "Conversion and implementation of state-of-the-art deep learning algorithms for the classification of diabetic retinopathy", arXiv preprint arXiv:2010.11692 (2020).

[105] T. Sabeenian and Shanthi, "RS Modified Alexnet architecture for categorization of diabetic retinopathy images", Comput. Electr. Eng. 2019, 76, 56–64.

[106] Dondeti, Venkatesulu, Jyostna Devi Bodapati, Shaik Nagur Shareef, and Naralasetti Veeranjaneyulu. "Deep Convolution Features in Non-linear Embedding Space for Fundus Image Classification", Rev. d'Intelligence Artif. 34, no. 3 (2020): 307-313.

[107] Bodapati, Jyostna Devi, Nagur Shareef Shaik, and Veeranjaneyulu Naralasetti. "Composite deep neural network with gated-attention mechanism for diabetic retinopathy severity classification", Journal of Ambient Intelligence and Humanized Computing 12, no. 10 (2021): 9825-9839.

[108] Majumder, S., and N. Kehtarnavaz, "Multitasking Deep Learning Model for Identification of Five Stages of Retinopathy", arXiv2021, arXiv:2103.04207.

[109] Patel, R., and Chaware, A. "Transfer Learning with Fine-Tuned MobileNetV2 for Diabetic Retinopathy", in Proceedings of the 2020 World Congress for Emerging Technology (INCET), Belgaum, India, June 5-7, 2020; IEEE: Piscataway, NJ, USA; pp. 1-4.

[110] Available available at: https://www.kaggle.com/c/aptos2019-blindness-detection/data (accessed on 21st May 2021).

[111] Hu, Jie, Li Shen, and Gang Sun. "Squeeze-and-excitation networks", In Proceedings of the IEEE conference on computer vision and pattern recognition, pp. 7132-7141. 2018.

[112] Sandler, Mark, Andrew Howard, Menglong Zhu, Andrey Zhmoginov, and Liang-Chieh Chen. "Mobilenetv2: Inverted residuals and linear bottlenecks", In Proceedings of the IEEE conference on computer vision and pattern recognition, pp. 4510-4520. 2018.

[113] Cao, Y., J., Lin, Xu, S., Wei, F., et al. "Genet: Non-local networks meet pressure networks and even beyond", Proceedings of the IEEE/CVF World Congress on Computer Vision Workshop, Seoul, Korea, Oct 27–28, 2019.

[114] Szegedy, C., Ioffe, S., Vanhoucke, V., and Alemi, A.A. "Inception-v4, inception-resnet, as well as the impact of feedback connections on learning", in Proceeding of the 31st AAAI Conference on Ai Technology, San Fran, CA, USA, 4–9 February 2017.

[115] F. Xception Chollet, "Deep learning with depthwise separable separable convolutions", in IEEE Conference on Computer Vision & Pattern Identification proceedings. Honolulu, Hawaii, USA; pages. 1251–1258; 21–26 July 2017.

[116] Maji, Debasis, and Arif Ahmed Sekh. "Automatic grading of retinal blood vessel in deep retinal image diagnosis", Journal of Medical Systems 44, no. 10 (2020): 180.

[117] Mariotti SP, Pascolini D (2012) "Estimates of vision impairment worldwide as of 2010",96(5):614-618 in Br J Ophthalmol.

[118] Mitchell P, Cumming RG, Attebo K, Panchapakesan J (1997) "Commonness of waterfalls in Australia: The Blue Mountains eye survey", Eye surgery 104(4):581-588.

[119] N. Congdon, J. Vingerling, R. Klein, S. West, D. Friedman, J. Kempen, B. O'Colmain, S. Y. Wu, and H. Taylor (2004) "Adult predominance of waterfall and pseudophakia/aphakia in the United States. Chicago, Illinois",Arch Ophthalmol",1960; 122(4):487-494.

[120] J.J. Kanski and A. Kubicka-Trzáska (2007) "A self-evaluation companion for clinical ophthalmology Churchill Livingstone",Elsevier.

[121] Vinogradov, S. V., Kohli, and A. D. (2005) " ‘5'-triphosphate nucleoside analogue cross-linked polymeric nanogel formulations: Cellular membrane function in drug release", 2(6):449–461 Mol Pharm.

[122] Klein BEK, R Klein, KLP Linton, Magli YL, and Neider MW (1990) "Assessing cataracts from pictures in the Beaver Dam Eye Study",Eye surgery 97(11):1428-1433.

[123] Soares JVB, JJG Leandro, RM Cesar, Jelinek HF, and Cree MJ (2006) "Segmenting retinal vessels with the 2-D Gabor wavelet and supervised learning",1214–1222 in IEEE Trans Drug Imaging 25(9).

[124] Kotyk, T., Chakraborty, S., Dey, N., Gaber, A.E., and V. Snasel (2016) "Semi-robotized framework for cup-to-disc measurement for detecting glaucoma utilizing characterization worldview", Proceedings of the Second International Afro European Gathering for Modern Progression AECIA 2015, Springer, pp 653-663.

[125] Lupascu CA, Tegolo D, and Trucco E (2010) "FABC: AdaBoost-enhanced retinal vessel division",1267–1274 IEEE Trans Inf Technol Biomed, 14(5).

[126] Memari, N., Ramli, A., Bin Saripan, M., Mashohor, and M. (2017) "Administered retinal vessel division from colour fundus pictures using matched filtering and the AdaBoost classifier", 12(12): e0188939 PLoS One.

[127] Fraz, M.M., P. Remagnino, A. Hoppe, S. Velastin, B. Uyyanonvara, and S. A. Barman (2011) "A supervised approach for segmenting retinal blood vessels based online strength, multiscale Gabor, and morphological data",IEEE International Gathering on Sign and Picture Handling Applications, 2011, p. (ICSIPA). 410-415 in IEEE.

[128] Dey N, Obreja CD, Ashour AS, Moraru L (2018) "For accurate assessment of retinal vascular diameter, combine Dempster and Shafer", Elsevier, pp. 149-160 in Delicate Registering Based Clinical Picture Examination.

[129] Lennon R. "Presenting remote identifying electronic picture investigation",2002. In the US: Esa/Esrin.

[130] Sekh AA, Maji D (2020) "Programmed retinal vein evaluating for analysis of profound retinal pictures. J Medical Systems ",44(10):1–14.

[131] Shih L., James J., and E. Sharifahmadian (2018) "Diabetic retinopathy seriousness levels are automatically classified. Int J Comp Appl 180:30–35.

[132] Yang Y, T Li, Li W, Wu H, Fan W, and Zhang W (2017) "Used two-stage profound convolutional brain organizations to detect and grade diabetic retinopathy lesions. International conference on computer-assisted intervention and medical image computing", 533-540 in Springer.

[133] Paing MP, S Choomchuay, and Yodprom MDR (2016) "Utilized fundus pictures to order diabetic retinopathy and recognise injuries", 2016 ninth Worldwide Gathering on Biomedical Designing (BMEiCON). IEEE, pages 1-5.

[134] Seoud L, Cheriet F, and Chelbi J (2015) "Programmed reviewing of diabetic retinopathy utilizing a public data set",Worldwide Ophthalmic Clinical Picture Examination Studio. Iowa College.

[135] Vibha L, Venugopal KR and Prasad DK (2015) "Computerized retinal fundus imaging can be utilized to early identify diabetic retinopathy. Late Advances in Keen Computational Frameworks", 2015 IEEE (RAICS). IEEE, pages 240-25.

[136] S. Roychowdhury, D. Koozekanani, and K. Parhi (2013) "DREAM: Utilizing AI to investigate diabetic retinopathy", 18(5):1717-1728 IEEE J Biomed Health Informatics.

[137] Gayathri S, Krishna AK, Gopi VP, Palanisamy P "Robotized twofold and multiclass order of diabetic retinopathy utilizing haralick and multiresolution highlights", (2020). 57497-57504 IEEE Access 8.

[138] Akram MU, Khalid S, Tariq A, Khan SA, and Azam F "The identification and characterization of retinal injuries for the evaluating of diabetic retinopathy was distributed", (2014). Comput Biomedicine 45:161-171.

[139] H. Pratt, F. Coenen, D. Broadbent, S. Harding, and Y. Zheng (2016) "Neural networks with convolutional layers for diabetic retinopathy", 90:200–205 in Procedia Computer Science.

[140] Mookiah MRK, Martis RJ, Acharya UR,Chua CK, Lim CM, Ng EYK, and Laude A (2013) "Evolutionary algorithm based classifier parameter tweaking for autonomous diabetic retinopathy evaluating: A half and half component extraction technique", 39:9–22 Knowledgebased Syst.

[141] Long, J., Shelhamer, E., and Darrell (2015) "Convolutional networks in their entirety for semantic segmentation", Page numbers 3431-3440 in: Procedures of the IEEE meeting on PC vision and example acknowledgment.

[142] Lian, S., Zhong, Z., Lin, X., Su, and Li (2018) "U-Net was guided by attention to segment the iris with accuracy ",56:296-304 J Vis Commun Image Represent.

[143] Bansal N., Dutta M. (2013) "Retina vessels identification method for biomedical side effects conclusion", 71 Int J Comput Appl (20).

[144] Van Ginneken, B., Niemeijer, M., and Staal J. (2004) "Ridge-based vascular segmentation in retinal colour pictures", 501–509, IEEE Trans Med Imaging, 23(4).

[145] Hoover A.D., Kouznetsova V., and M. Goldbaum (2000) "Blood vessel location in retinal pictures by piecewise threshold examining of a matched channel reaction", 203–210. IEEE Trans Med Imaging, 19(3).

[146] Fraz MM, Hoppe A, Remagnino P, Rudnicka AR, Uyyanonvara B, Owen CG, and Barman SA 30 (2012) "An ensemble classification-based approach was used to segment retinal blood vessels", 2538–2548. IEEE Trans Biomed Eng, 59(9).

[147] A. Budai, R. Bock, A. Maier, J. Hornegger, and G. Michelson (2013) "powerful vessel division in fundus pictures", International Journal of Biomedical Imaging 2013.

[148] Prentai P, Lonari S, Vatavuk Z, Beni G, Subai M, Petkovi T, Dujmovi L, Malenica-Ravli M, Budimlija N, Tadi R (2013) "Diabetic retinopathy images database (DRiDB): a clever data set for diabetic retinopathy screening program research eighth Worldwide Discussion on Picture and Sign Handling and Analysis", 2013, p. (ISPA). IEEE, pages 711–716.

[149] Estrada, R., Allingham, M.J., Mettu, P.S., Cousins, S.W., Tomasi, and S. (2015) "Using topology estimation, classify the retinal arteries and veins", 2518–2534 IEEE Trans Med Imaging 34(12).

[150] Holm, S., Russell, G., Nourrit, and N. McLoughlin are 34. (2017) "DR HAGIS is a fundus picture data set for the programmed extraction of diabetes patients' retinal surface vessels", J. Med. Imaging 4(1): 14503.

[151] Roychowdhury, S., D., and K. Koozekanani (2014) "Segmenting blood vessels in fundus images using subimage classification and main vessel extraction", IEEE J Biomed Health Inform 19(3):1118-1128.

[152] Li Q, Xie L, Feng B, Liang P, Zhang H, and Wang T. (2015) "A multimodal learning strategy for segmenting vessels in retinal pictures", 109–118, IEEE Trans Prescription Imaging 35(1).

[153] Alom MZ, Yakopcic C, Hasan M, Taha TM, and Asari VK "U-Net (R2U-Net) for Clinical Picture Division",(2018) Intermittent Remaining Convolutional Brain Organization based.

[154] Wang, B., Qiu, S., and He, H. (2019) "Segmenting retinal vessels using a dual-encoding u-net. At: The Global Meeting on Clinical Picture Registering and PC Helped Mediation", 84–92 in Springer.

[155] S.Maiti, D.Maji, A.K. Dhara, G. Sarkar "Programmed discovery and division of the optic disc that using a modified Network of convolution algorithm", (2022). Biology of Signal Processing in Medicine 74:103514.

[156] Raghavendra, H. Bhandary, U. Fujita, S.V. Gudigar, A. Tan, J.H. Acharya, and U.R., "Deep convolution neural networks for official diagnosis of glaucoma utilizing digital fundus pictures", Inf. Sci. 2018, 441, 41–49.

[157] Chetoui, M. Akhloufi, M.A "Explainable Diabetic Retinopathy with EfficientNET", in Proceeding of the 2020 42nd Annual World Congress of the IEEE Bioengineering in Medicine & Biology Association (EMBC), Montréal, QC, Canada, 20-24 July 2020; IEEE: Newark, NJ, USA; pp. 1966-1969.

[158] Simonyan, K., Zisserman, A "deep convolutional networks for large-scale image recognition", arXiv 2014, arXiv:1409.1556.

[159] Hashimoto, N. Fukushima, R.; Takagi, D. Koga, Y. Ko, K. Kohno, K. Nakaguro "Multi-scale Domain-adversarial Numerous CNN for Cancer Subtype Categorization with Unannotated Histopathological I Images", In Deliberations of the IEEE/CVF Conference on Computer Vision & Pattern Recognition, Seattle, WA, USA, 13-19 June 2020; pp. 3852-3861.

[160] Gargeya, R., Leng, T "Automated detection of diabetic retinopathy using deep learning", Ophthalmology 2017, 124, 962-969.

[161] Szegedy, Y. Sermanet, W. Jia, C. Liu, P.; Reed, S. Anguelov, D. Vanhoucke, D. Erhan, V. Rabinovich, A "Going deeper with convolutions", In Proceeding of the Conference on Computer Vision & Algorithmic, Boston, MA, America, 7-12 June 2015; pp. 1-9.

[162] Wang, S. Yin, x, G. Wei, W. Jia, B. Zheng, Y. Yang, G "Hierarchical retinal blood vessel describe the characteristics on feature and ensemble learning", Neurocomputing 2015, 149, 708-717.

[163] S. J. Pan and Q. Yang, "A survey on transfer learning," IEEE Trans. Knowl. Data Engineering. 2009, 22, 1345–1359.

[164] Rao, Mihir, Michelle Zhu, and Tianyang Wang. "Conversion and implementation of state-of-the-art deep learning algorithms for the classification of diabetic retinopathy." arXiv preprint arXiv:2010.11692 (2020).

[165] T. Sabeenian and Shanthi, "RS Modified Alexnet architecture for categorization of diabetic retinopathy images", Comput. Electr. Eng. 2019, 76, 56–64.

[166] Dondeti, V., Bodapati, J. D., Shareef, S. N., & Veeranjaneyulu, N. (2020). Deep Convolution Features in Non-linear Embedding Space for Fundus Image Classification", Rev. d'Intelligence Artif., 34(3), 307-313.

[167] Patel, Vinod, Salwan Rassam, Richard Newsom, Jutta Wiek, and Eva Kohner. "Retinal blood flow in diabetic retinopathy", British Medical Journal 305, no. 6855 (1992): 678-683.

[168] Fevereiro-Martins, Mariza and Marques-Neves, Carlos and Guimarand Bicho, Manuel "Retinopathy of prematurity: A review of pathophysiology and signaling pathways"in Current Opinion in Ophthalmology, Elsevier, 2023, volume-68,PP-175-210.

[169] Chen X, Wang Y "Update on Screening and Management of Retinopathy of Prematurity" in Journal of Current Treatment Options in Pediatrics, Springer-2022, volume-8,PP- 246—261.

[170] Tsai, Andrew SH and Acaba-Berrocal, Luis and Sobhy, Myrna and Cole, Emily and Ostmo, Susan and Jonas, Karyn and Campbell, J Peter and Chiang, Michael F and Chan, RV Paul" Long-term neurodevelopmental outcomes of premature infants in Singapore" in Pediatric Research , Ann Acad Med Singap,2023, volume-47,PP-63-70.

Delasios Mayi
20/4/2023